The Hong Kong Polytechnic University

Department of Building Services Engineering

Energy Performance and Optimal Control of Air-conditioned Buildings Integrated with Phase Change Materials

Na ZHU

A thesis submitted in partial fulfillment of requirements for the

Degree of Doctor Philosophy

June 2011

CERTIFICATE OF ORIGINALITY

The research described in this thesis is the original work except the sources quoted. It was carried out at the Department of Building Services Engineering, The Hong Kong Polytechnic University under the supervision of Prof. Shengwei Wang and Dr. Fu Xiao.

Na ZHU

Department of Building Services Engineering

The Hong Kong Polytechnic University

Hong Kong, P.R. China

June 2011

ABSTRACT

Abstract of thesis entitled: Energy performance and optimal control of buildings integrated with phase change materials

Submitted by: Na ZHU

For the degree of: Doctor of Philosophy

at The Hong Kong Polytechnic University in June, 2011

Thermal energy storage (TES) systems using phase change materials (PCMs) have been recognized as one of the advanced energy technologies in enhancing energy efficiency and sustainability of buildings. The use of PCMs in buildings provides the potential for a better indoor thermal comfort for occupants due to the reduced indoor temperature fluctuations, and lower overall energy consumption due to the load reduction/shifting. This thesis presents an overview of the previous research work on dynamic characteristics and energy performance of buildings due to the integration of PCMs. The research work on dynamic characteristics and energy performance of buildings using PCMs both with and without air-conditioning is reviewed. Since the particular interest in using PCMs for free cooling and peak load shifting, specific research efforts on both subjects are reviewed separately.

The use of phase change materials (PCMs) to enhance the building energy performance has attracted increasing attention of researchers and practitioners over the last few years. Thermodynamic models of building structures using PCMs are

essential for analyzing their impacts on building energy performance at different conditions and using different control strategies. There are few PCM models of detailed physics providing good accuracy in simulating thermodynamic behavior of building structures integrated with PCM layers. However, simplified models with acceptable accuracy and good reliability are preferable in many practical applications concerning computation speed and program size particularly when involving large buildings or models are used for online applications. A simplified physical dynamic model of building structures integrated with SSPCM (shaped-stabilized phase change material) is developed and validated in this study. The simplified physical model represents the wall by 3 resistances and 2 capacitances and the PCM layer by 4 resistances and 2 capacitances respectively while the key issue is the parameter identification of the model. The parameters of the simplified model are identified using genetic algorithm (GA) on the basis of the basic physical properties of the wall and PCM layer. Two GA-based preprocessors are developed to identify the optimal parameters (resistances and capacitances) of the model by frequency-domain regression and time-domain regression respectively. Validation results show that the simplified model can represent light walls and median walls integrated with SSPCM with good accuracy.

This thesis also presents the studies on the thermodynamic characteristics of buildings enhanced by PCM and on the investigation of the impacts of PCM on the building cooling load and peak cooling demand at different climates and seasons as well as the optimal operation and control strategies to reduce the energy consumption and energy cost by reducing the air-conditioning energy consumption and peak load.

An office building floor with typical variable air volume (VAV) air-conditioning system is used and simulated as the reference building in the comparison study. The envelopes of the studied building are further enhanced by integrating the PCM layers. The building system is tested in two selected cities of typical climates in China including Hong Kong and Beijing. The cold charge and discharge processes, the operation and control strategies of night ventilation and the air temperature set-point reset strategy for minimizing the energy consumption and electricity cost are studied. This thesis presents the simulation test platform, the test results on the cold storage and discharge processes, the air-conditioning energy consumption and demand reduction potentials in typical air-conditioning seasons in typical China cites as well as the impacts of operation and control strategies.

PUBLICATIONS ORIGINATED FROM THIS STUDY

Journal Papers

Zhu N, Ma ZJ and Wang SW. Dynamic characteristics and energy performance of buildings using phase change materials: A review. Energy Conversion and Management 2009; 50(12):3169-3181.

Zhu N, Wang SW, Xu XH and Ma ZJ. A simplified dynamic model of building structures integrated with shaped-stabilized phase change materials. International Journal of Thermal Sciences 2010; 49(9):1722-1731.

Zhu N, Wang SW, Ma ZJ and Sun YJ. Energy Performance and Optimal Control of Air-conditioned Buildings with Envelopes Enhanced by Phase Change Materials. Under publish, Energy Conversion and Management.

Wang SW, Sun ZW, Sun YJ and Zhu N. Online Optimal Ventilation Control of Building Air-conditioning Systems. Indoor and Built Environment 2010;20(1):129-136.

Sun ZW, Wang SW and Zhu N. Model-based Optimal Control of Outdoor Air Flow Rate of An Air-Conditioning System with Primary Air Handling Unit. Revision submitted, Indoor and built environment.

Conference Paper

Zhu N, Wang SW and Ma ZJ. A Simplified Dynamic Model of Building Structures integrated with SSPCM Using GA-based Parameter Identification. International Conference on Applied Energy, Singapore, 21-23, April 2010.

Wang SW, Sun YJ, Huang GS and Zhu N. A control scheme of enhanced reliability for multiple chiller plants using merged building cooling load measurement. 8th International Conference for Enhanced Building Operations, Berlin, Germany, October, 2008.

Published Book

Translation, Chapter 2 of《Intelligent Buildings and Building Automation》, Chinese version published by China Architecture & Building Press in Jan 2010.

ACKNOWLEDGEMENTS

I am deeply indebted to Prof. Shengwei Wang, my supervisor, and Dr. Fu Xiao, my co-supervisor, for their available supervision, invaluable suggestions, patient encourage, continuous support, and extensive cultivation over the past three years.

I would like to thank colleagues, especially Dr. Zhenjun Ma, Dr. Yongjun Sun, in the team for their sincere care and help. The long road to accomplish this research is memorable because of their company.

Finally, I would like to express my deepest appreciation to my family members: especially my parents, for their unconditional trust and support in my life. This thesis is to them.

LIST OF FIGURES

LIST OF TABLES

NOMENCALTURE

A	air
AHU	air handling units
Avg	average
C	capacitance (kJK^{-1})
CAV	constant air volume
c_p	specific heat ($kJkg^{-1}K^{-1}$)
D	thickness of materials (mm)
DDC	Direct Digital Control
DL	demand-limiting
EMCS	energy management and control systems
f	fitness function
GA	genetic algorithm
H	convective heat transfer coefficient ($Wm^{-2}K^{-1}$)
H	enthalpy ($kJkg^{-1}$)
HDPE	high-density polyethylene
In	indoor air
J	objective function
K	thermal conductivity ($Wm^{-1}K^{-1}$)
LHTES	latent-heat thermal energy storage
LS	load-shifting

MPCM	microencapsulated phase change material
N	the number of frequency points
N	number of occupants
NVP	night ventilation system
p	phase change material
P	pressure (Pa)
PC	personal computer
PCM(s)	phase change material(s)
PL	phase lag (rad)
PVC	polyvinyl chloride
Q	cooling/heating load or heat (kW)
R	resistance and (KkW^{-1})
SSPCM	shape-stabilized phase change material
T	temperature (℃or K)
TES	thermal energy storage
TIM-PCM	thermal interface material-phase change material
TOU	time-of-use
u	velocity (m/s)
VAV	variable air volume
VIP	vacuum insulation panel
W	weighting factor
ρ_a	specific mass of are (m^3/s)

Greek symbols

β_i	*i*-th element of coefficient vector
ρ	density (kgm^{-3})
ω	frequency($rads^{-1}$)
η	saving rate

Subscripts

eo	equipments and occupants
in	inside or indoor
T	temperature (℃or K)
p	phase change material (pcm)
sol	solar air
s	simplified model
t	theoretical model
w	wall

Energy Performance and Optimal Control of Air-conditioned Buildings Integrated with Phase Change Materials

Table of Contents

CHAPTER 1 INTRODUCTION

1.1 Motivation

Over the last two or more decades, many efforts have been made on the development and application of various PCMs in buildings. It is reflected by the fact that more than ten solid and comprehensive review papers concerning the use of PCMs in various applications have been published and can be readily available in literature [Salyer IO and Sircar AK, 1997. Etheridge D, Murphy K and Reay D, 2006. et al.]. The studies related to the use of PCMs in buildings have addressed PCM developments [Khudhair AM and Farid MM, 2004. Pasupathy A, Velraj R and Seeniraj RV, 2008. Ghoneim AA, Klein SA and Duffie JA, 1991] and their performance enhancement and analysis (i.e., heat transfer [Zhang YW and Faghri A, 1996. Stritih U, 2003. Darkwa K and Kim JS, 2004], thermal physical properties [Hadjieva M, Kanev S and Argirov J, 1992. Neeper DA, 2000], long-term stability [Zalba B, Marin JM, Cabeza LF, 2003], fire characteristics [Banu D, Feldman D, Haghighat F, Paris J and Hawes D, 1998], etc.), PCM incorporation methods (i.e., direct incorporation [Feldman D, Banu D, Hawes D and Ghanbari E, 1991], immersion [Banu D, Feldman D, Haghighat F, Paris J and Hawes D, 1998], encapsulation [Hawlader MNA, Uddin MS and Khin MM, 2003. Schossig P, Henning HM, Gschwander S and Haussmann T, 2005], and laminated PCM board [Darkwa K and Kim JS, 2004], etc.), and their various applications in buildings, including PCMs in building walls [Neeper DA, 2000. Peippo K, Kauranen P and Lund PD, 1991], PCMs in other building components other than walls [Benard C, Gobin D and Gutierrez M, 1981. Athienitis AK, 1994], PCMs in heat and cold storage units [Zalba B, Marin JM, Cabeza LF and Mehling H, 2004], the dynamic characteristics and the energy performance of buildings using PCMs [Zhu N, Ma ZJ and Wang SW, 2009], etc. These efforts have resulted in a number of commercial PCMs readily available in the international market and that can be easily integrated with buildings for various applications.

The thermal performance enhancement of a building due to the use of PCMs depends on many factors, including climate, design, orientation of the construction, and the quantity and types of PCMs used [Ibáñez M, Lázaro A, Zalba B and Cabeza LF, 2005]. Therefore, proper modeling of buildings and integrated PCMs, and detailed simulation of the thermal behavior of the buildings using PCMs are essential. They can play important roles in assisting the proper selection of the most promising PCMs, testing and evaluating the performances of alternative operation/control strategies and design options, prior to field validation and application.

Over the last three decades, many efforts have been made on the development of proper models for buildings and their associated thermal energy storage systems. At building level, many researchers have developed various reference models (load models or energy performance models) for load prediction or cost saving estimations, including physical models [Lawrence Berkeley Laboratory, 1982. Kelin SA et al. 1990], data driven models [Ferrano F and Wong K, 1990. Reddy TA and Claridge DE, 1994] and gray-box models [Braun JE and Chaturvedi N, 2002. Liao Z and Dexter AL, 2004].

Many efforts have also been made on the developing proper models for thermal energy storage (TES) systems, especially for latent TES systems. In general, those models can be categorized into two groups, models based on first law of thermodynamics and models based on second law of thermodynamics. Kurkulu et al. [1996] proposed a mathematical model for prediction of the thermal performance of a square cross-sectioned PCM store. Gong and Mujumdar [1997] developed a finite-element model to simulate the cyclic thermal process occurring in a shell and tube latent heat thermal storage exchanger. Kang et al. [1999] and Zhang et al. [2001] proposed generic models for analyzing the thermal performance of latent heat TES systems. Halawa et al.[2005] developed a two-dimensional model to analyze the characteristics of a PCM thermal storage unit for roof integrated solar heating systems. Xu and Zhang et al [2005] developed a model for studying the thermal performance of a shape-stabilized PCM floor. Dwarka and Kim [2005] presented a mathematical model for comparing the thermal performance of randomly mixed and laminated PCM drywall system. A two-dimensional separate phase formulation was used by Benmansour et al. [2006] to develop a numerical analysis of the transient response of a cylindrical packed bed thermal energy storage system. In addition, a solid review of mathematical modeling on latent heat TES systems using PCMs has been done by Verma et al. [2008] recently.

Using above models, the simulation of the “actual” performance of various

PCMs in buildings and the performances of alternative design options can be studied and tested in the virtual environment. Peippo et al. [1991] discussed the use of PCMs walls for short-term heat storage in a building simulation environment. Jokisalo et al. [2000] simulated the thermal behavior of a single room using PCM structures using TRNSYS program. Ibáñez et al. [2005] presented a simple methodology for the energetic simulation of buildings including elements with PCMs using TRNSYS. Thermal performance test and numerical simulation of a prototype cell using light wallboards coupling vacuum isolation panels and PCM were studied by Ahmad et al. [2006] using TRNSYS.

These works provided the foundations for successful use of PCMs in buildings. However, these studies were focused on the particular applications and the general guidelines for the proper selection and use of PCMs in buildings were not provided. Particularly, most of the existing models are too complex and not convenient for practical applications on full scale buildings building because they were mostly developed for detailed analyzing the thermal characteristics of PCMs. For practical applications of PCMs in building performance enhancement and optimal control of buildings using PCMs, models which are accurate and simple enough and convenient for use are still missing.

Proper control and operation of buildings and their associated components have significant impacts on energy or cost efficiency of buildings besides proper system designs and selection as well as maintenance of individual components. Aiming at enhancing system operating efficiency and improving system control robustness, many researchers and experts in the HVAC&R field have devoted considerable efforts on energy efficient control and operation of buildings during the past two decades. Braun [1990] applied optimization routines to computer simulations of buildings and their associated cooling systems in order to estimate cost savings associated with optimal control of building thermal mass. Rabl and Norford [1991] used a simple building model to study the impact of building pre-cooling on peak cooling loads. Reddy et al. [1991] proposed the alternative practical strategies of peak removing that use the opportunities offered by modern electronics and a more intelligent use of the thermal mass storage inherent in the structure and furnishings of the house. Andresen and Brandemuehl [1992] demonstrated the cost saving potentials in peak cooling rate associated with using pre-cooling strategies. Kintner-Meyer and Emery [1995] presented a comprehensive analysis of optimal control of HVAC systems considering the building thermal mass and cold storage equipment.

Nagai et al. [2002] described a calculation method for optimal dynamic control utilizing the thermal effect of building envelope to minimize annual energy consumption, annual peak energy/demand, and annual energy cost. Braun [2003] attempted to provide an assessment of the state of the art in load control using building thermal mass and to identify the steps necessary to achieve widespread application of appropriate control strategies. Henze and Le et al. [2007] systematically evaluated the merits of the passive building thermal capacitance to minimize energy cost for a design day using optimal control. The evaluation was conducted by means of a sensitivity analysis utilizing a dynamic building energy simulation program coupled to a popular technical computing environment. Henze and Pfafferott et al. [2007] investigated building thermal mass control of commercial buildings to reduce utility costs with a particular emphasis on the individual impacts of both adaptive comfort criteria and of heat waves. Lee and Braun [2006, 2008] paid considerable efforts on development and evaluation of demand-limiting strategies using building thermal mass.

These studies have demonstrated that optimal control of buildings using building thermal mass can reduce the peak loads greatly and, therefore, achieve significant energy or cost savings. However, the studies on optimal control of active buildings using PCMs as TES systems are still inadequate, or even missing.

Therefore, the simplified SSPCM building model, the model parameter estimation method, and accurate building cooling load calculation method as well as optimal control strategies for building and HVAC&R systems are developed in this PhD project. The dynamic characteristic and energy performance are analyzed in different weather profiles and different electricity price policies.

1.2 Aim and objectives

This project aims at studying on the thermodynamic characteristics of air-conditioned buildings enhanced by PCMs; investigating the impacts of PCMs on the building energy performance; and developing the optimal control strategies for their air-conditioning systems. The outputs of the project provide useful guidance, methods and tools for the application of PMC in buildings, the performance assessment and control of buildings integrated with PCMs to reduce their overall energy consumptions and maximize their energy/cost saving.

This project aim is achieved by addressing the following objectives/tasks:

1). Develop and validate the simplified dynamic models of building structures integrated with PCMs;

2). Study the thermodynamic characteristics of buildings integrated with PCMs in various applications (i.e., different climate conditions, etc.) and the effects of PCMs on the building indoor environment;

3). Study the energy performance of the buildings integrated with PCMs and the impacts of PCMs on the building energy consumption;

4). Develop and validate the optimal control strategies for air-conditioned buildings and assess their energy impacts in different climate conditions and electricity pricing policies (i.e. time-base pricing and energy-plus-demand-base pricing). The optimal control strategies will be developed to determine the cost efficient control settings using a system approach to maximize the overall system operating efficiency without scarifying the indoor thermal comfort.

The above objectives/tasks will be achieved through detailed simulation tests of the building system of a full scale building integrated with PCMs and the experimental study on a building of reduced scale (i.e. an office room). As the outputs, this project will provide general guidelines for proper use of PCMs in buildings for load reduction/shifting and load leveling, and provide a systematic methodology for developing proper operation and optimal control strategies for air-conditioned buildings integrated with PCMs as TES systems.

Electrical demand varies significantly during the day and night due to the changes of weather conditions and the demand by industrial, commercial and residential activities. In hot climate, a major part of the load variation is due to the air-conditioning. This variation leads to a differential pricing system for peak and off peak periods of electrical energy use. Significant economic benefits might be achieved if some of the peak load could be shifted to the off peak period via proper technologies and advanced control algorithms, or/and the ambient air of lower temperature at night can be used to reduce the cooling load of the building at daytime. A building integrated with distributed thermal energy storage materials could shift certain amount of the load in buildings from peak to off peak time periods and provides extra potential of cooling using ambient air at night. The use of phase change materials (PCMs) as latent TES systems is one of the feasible approaches for such purpose, and therefore minimizes building operating energy/costs and reduces CO_2 emissions. Other benefits can also be achieved including improved indoor thermal comfort owing to the relatively small temperature variations.

PCMs have been considered for TES systems in buildings since 1980s. With the advent of PCMs implemented in various building wall covering materials, TES systems can be part of the building structure even for light weight buildings nowadays. In the building related fields, many efforts have been made on the development of PCMs for heating and cooling of buildings in different climate conditions, the testing and analysis of their thermal and heat transfer performances, and the modeling of PCM layers as TES systems, as well as the demonstration of their performances in various applications. These efforts have resulted in fruitful outputs and a number of commercial PCMs are readily available in market.

To successfully apply PCMs in buildings to minimize the overall operating energy/cost, the selection of the most promising PCM and proper incorporation techniques, the proper system design and optimal control are among the most important issues. In the available literature, the first three issues have been widely addressed. Although many efforts in the building control field have been made on the control and control optimization of buildings with thermal mass or ice storage systems, and on the control and optimization of air-conditioning systems and their related components, however, the detailed studies on optimal control of air-conditioned buildings with PCMs as TES systems are still inadequate. For buildings integrated with PCMs as TES systems, significant reductions in peak cooling loads and in energy consumption are possible by making use of optimal control strategies. There is also no convenient tool available for the test and evaluation thermodynamic performance of different integration of the PCMs with buildings. To optimize the design and control, a better understanding of thermodynamic characteristics of buildings with PCMs and the effects of PCMs on the building cooling load and indoor environment is essential.

1.3 Organization of the thesis

This chapter described the aim and objective of this thesis. The aim is to study on the thermodynamic characteristics and energy performance of the PCMs buildings; and develop optimal control strategies for air-conditioned buildings including PCMs as TES systems. The objective will be achieved through four subtasks as above.

Chapter 2 presents the literature review, including the applications of PCMs in buildings for free cooling and peak load shifting; the applications of PCMs in passive and air-conditioned buildings.

Chapter 3 presents a simplified model of shape-stabilized phase change materials (SSPCM) building structure and the optimal nodal placement. A GA-based estimator is developed to optimize the parameters of simplified models of building envelopes by comparing the frequency response characteristics of the simplified models with theoretical frequency response characteristics.

Chapter 4 presents the validation of optimal nodal placement of simplified models of building envelopes. Three representative constructions are used to validate performance of the optimal nodal placement. The validation shows that the simplified model with the optimal nodal placement performs better than the same order simplified models with other configurations.

Chapter 5 presents the specification of the building and air-conditioning VAV system. The simplified building model is also introduced. The test conditions and control strategies are introduced in the chapter. The test condition includes the weather profile and characteristic of the building. The control strategies include normal control, demand-limiting (DL) control and load-shifting (LS) control.

Chapter 6 presents the indoor thermal environment of air-conditioned building integrated with shape stabilized phase change materials (SSPCM). It studies the indoor temperature of zones in air-conditioned SSPCM building. The energy performance of SSPCM air-conditioned building under normal control is investigated.

Chapter 7 presents the performance of cold storage in SSPCM building when using night ventilation. Night ventilation plays an important role in free cooling for buildings in summer, it's an effective method to save energy if the phase change materials can store cold during night and release it during day.

Chapter 8 presents the optimal operation method of SSPCM buildings for peak demand reduction. Demand-limiting control strategy is effective in reducing the peak cooling loads in summer, and therefore the peak energy consumption can also be reduced without sacrificing the indoor thermal comfort.

Chapter 9 presents the optimal operation strategy of SSPCM buildings for load-shifting. The use of PCMs in buildings can help in shifting considerable amount of building loads from peak periods to off-peak periods. Therefore, significant economic benefits can be achieved for places where a time-based pricing system is adopted. The reduction of sizes of HVAC systems is also possible.

Chapter 10 presents the main conclusions and achievements of researches in this project and the optimal control strategy for reducing the overall electricity consumption and maximizing the cost saving.

CHAPTER 2 LITERATURE REVIEW

This chapter provides a comprehensive review on previous studies associated with the investigation and evaluation of dynamic characteristics and energy performance of buildings using PCMs, as well as the control methods concerning the use of building thermal masses, to present the state of the art.

2.1 Introduction

The building sector is one of major energy consumers and its contribution toward global energy consumption is about 40% [DOE, 2007, HKES, 2008]. Due to the rapid increase in the living standard together with climate changes and economic development, the growing trend of energy use in buildings might be continuously experienced in the future. Promoting energy efficiency and conservation in buildings is therefore becoming one of major issues of concern to governments and societies today.

Over the past two decades, many scientists, environmentalists and international communities have devoted considerable efforts on promoting energy efficiency and sustainability of buildings, which have resulted in a number of energy technologies and green strategies with different degrees of promise available in literature. Among them, the use of thermal energy storage (TES) systems is received increasing interest, which has been recognized as one of effective approaches to reducing energy consumption of buildings. A TES is a heat or cool storage that allows high or low temperature thermal energy to be stored temporarily for later use. Therefore, it can be used to assist in efficient use and provision of thermal energy whenever there is a mismatch between energy supply and demand, and the places where a differential pricing system for peak and off-peak periods of energy use is adopted. Higher energy storage density and reversibility are two basic requirements on the materials for TES systems. In general, there are three approaches that can provide a thermal energy function, i.e., sensible heat, latent heat and chemical energy (reversible reactions). For a particular application, which one is more appropriate mainly depends on storage periods required (i.e., diurnal or seasonal), economic viability and operating conditions [Dinçer I and Rosen MA, 2002]. Among these three approaches, the latent heat TES systems using phase changes materials (PCMs) have attracted wide concern for building applications due to their ability to provide high energy storage density and the characteristics to store thermal energy at relatively constant temperatures [Pasupathy A and Velraj R et al, 2008. Verma P and Varun et al, 2008].

The investigations on PCMs as TES systems in buildings have a long history. Already in the 1940s, Telkes [1949] investigated the use of sodium sulfate decahydrate to store solar energy and used it for space heating during night and on cloudy days. The first experimental application of PCMs for solar energy storage in buildings was carried out by Telkes [1974] in early 1970s. Since then, a considerable amount of research work has been accomplished. It is reflected by the fact that several books and technique reports, a dozen of review papers and thousands of research papers that address the use of PCMs in buildings available in literature [Dinçer I and

Rosen MA, 2002. Mehling H and Cabeza LF, 2008 et al.]. These research efforts have addressed the development of PCMs suitable for space heating, cooling and air-conditioning (HVAC) in various climate conditions, the development and investigation of effective encapsulation methods, the analysis and enhancement of PCM thermo-physical, heat transfer performance and long term stability, and mathematical modeling on PCM storage systems as well as the demonstration of thermal performance enhancement and energy saving opportunities of various building applications due to the use of PCMs. The results obtained from these studies have demonstrated that the proper use of PCMs in buildings can help reduce energy consumption and CO_2 emissions, and improve indoor thermal comfort for occupants due to the relatively small temperature variations. A reduction in size of HVAC equipment and its operational cycling frequency are also possible.

In building applications, PCMs can be integrated into building covering materials such as concrete, gypsum wallboard, plaster, etc., as part of building structures for lightweight or even heavyweight buildings to increase the thermal mass. They can also be installed in water circuits or air circuits of HVAC systems as thermal energy storage tank to provide functional purposes. The use of PCMs in buildings can provide different functions for different applications. For instance, they can be used for free cooling of buildings, building peak load shifting, solar energy utilization, waste heat recovery, etc. These functions can be achieved passively or actively. Here, the passive means that the use of PCMs in the structure of buildings and the melting and freezing of PCMs are realized without resort to mechanical equipment. The active means that the charging and discharging of energy in PCM storages are achieved with the help of mechanical equipment.

However, the successful use of PCMs in buildings depends on many factors, such as the type and quantity of PCMs used, the encapsulation method used, the location of PCMs in building structures, building design and orientation, equipment design and selection, climate condition, utility rate policy, occupancy schedule, system control and operational algorithms, etc. To properly use PCMs in buildings, a good knowledge on dynamic characteristics and energy performance of buildings using PCMs is essential, which can help building practitioners fully understand building temperature response characteristics and potential energy savings due to the use of PCMs. It could also help building designers adopt proper design options and concepts in the decision making process during the initial planning and design stages and help operators utilize advanced control and operational algorithms to maximize system operating efficiency and provide better indoor environmental quality.

2.2 Applications of PCMs in buildings for free cooling

Free cooling is a technique defined as "that amount of cooling which can be obtained from existing, additional or modified system components during low ambient conditions and used to partly or fully offset the load on mechanical refrigeration plant" [De Saulles, 1996]. In building applications, there have two free cooling approaches, i.e., the water side free cooling and air side free cooling. The water side free cooling often uses evaporative cooling towers to cool down the chilled water directly without resort to the mechanical cooling while the air side free cooling is to use fresh air and/or re-circulated indoor air to cool down a building. It is often understood to store outdoor cool during low ambient conditions in night and supply it with a time delay for space cooling during daytime. It is worthy noticing that free cooling is not really free. In some cases, water pumps and cooling tower fans are used in water side to provide the circulation force and ventilation fans and/or heat pipes or water piping (e.g., capillary tubes) are used in air side to provide enhanced heat transfer between air and PCM storages.

During the past 20 years, different designs of ventilation systems using PCMs have been proposed and their performance for free cooling of buildings has been investigated [Butala V and Stritih U, 2006, 2007. Stritih U and Butala V, 2007 et al.]. The concepts of ideal thermo-physical properties for free cooling of buildings with constant thermal physical property materials were put forward by Zhang et al. [2006]. For external walls, the best material should have large ρc_p (i.e., the product of specific heat and density) and small thermal conductivity k. For internal walls, the best material should have large ρc_p and k. The ceiling and floor free cooling principles were explained by Stritih and Butala [2006, 2008, 2007]. An experimental set-up was also established for analyzing the heat transfer within the free cooling system, in which RUBITHERM® RT 20 with a melting point of 22°C was used as the energy storage media. Air temperatures and heat fluxes as a function of time were presented for different air velocities and inlet temperatures. One-week measurement under real conditions showed that the use of this PCM can reduce the indoor temperature fluctuation and the need for additional cooling and air-conditioning, and therefore can save electricity consumption. A number of PCMs suitable for free cooling applications were summarized in Ref. [Butala V and Stritih U, 2008].

An installation that allows testing the performance of PCMs in free cooling systems was designed by Zalba et al. [2004]. The major influence parameters like ratio of energy/volume in encapsulates, load/unload rate of the storage, and cost of the installation were determined. The statistical analysis showed that the thickness of the encapsulation, the inlet temperature of air, air flow rate and the interaction thickness × temperature have significant influences on the solidification process, while the inlet air temperature has significant impacts on the melting process.

The free cooling of a low energy building using latent-heat thermal energy storage (LHTES) devices integrated into a mechanical ventilation system was investigated in Ref. [Arkar C and Vidrih B, 2007. Arkar C and Medved S, 2007]. The PCM considered was the spheres of encapsulated RT20 paraffin. The temperature response function of the LHTES was established based on a numerical model developed and then used in the TRNSYS building thermal response model to predict the outlet air temperatures of the storage under a periodic variation of the inlet ambient air temperature and defined operating conditions. Numerical simulations showed that free cooling can help reduce the size of the mechanical ventilation system and provide better thermal comfort conditions. A PCM with a melting temperature between 20°C and 22°C is the most suitable for free cooling in the case of a continental climate.

The free cooling potential of using PCMs in buildings in different climate conditions was studied by Takeda et al. [2004] and Medved and Arkar [2008]. Both studies have indicated that the potential of free cooling mainly depends on the amplitude of the ambient air temperature variations. Takeda et al. [2004] investigated the ventilation load reduction by using a ventilation system that features direct heat exchange between ventilation air and granules containing a PCM for eight cities in Japan by simulations. The results showed that both ventilation load and building cooling load can be reduced by using such a system. Medved and Arkar [2008] selected six cities in Europe to investigate the correlation between the climatic condition and the free cooling potential of using PCMs in buildings. The results showed that the optimal PCM should have a melting temperature that approximately equals to the average ambient air temperature and the free cooling potential is proportional to the average daily variation range of the ambient air temperature.

The free cooling of buildings using PCMs at temperature conditions in a typical desert region in summer was studied by Mozhevelov et al. [2006]. The numerical simulation on a real size room by PCM-based units showed that, with a proper PCM choice and system design, passive night cooling is sufficient to solidify the melted material in a melting-solidification cycle of 24 hours. It is also shown that it is possible to provide thermal comfort conditions by means of the PCM-based temperature moderation in a properly designed structure under a desert climate environment.

To help apply shape-stabilized phase change material (SSPCM) plates in buildings for free cooling in summer, a numerical analysis on thermal effects of SSPCM plates as inner linings on the indoor air temperature under night ventilation conditions was carried out by Zhou et al. [2009]. The results showed that the SSPCM plates could decrease the daily maximum temperature by up to 2°C due to the cool storage at night. The air change per hour (ACH) at night needs to be as high as possible but the ACH at daytime should be controlled properly.

Kang and Jiang [2003] proposed a night ventilation system integrated with a PCM packed bed storage (NVP) system. A mathematical model, which considers the building thermal inertia, the model of storage and the ventilation scheme, was developed to analyze the system thermal behavior, optimal design and control performance. An experimental installation was also introduced to test the thermal performance including the effects on decreasing the room temperature and energy consumption. The results showed that the NVP system can improve the thermal comfort level of indoor environment obviously. However, the energy saving due to the use of this system was not addressed.

Aiming at reducing the need for air-conditioning use and solving poor thermal conductivity of PCMs for building applications, novel ventilation cooling systems using PCMs in combination with heat pipes and fans were proposed in Refs [Turnpenny JR and Etheridge DW, 2000, 2001, Etheridge D and Murphy K, 2006].

The economic and environmental benefits of using the heat pipe/PCM system over a standard air-conditioning unit were estimated by Turnpenny and Etheridge [2000, 2001]. The results showed that this kind of system can offer substantial capital and running cost savings. If the proposed system was installed in 2000 offices instead of using air-conditioning, about 430 tones CO_2 emissions can be reduced. The processes of cooling of the PCM storage during night operation and cooling of the room air during daytime operation by using this system were tested in Ref. [Etheridge D and Murphy K, 2006]. The results showed that the proposed system can perform properly as expected.

The results obtained from the above studies have primarily demonstrated that the free cooling technique by using PCMs in buildings can provide better indoor thermal comfort, and help reduce the need of air-conditioning use and sizes of air-conditioning systems. However, this concept is only feasible in climate conditions with relatively large temperature differences between day and night in summer. It is also worthy noticing that the selection of PCMs plays significant roles in the successful use of the free cooing technique in buildings. The selected PCMs should have capability to ensure that the cooled air temperature is within the acceptable comfort levels of occupants.

2.3 Applications of PCMs in buildings for peak load shifting

Electrical demands vary significantly during the day and night due to the changes of weather conditions and the demands by industrial, commercial and residential activities. In many countries, electrical demands and time-of-use (TOU) utility rates have been designed to encourage shifting of electrical loads from peak periods to off-peak periods. Since PCMs as TES systems in buildings can store cool energy by using nighttime cheap electricity or free one from nature environment, and use it with a time delay for space cooling in summer. Therefore, they can be used for peak cooling load shifting/reduction. In the meantime, they can be used for peak heating load shifting/reduction in cold climate conditions in winter.

In literature, there are a number of studies that specifically focused on the peak load reduction/shifting of buildings by using PCMs. The use of PCM technologies in buildings for peak load shifting/reduction was addressed in Refs [Roth K and Westphalen D, 2007, Stovall TK and Tomlinson JJ, 1995, Athienitis AK and Liu C et al. 1997, Weinläder H and Beck A, 2005]. The economic feasibility of using PCM storages for peak shaving was presented in the final report of Annex 17: Advanced thermal energy storage through phase change materials and chemical reactions-feasibility studies and demonstration projects [Hauer A and Mehling H, 2005]. It is showed that the pay back cycle of the system using PCMs is strongly affected by the price of the PCM used and the price of energy charged, as shown in Figure 2.1.

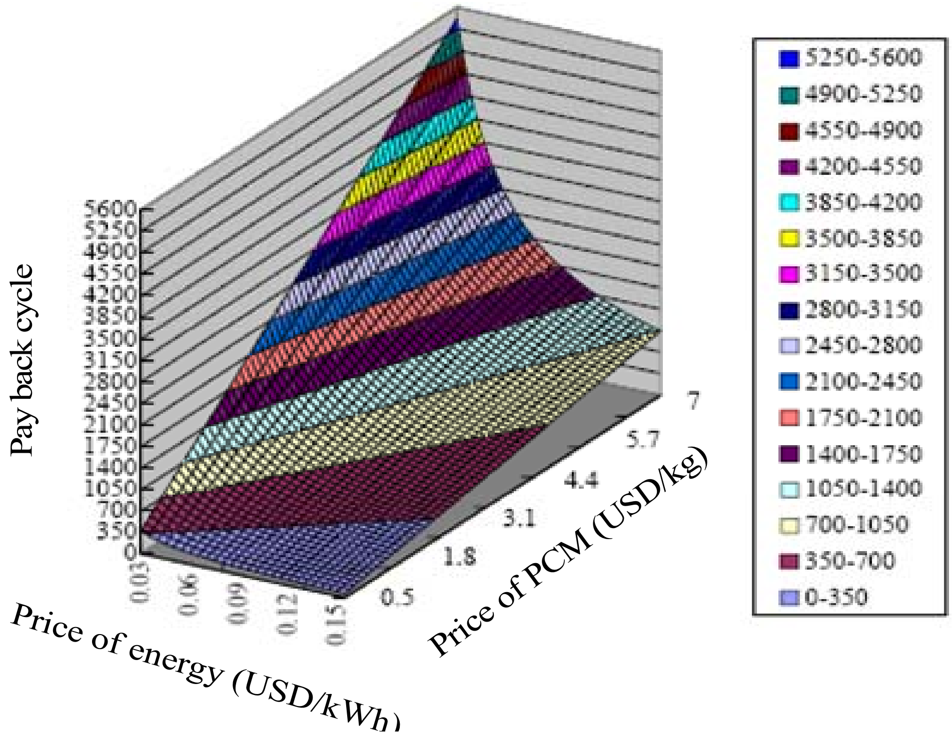

Figure 2.1 Relationships among the pay back cycle, price of energy and price of PCM

Halford and Boehm [2007] numerically studied the potential of peak cooing load shifting by using PCMs in buildings. In their study, the PCM was installed within the ceiling and wall insulation to assist in delaying the peak air-conditioning demand. The results showed that the use of PCMs can help achieve an 11–25% and 19–57% maximum reduction in peak cooling load as compared with the 'mass but no phase change' case and 'insulation only' case, respectively. The 'mass but no phase change' case meant that the system had the mass of the PCM but the PCM was not allowed to change phase while the 'insulation only' case referred to a purely resistive R-19 wall.

An air distribution system with PCMs in air ducts was proposed by Yamaha and Misaki [2006] for peak load shaving. In their study, the PCM storage was charged from 5:00 AM to 8:00 AM. As shown in Figure 2.2(1), at the charging mode, the air flowed through the closed circuit of the PCM storage tank and air conditioner simultaneously. When the charging operation finished, the ordinary air-conditioning operation was started, in which the air was assumed to bypass the PCM storage tank, as shown in Figure 2.2(2). The discharging operation was occurred from 1:00 PM to 4:00 PM. At this operation mode, the air flowed through the PCM tank to the room, as shown in Figure 2.2(3). The simulation study based on a part of one floor of an office building in Japan showed that the use of 400 kg PCM in the proposed system for a room with $73.8m^2$ surface could maintain a constant indoor temperature without using any cold source in a hot summer day. The melting temperature suitable for the system was around 19°C, which can be achieved by using MT19.

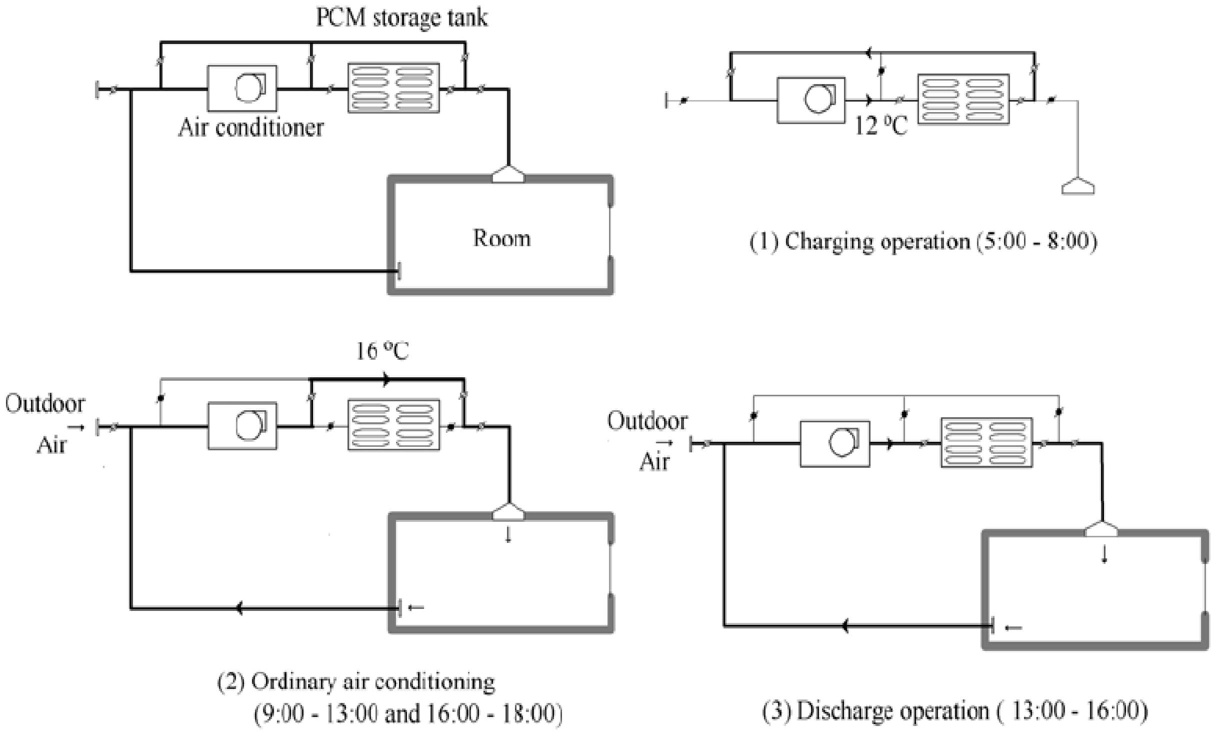

Figure 2.2 Schematics of the HVAC system proposed by Yamaha and Misaki

The effects of the peak shaving control of air-conditioning systems using the PCM ceiling board in an office building in Tokyo, Japan were examined by Kondo and

Lbamoto [2006]. In their study, the charging period was from 5:00 AM to 7:00 AM and the peak shaving period was from 1:00 PM to 3:00 PM. During the charging period, the cooled air from the AHU flows into the ceiling chamber space and cools down the PCM ceiling board, and therefore stores the cooling thermal energy. During the peak shaving period, the air from the room returns to the AHU via the ceiling chamber space. The results from numerical simulations showed that the maximum thermal load using the PCM ceiling board was reduced by 9.4% as compared to the conventional rock wool ceiling board. The overall running cost was 96.6% lower than that of the rock wool ceiling board due to the use of discounted nighttime cheap electricity.

The thermal performance of the phase change wallboard was experimentally and numerically investigated by Kissock and Hannig et al. [2008]. Two test cells (1.22m×1.22m×0.61m) using common light-frame construction practices were constructed for experimental study. The conventional wallboard was installed in one of the test cells, and the wallboard imbibed to 29% by weight with K18 was installed in the other test cell. A finite-difference simulation model was modified and validated by using experimental data to predict interior wall temperatures in the test cells. The results indicated that peak temperatures in the PCM test cell were up to 10°C less than that using the conventional wallboard during sunny days. The modified model has satisfactory prediction performance. This validated model was further used in Ref. [Kissock JK and Limas S, 2006] to investigate the diurnal load reduction through phase change building components. The simulation studies based on typical meteorological weather data in Dayton, Ohio showed that the addition of 10% K18 to the concrete in concrete sandwich walls can reduce peak and annual cooling loads through the wall by 19% and 13%, respectively. The addition of the PCM to low-mass steel roofs can reduce the peak and annual cooling loads through the roof by 30% and 14%, respectively. The addition of the PCM to gypsum wallboard in frame walls can reduce the peak and annual cooling loads through the wall by 16% and 9%, respectively.

A thermally enhanced frame wall that reduces peak air-conditioning demand in residential buildings was presented by Zhang and Medina [2005]. Two identical test houses (1.83m×1.83m×1.22m) of conventional residential construction were used for experimental study. One house was used as a control house and the other as a retrofit house with the PCM frame wall. The results from the field tests showed that the retrofit house using the PCM frame wall with a 10% PCM concentration can reduce the wall peak heat flux and space cooling load about 15% and 8.6% respectively, as compared to the control house. It is also shown that the west and north walls achieved more heat rate reductions than the south wall and the load shifting was spread over many hours from about midnight until about 1:00 PM.

A PCM structural insulated panel (PCMSIP) was proposed by Medina and King et al. [2008], in which the SIP technology was utilized as a structural vehicle for thermal insulation, and the PCM was used to provide distributed thermal mass. The experimental results during the summer period indicated that a PCMSIP with 10%

and 20% PCM concentrations can reduce the peak heat flux by an average of 37% and 62%, respectively. The average reductions in daily heat transfer across the PCMSIPs were 33% and 38% for concentrations of 10% and 20% PCM. It is also shown that the greater the temperature difference between day and night, the better the PCM works to reduce the heat flux.

The application of PCM wallboards in buildings for peak load reductions was studied by Lv and Feng [2007]. A test was conducted in a 5.0m×3.3m×2.8m experimental room with a 1.5m×1.5m window in the south wall and a 1.0m×2.0m wooden door in the north wall. The results showed that the PCM wallboard room could greatly reduce the operating cost of HVAC systems and transfer electric power peak load to valley. When indoor temperature exceeds 18.49°C in summer, the PCM in wallboards will melt and absorb 39.12kJ/kg energy before completely melting at 24.26°C, which can maintain indoor temperature in the comfortable range and decrease the cooling load of the air-conditioning system.

A new floor air-conditioning system using granular PCM was studied in Ref. [Hauer A and Mehling H et al. 2005, Nagano K and Takeda S, 2006]. Figure 2.3 is a concept diagram of the system proposed. In this system, latent heat was stored in the PCM that was embedded directly below OA floor boards in the form of granules. The PCM packed bed was permeable to air suitable for use in floor supply air-conditioning systems. During night, the circulation of cold air through the under floor space allows cold energy to be charged to the concrete slab, OA floor board and

PCM packed bed. During daytime, the stored energy in turn can be used to remove the cooling load in the room. The charging/discharging experiments to simulate an office air-conditioning system over 24 hours periods showed that about 89% daily cooling load could be stored during night for the system that used a 30mm thick packed bed of the granular PCM.

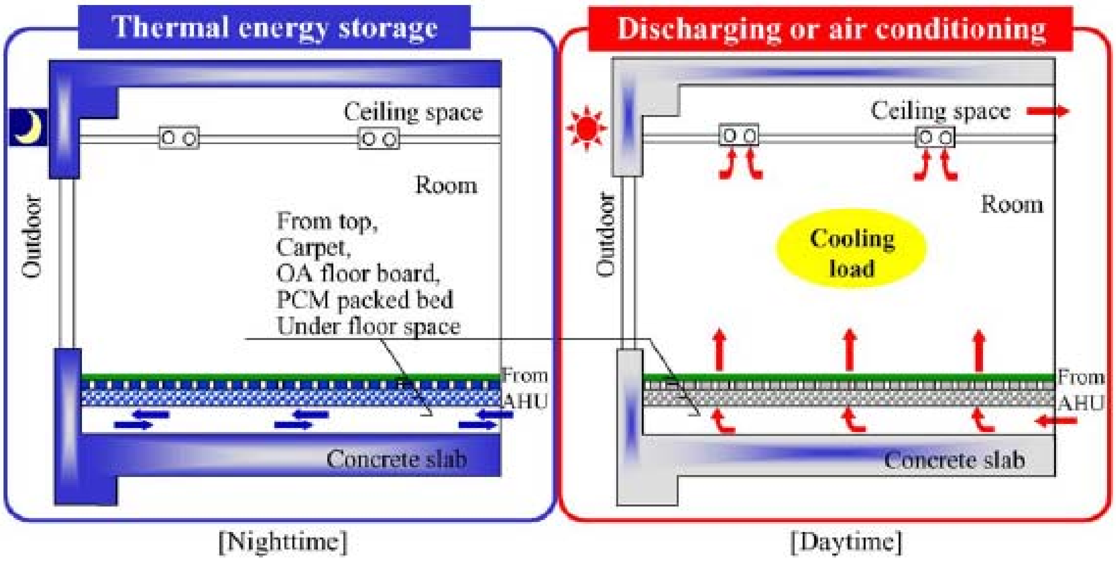

Figure 2.3 A concept of the floor supply air-conditioning system

To estimate the load reduction potential of phase change wallboards in office buildings, a numerical study using RADCOOL was conducted by Stetiu and Feustel [1998]. The results showed that the use of PCM wallboards coupled with mechanical night ventilation in office buildings can offer the opportunity for system downsizing in climates where the outside air temperature drops below 18°C at night. About 28% peak cooling load reduction can be achieved for a prototype IEA building located in California climate condition. However, for climates where the outside air temperature remains above 18°C at night, the use of PCM wallboard coupled with mechanical night ventilation only cannot lead to energy or peak power saving opportunities.

The above studies have demonstrated that the use of PCMs in buildings can help shift considerable amount of building loads from peak periods to off-peak periods. Therefore, significant economic benefits can be achieved for places where a differential pricing system is adopted. A reduction of sizes of HVAC systems is also possible. However, most of these studies were carried out based on numerical simulations or prototype experiments. The detail energy savings of using PCMs for peak load shifting within a long period were not provided in most of these studies.

2.4 Applications of PCM in air-conditioned buildings

In building applications, PCM storages can be integrated into other systems, such as solar heat pump systems, heat recovery systems, floor heating systems, etc., as active applications to provide functional purposes and enhance the heat transfer performance of PCM storages. In this section, the studies associated with the applications of PCMs in air-conditioned building systems are summarized.

The performance of the combined solar heat pump system with the PCM (i.e., $CaCL_2 \cdot 6H_2O$) storage for space heating was experimentally and theoretically investigated in several studies [Kaygusuz K, 1995, 1999, 2003. Esen M, 2000]. Figure 2.4 is the schematic overview of the experimental heating system used in these studies. The effects of various system parameters on the response of indoor air temperature of the building, the temperature variation of the PCM in the energy storage tank and the temperatures of the heat transfer fluid (water) in the solar collectors and energy storage tank for series, parallel and dual source heat pump systems were investigated in Refs [Kaygusuz K, 1995, 1999, 2003]. The results showed that the dual source system saved a net energy of 12056kWh while the parallel system saved 10120kWh and the series system saved 9390kWh net energy per heating season for the case studied as compared with a conventional system. It is also showed that the PCM storage is an important component for solar-assisted heat pump systems in moderate climate conditions, and $CaCL_2 \cdot 6H_2O$ is preferable as a storage material in such climate conditions technically but economic feasibility should be considered. It is worthy noticing that a switch over temperature was used to control the series solar heat pump systems to be changed from using direct solar heating to using the heat pump, or vice versa. To describe the diurnal transient behavior of the PCM storage in the charging and discharging processes, a theoretical model was developed by Esen M [2000]. A comparison between mathematical results of the model with experimental data showed reasonable agreement. It is also showed that the PCM cylinders with smaller radii will melt at a shorter time and can store much more heat energy than that with thicker radii.

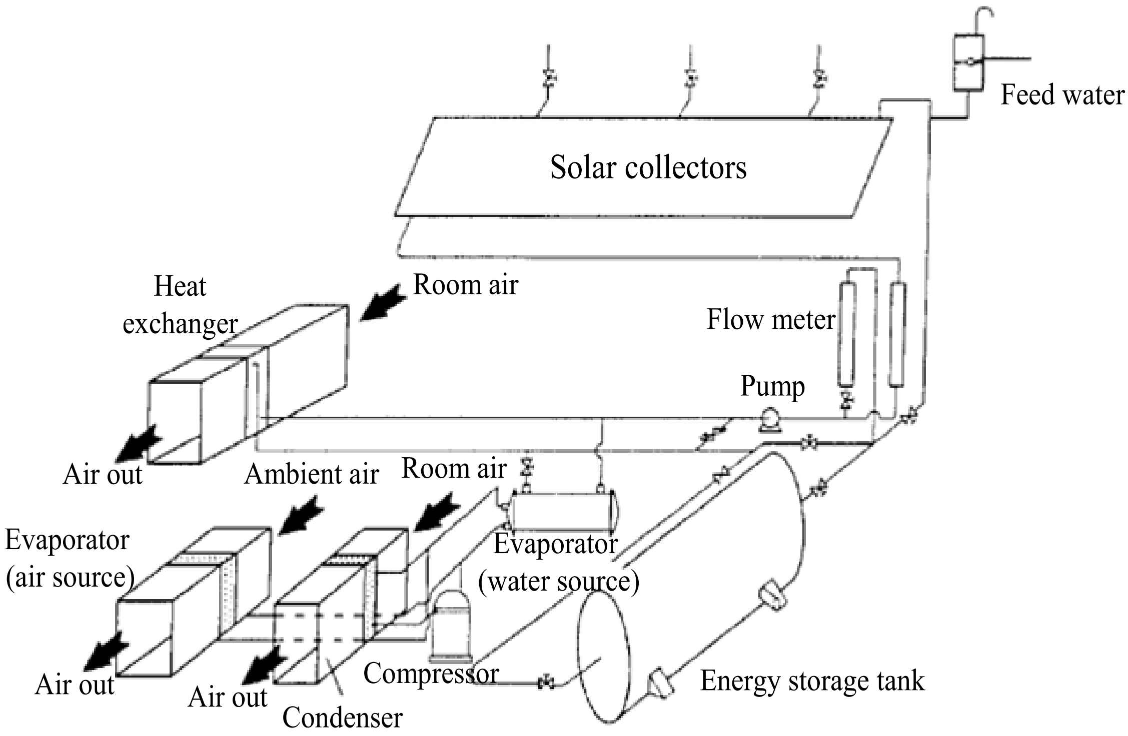

Figure 2.4 Schematic overview of the heating system

A hybrid PCM storage system for managing solar and electric energy was proposed by Hammou and Lacroix [2006]. Solar energy was stored during sunny days and released later at night or during cloudy days while electric energy was stored during off-peak periods and used during peak periods. A heat transfer model of the hybrid PCM storage was developed and used to examine the effect of various storage materials and operating conditions on the thermal behavior of the storage. The simulation results based on a test room in the city of Montréal, Canada showed that the electricity consumption for space heating can be reduced by 32% and more than 90% of electricity was consumed during off-peak hours.

The feasibility of using an integrated flat plate solar collector and a PCM storage tank to provide energy for residential units was investigated by Hassan and Beliveau

[2008]. The system was operated by controlling the fluid circulation pump and fluid path. The fluid path was altered based on changes in system and service temperatures or changes in the level of solar radiation and ambient temperature. Figure 2.5 illustrates the alternative energy supply paths. The simulation results based on a selected building in Blacksburg showed that the proposed system could supply 88% of the space heating and hot water requirements throughout the year saving the homeowner about 61.5% of the annual heating bill and reducing the need for non-renewable energy. However, the authors pointed out that the use of the PCM storage system was not economical for the considered conditions.

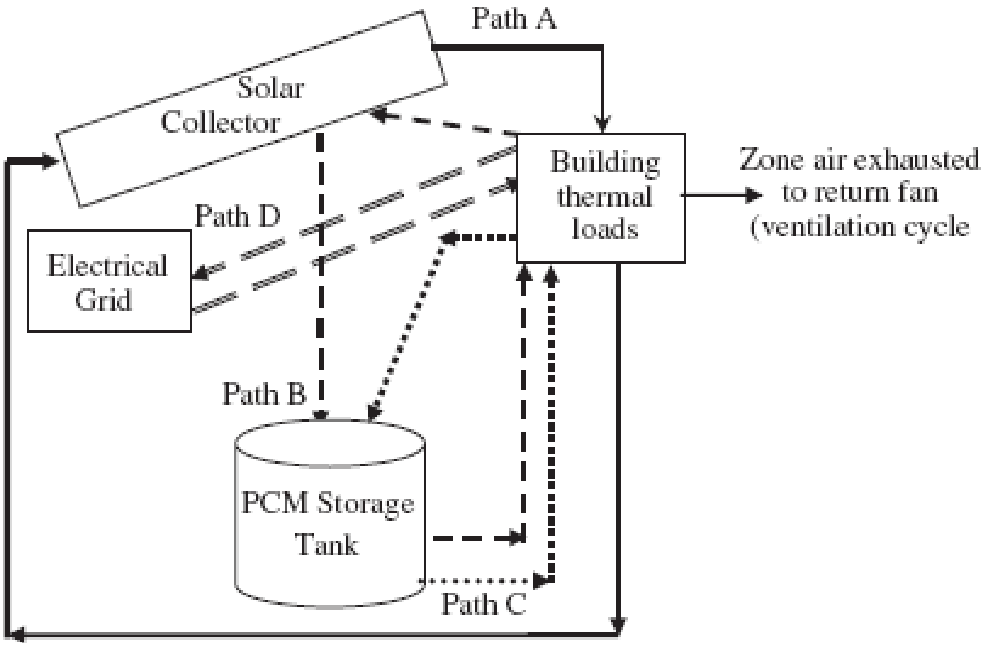

Figure 2.5 Alternative energy supply paths

A solar-driven absorption cooling system using PCM storage was designed in Ref. [Schweigler C and Hiebler S et al. 2007]. During the heating operation, the PCM storage balances the heat generated by the solar system and other heat sources to supply adequate heat for buildings. In the cooling mode, the PCM storage serves as a reject heat sink for the absorption chillers in addition to a dry cooling system. An analysis of the thermal design of different system components showed that the introduction of the PCM storage can reduce the oversize of the solar collector system arising from the application of dry air cooling as compared with a standard system design with wet cooling towers. It is also showed that the PCM storage has a positive effect on solar gain by allowing for a low operating temperature of the solar collectors.

The under-floor electrical heating system with the SSPCM storage was experimentally and numerically studied in Refs [Lin KP and Zhang YP et al. 2005, 2007. Zhang YP and Lin KP, 2006]. The proposed system can charge heat by using nighttime cheap electricity and discharge it during daytime when necessary. An experimental study was carried out on an experimental house while the numerical study was conducted using an enthalpy model. The results showed that the indoor temperature can be increased greatly. The temperature of the PCM plate can be kept at the phase transition temperature for a long period after heaters stopped working. It is worthwhile to notice that the conventional control strategies were used in these studies. A hybrid heating system combined with the thermal storage using SSPCM plates was investigated in Ref. [Zhou GB and Zhang YP et al. 2007] numerically. The results indicated that the thermal storage effect of the SSPCM plates can improve the indoor thermal comfort level and save about 47% of normal and peak hour energy use and 12% of total energy consumption in winter in Beijing.

The potential of using the PCM storage in under-floor electrical heating systems was also investigated in Refs [Farid MM and Chen XD, 1999, Farid MM and Kong WJ, 2001]. The simulation results from Ref. [Farid MM and Chen XD] indicated that a 30mm PCM layer located between the heater and the floor tiles with a melting point close to 40°C is sufficient to provide uniform heating throughout the day when the heater was applied only 8 hours during the night, which allows a shift of 7.2MJ/m^2 day of electricity from peak periods to off-peak periods. Two concrete slabs with dimensions of 0.5m×0.5m×0.095m were constructed in Ref. [Farid MM and Kong WJ, 2001] to simulate the under-floor heating systems with and without the PCM storage. The results showed that the system with $CaCl_2 \cdot 6H_2O$ as thermal energy storage can provide uniform heating throughout the day and can keep the floor surface near the desired temperature of 24°C if the system is designed properly.

A roof integrated solar heating system using a PCM storage was experimentally and numerically investigated in Ref. [Saman W and Bruno F, 2005]. Figure 2.6 is the schematic of the system proposed, which utilizes the existing roof as a solar collector/absorber and incorporates PCM storage to store heat during the day and release it to heat the living space during night or when there is no sunshine. This system was installed in a house in Adelaide, Australia. The results showed that the effect of sensible heat was perceived in the initial periods of melting and freezing processes. A higher inlet air temperature and air flow rate can increase heat transfer rates and shortens the melting time, but a higher air flow rate increased outlet air temperatures. For freezing, a lower inlet air temperature and a higher air flow rate can increase heat transfer rates and shortens the freezing time, but a higher air flow rate reduced outlet air temperatures.

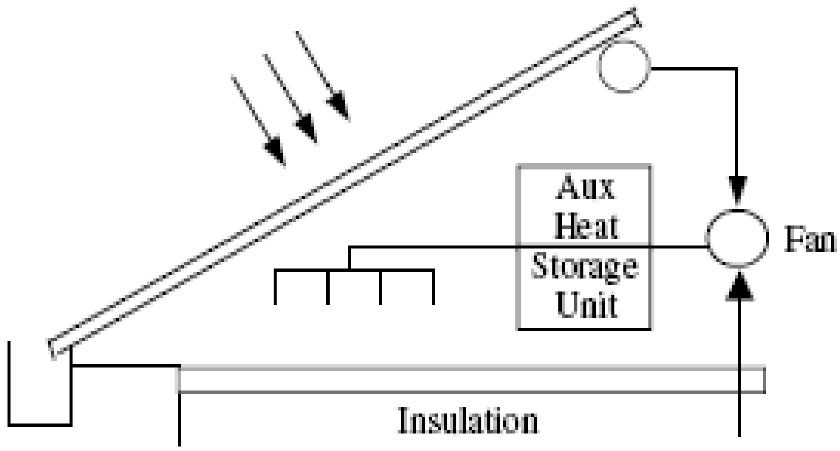

Figure 2.6 Schematic of the roof integrated solar heating system

A thermally activated ceiling panel with the PCM storage, as shown in Figure 2.7, was proposed in Ref. [Koschenz M and Lehmann B, 2004] for applying in lightweight and retrofitted buildings. The PCM in the ceiling panels melts during daytime upon exposure to the thermal loads and freezes during night by means of an integrated water pipe system. The simulation study using TRNSYS and laboratory tests demonstrated that a 5.0cm layer of microencapsulated phase change material (MPCM) (25% by weight) and gypsum is sufficient to maintain a comfortable room temperature in standard office buildings.

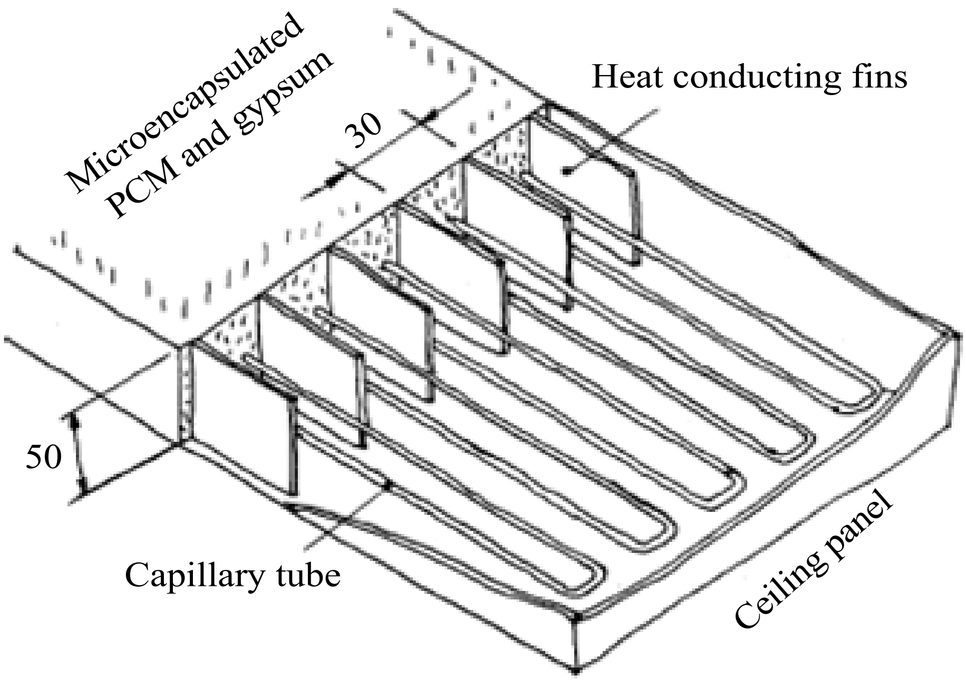

Figure 2.7 Schematic of the thermally activated ceiling panel with PCM

Ismail and Henríquez [2001] proposed a concept of a window with moving PCM curtains. The window was double sheeted with a gap between the sheets and an air vent at the top corner. The sides and the bottom were sealed with the exception of two holes at the bottom, which were connected by plastic tubes to a pump and a PCM tank. When the temperature difference reaches a pre-determined set-point, the pump will start to work and the liquid PCM will be pumped out of the tank to fill the gap between the glass panes. The experimental and simulation results showed that the proposed concept of the PCM filled window system is thermally effective, and the green colored PCM is more effective in reducing radiated energy gains.

The thermal performance of a building roof incorporating an inorganic eutectic PCM for thermal management of a residential building in India was studied by Pasupathy et al. [2008]. To solve the PCM that does not change to the solid state during night hours in hot summer months, a water tank with a capacity of 200L was used to provide the circulating water through the PCM panel to remove the heat from the PCM slab and the ceiling. The experimental study with one single layer of the PCM showed that the quantity of water required was very large (about 830 kg/m^2 for the case studied), which is not easily available during the summer months.

A low energy air-conditioning system that combines the cooled ceiling, microencapsulated phase change material (MPCM) slurry storage and evaporative cooling technologies was proposed by Wang et al. [2008]. The major feature of the system was that the thermal energy storage using the MPCM slurry enables the evaporative cooling to be stored in the MPCM slurry at 24 hours operation mode whenever the wet-bulb temperature reaches the predetermined set-point. The simulation results indicated that this new system can offer energy saving potential up to 80% under northwestern China and up to 10% under southeastern China.

Gu and Liu et al. [2004] proposed a heat recovery system using PCMs to recover the rejected heat from air-conditioning systems to produce domestic hot water for washing and bathing. The proposed thermal energy recovery system consisted of a conventional air-conditioning system, two heat recovery accumulators and an auxiliary electric water heater. The thermodynamic calculation showed that the integrative energy efficiency ratio of the system can be improved effectively when all rejected sensible and latent heat from air-conditioning systems can be recovered.

A phase change energy storage system consisting of sections of different materials with different melting temperatures was proposed by Vakilaltojjar and Saman et al. [2001] for air-conditioning applications, in which the PCMs were placed in thin flat containers and air was passed through gaps between them. The simulation study showed that the air velocity profile at the entrance does not affect the heat transfer characteristics and the outlet air temperature considerably. A better performance can be obtained by using smaller air gaps and thinner PCM slabs.

Different active systems presented in above studies have showed that they are thermally effective and technically feasible. However, the economic benefits and pay back periods due to the use of these active systems should be analyzed carefully before they are implemented in practice.

2.5 Applications of PCM in buildings without air-conditioning

In most passive applications, PCMs were integrated into building envelopes (i.e., walls, roofs, and floors) as part of building structures to increase the building thermal mass. During daytime, the PCM undergoes a melting process by absorbing part of solar heat flowing through the building structure. During night, the PCM solidifies and releases the stored heat into surrounding environments when outdoor or indoor temperature falls. Therefore, they can prevent the indoor environment from overheating during daytime in hot summer and provide heat for space heating during night in cold winter. Since there is a considerable amount of studies associated with dynamic characteristics and energy performance of buildings using PCMs in passive manners, the related studies are reviewed in the following by three categorizes according to different research methods used, i.e., simulation, experiment, combined simulation and experiment.

2.5.1 Studies based on simulations

The dynamic characteristics and/or energy performance of buildings using PCM walls were numerically investigated in a number of studies [Feustel HE and Stetiu C, 1997. Neeper DA, 2000, Peippo K and Kauranen P et al. 1991]. The optimization of a multi-component PCM wall for direct gain passive solar houses was studied by Peippo and Kauranen et al. [1991] using a building energy simulation code FHOUSE. The results showed that the annual auxiliary heating energy of a 120m^2 house in Helsinki, Finland and Madison, Wisconsin can be reduced by 2GJ (6%) and 3GJ (15%) respectively, when the proposed PCM wall is used. It is also showed that the optimal diurnal heat storage can be achieved when the PCM has a phase change temperature of 1~3°C above the average room temperature.

Thermal dynamics of PCM wallboards were studied in Ref. [Neeper DA, 2000] through simulations. Three parameters, i.e., the melting temperature of the PCM, temperature range over which melting occurs, and latent capacity per unit area, that affect the energy to be passively stored and released during a diurnal cycle, were examined. The results showed that the maximum diurnal energy storage occurred when the PCM melting temperature was close to the average room temperature with a narrow transition range. The optimal melting temperature depended on the average room temperature. The optimization of a PCM wallboard for building applications was studied by Kuznik and Virgone et al. [2008]. The simulation study using an in-house numerical code CODYMUR showed that an optimal PCM thickness existed for a given application and indoor room temperature fluctuations can be reduced by using PCM wallboard.

The thermal performance of the PCM wallboard for residential cooling applications was studied by Feustel and Stetiu [1997] using a thermal building simulation program RADCOOL. The simulation for a living room with PCM-treated wallboards (0.015m) containing 20% paraffin in all walls and ceiling showed that the room air temperature can be reduced significantly when heat can be stored in PCM-treated wallboards. The use of double PCM wallboards can keep the room temperatures close to the upper comfort limits without using any mechanical cooling.

A verified TRNSYS code was used by Stovall and Tomlinson [1995] to analyze the potential benefits of using a PCM wallboard for passive solar applications with thermostat control. The results showed that the PCM wallboard did not improve the occupant comfort level with the traditional thermostat control but can provide significant load management relief. The installation of the PCM wallboard for a house ($221m^2$) in Boston can result in about 190 USD annual cost savings with a 3~5 year payback period. Onishi and Soeda et al. [2001] investigated the effects of the PCM storage wall (Trombe wall) on the performance of a hybrid heating system using a CFD code 'SCIENCE'. Simulation results showed that the system with PCM storages could consume less energy than those without using PCM storages on fine days.

However, the energy consumption is almost the same in both systems on cloudy days. The reason is that the PCM did not work effectively on cloudy days.

The energy saving potential and temperature regulation effects resulting from the use of PCMs in a building cavity wall was numerically investigated by Huang et al. [2004]. Five cases in which walls (i.e., cavity, exterior surface, and interior surface) were augmented with various quantities of granulate PCMs GR41 and GR27 were studied. The results showed that a cavity wall augmented with a 20mm of GR27 PCM and a 20mm air space cavity can help maintain the temperature of the interior wall surface satisfying thermal comfort requirements and preventing the formation of condensation in the cavity of the wall during the simulated time period. De Grassi et al. [2006] evaluated the thermal behavior of dry assembled PCM containing walls. A statistic approach based on the time series analysis method was used to represent a valid instrument to evaluate the effects of the thermal inertia increase on the heat transmission process that occurs between the elements of a building. The simulation results showed that the indoor thermal comfort can be improved due to the insertion of PCM inside dry assembled walls.

To prevent building overheating in Mediterranean climatic conditions, the thermal behavior of glazed ventilated facades of buildings using PCMs was investigated in Refs [Faggembauu D and Costa M et al. 2003]. The glazed ventilated facades were made up of two layers of different materials, opaque or transparent, that were separated by an air channel used to collect or evacuate the solar radiation absorbed by the facade. The simulation results showed that the use of the PCM in the opaque zone can result in a reduction of heat gains and heat losses, although the net values remained nearly constant. However, depending on the proportion of the facade with the PCM, the effect was relatively small since the main gains were direct gains through the transparent area.

The numerical modeling and thermal simulation of PCM-gypsum composites using ESP-r were presented in Refs. [Heim D and Clarke JA, 2004. Heim D, 2006]. The behavior of the PCM was modeled using the concept of special materials within ESP-r. The effect of the phase transition was added to the energy balance equation as a latent heat generation term according to an effective heat capacity method. The numerical analysis showed that the use of PCM composites in buildings is thermally effective. Solar energy stored in the PCM-gypsum panels can reduce the heating energy demand by up to 90% during the heating season studied. The behavior of a transparent insulation material (TIM)-PCM wall and its influence on the internal wall temperature were studied in Ref. [Heim D, 2004] using ESP-r. The results showed that the efficiency of thermal interface material-phase change material (TIM-PCM) wall systems was similar to a transparently isolated ordinary ceramic wall for the case studied. However, the use of the PCM highly improved thermal conditions on internal surfaces.

Thermal analysis of a building brick containing PCMs was studied in Ref. [Alawadhi EM, 2008]. The objective of the brick-PCM system was to reduce the heat flow from outdoor space by absorbing the heat gain in the brick before it reaches the indoor space during daytime. A paramedic study was conducted to assess the effects of different design parameters, including the quantity and type of PCMs used, and the location of PCMs in the brick. The results indicated that the heat flux at the indoor space can be reduced by 17.55% when three PCM cylinders were introduced and located at the centerline of the bricks. The increase of the quantity of PCMs has a positive effect to reduce the heat gain through bricks.

To identify the promising PCMs suitable for solar space heating, a numerical study was carried out by Khalifa and Abbas [2008]. A numerical model was developed to verify the suitability of three selected materials as thermal storage mediums under actual weather conditions of Iraq. The room temperature fluctuation in the zone was evaluated for each material using different thickness. The results showed that that an 8cm thick storage wall made from the hydrated salt was capable of maintaining the comfort temperature in the zone with the least room temperature fluctuation.

The thermal performance of passive solar buildings using the SSPCM was numerically studied in Refs [Xu X and Zhang YP et al.2005. Zhou GB and Zhang YP et al.2007] using an enthalpy model. Figure 2.8 presents the schematics of the SSPCM floor system studied [Zhou GB and Zhang YP et al. 2008]. In these studies, the effects of the thermo-physical properties of the SSPCM, inner surface convective heat transfer coefficient, location and thickness of the SSPCM plate and wall structure (external thermal insulation and wallboard material) on the room air temperature were investigated. The results showed that the thermal storage effect of the SSPCM plates can help reduce indoor temperature swings. The effect of PCM plates located at the inner surface of interior walls is superior to that of exterior south walls. In order to analyze and evaluate energy efficient effects of the PCM wallboard and floor, two parameters, namely modifying factor of the inner surface heat flux ‘α’ and ratio of the thermal storage ‘b’, were put forward in Ref. [Zhang YP and Lin KP et al. 2008]. The analysis and simulation results showed that the PCM external wall can save more energy by increasing heat of fusion, decreasing thermal conductivity and selecting proper melting temperature (α<1). The PCM internal wall can save more energy by increasing heat of fusion and selecting appropriate melting temperature and thermal conductivity. The most energy efficient approach to apply PCMs in solar houses is in internal walls.

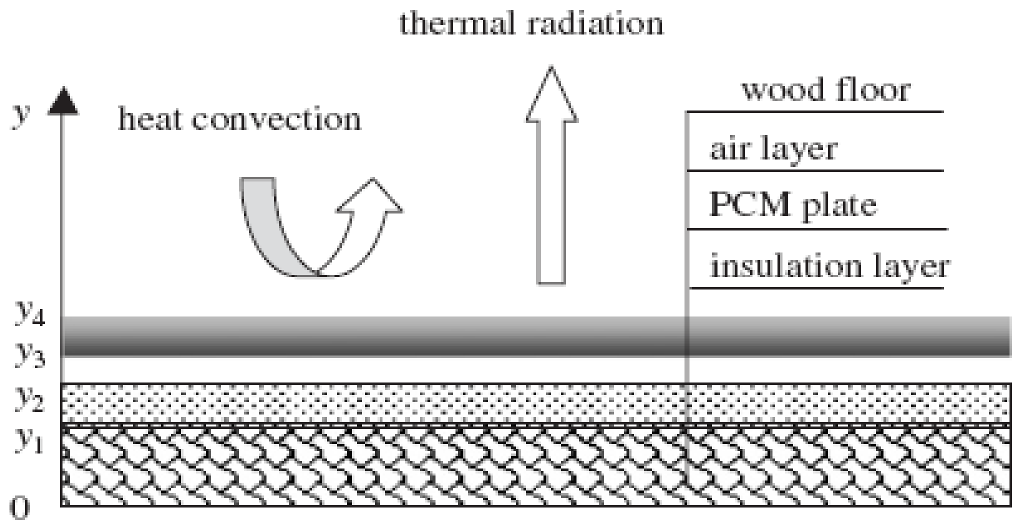

Figure 2.8 Schematic of the heat transfer in the floor

2.5.2 Studies based on experiments

There are also a number of studies that use the experimental approach to investigate the building performance through the passive use of PCMs. The dynamic characteristics and/or energy performance of test rooms using PCM walls have been experimentally evaluated by comparing with that of using ordinary walls in several studies [Lv SL and Zhu N et al. 2006. Kuznik F and Virgone J et al. 2008 et al.]. The results from these studies have showed that the fluctuations of indoor temperature of rooms using PCM walls were lower than that using the ordinary walls. The experimental results from Ref. [Lv SL and Zhu N et al. 2006] under the climatic conditions in winter in the northeast of China showed that the maximum of indoor temperature fluctuation of the ordinary wall room was 3.74°C while the maximum value in the phase change wall room was 2.59°C. The experimental results in a summer repetitive day by Kuznik et al. [2008] showed that the indoor temperature for the case without the PCM fluctuated from 36.6°C to 18.9°C while for the PCM case it varied from 32.8°C to 19.8°C, which proved that the PCM walls can decrease temperature fluctuations by 4.7°C. The results obtained by Schossig et al. [2005] showed that, during the summer season, the temperature in the PCM test room can be reduced by up to 4K. In the reference room, the temperature was higher than 28°C for more than 50 hours, while the PCM test room was higher than 28°C for only about 5 hours. The experimental results from Scalat et al. [1996] showed that thermal effects of PCM wallboards can help maintain the room temperature within the human comfort zone for protracted periods of time after the heating or cooling system was shut off. The results by Lai and Chiang [2006] showed that the PCM-treated brick had a better daytime thermal insulation effect than the ordinary hollow brick, and the PCM-treated brick can provide more effective indoor heat preservation at night when temperatures fall below outdoor temperatures. The results from Ref. [Lee T and Hawes DW et al. 2000] showed that the use of PCMs in blocks can increase their heat storage capacity greatly, which can therefore render the feasibility to use low cost heat, such as solar energy and waste heat whose supply may be asynchronous with the demand.

Based on the discussion and experimental study on the thermal properties of new materials for solar thermal storages, Nikolić et al. [2003] presented that the impregnation of PCMs into passive solar walls is particularly suitable for the areas with fluctuating climates to act as temperature regulators and minimize overheating in buildings.

The thermal performance of the SSPCM floor in passive solar buildings was studied by Zhang et al. [2006]. The experiment was conducted on an outdoor cabin, in which the floor was composed of a 50mm thick polystyrene insulation layer and 8mm thick SSPCM plates. The results showed that the mean indoor temperature of a room with the PCM floor was about 2°C higher than that of the room without a PCM floor, and the indoor temperature swing was obviously minimized.

2.5.3 Studies based on experiments and simulations

In literature, there are also a number of studies that use combined experiment and simulation approaches to investigate the performance of buildings using PCMs passively. The dynamic characteristics and/or energy performance of buildings using PCM walls were also numerically and experimentally investigated in a number of studies [Ahmad M and Bontemps A et al. 2006 et al.]. Ahmad et al. compared the performance of three types of wallboards, including a polycarbonate panel filled with paraffin granulates, a polycarbonate panel filled with polyethylene glycol PEG 600, and a polyvinyl chloride (PVC) panel filled with PEG 600 and coupled to a vacuum insulation panel (VIP). The results showed that the PVC panel filled with PEG 600 can provide much better thermal performance in lightweight buildings. With this result, Ahmad et al. [2006] tested the performance of a prototype test-cell with the PVC panel with PEG 600 and coupled to a VIP by comparing with that of a test-cell with ordinary wallboards. The results showed that the test-cell using the PCM wallboard can reduce the indoor temperature amplitude of around 20°C on a daily cycle in summer.

A TIM-PCM external wall system for solar heating and day-lighting was experimentally and theoretically investigated by Manz et al. [1997]. The PCM was filled into a glass container. A part of the incident solar radiation was used for day-lighting and the rest was used for space heating. The results showed that the use of PCMs in walls has a positive effect on building performance. A higher utilization of solar gains could be expected because more evenly distributed energy flows into the building.

To investigate the thermal performance and benefits due to the use of PCM gypsum boards in passive solar buildings, an experimental and simulation study on a direct gain outdoor test room was carried out by Athienitis et al. [1997]. The results showed that the application of the PCM gypsum board in passive solar buildings can reduce overheating and provide great potential for reducing energy consumption and peak loads. Compared with the ordinary board, the use of PCM gypsum board can increase about 10MJ heat transfer from the wall to the room, which equals to about 15% of the total heating load.

The effects of the PCM wallboard on heating energy consumption and energy conservation rate were studied in Ref. [Chen C and Guo HF et al. 2008]. Based on experimental investigations of heat storing/releasing properties of materials and numerical analysis of the performance of the PCM room, it is showed that the application of proper PCMs to the inner surface of the north wall can enhance the indoor thermal comfort and increase the utilization rate of solar radiation. The energy saving rate of heating season (η) increased with the increase of the phase change enthalpy and thickness. The saving rate η can reach up to 10% during a whole winter when the optimal thickness is set at 30mm and the phase change enthalpy of the PCM is 60kJ/kg.

Darkwa and his colleagues have devoted considerable efforts on the evaluation of the thermal performance of two integrated gypsum-based PCM systems (i.e., randomly mixed and laminated PCM wallboards) in building applications through simulation and experiments [Kim JS and Darkwa K, 2003. Darkwa K and Kim JS et al. 2005. Darkwa K and O'Callaghan PW, 2006]. The results showed that the laminated PCM wallboard can perform thermally better than the randomly PCM wallboard. The laminated PCM wallboard with a narrow phase change zone is more effective in moderating the nighttime temperature in passive solar buildings, which could increase the minimum room temperature at night by about 17% more than the randomly mixed type. In addition, the authors pointed out that heat transfer enhancement materials are essential for the successful use of PCM drywall systems in buildings.

To test the suitability of using PCMs to solve overheating of sandwich panels for prefabricated walls of lightweight buildings, the thermal behavior of four prototypes of sandwich panels containing eutectic salts with different insulation thickness, and/or different PCM thickness, and/or with and without air layers were studied by Carbonari et al. [2006]. The results showed that the use of the PCM in sandwich panels can help remain a relatively constant indoor temperature. The introduction of an air layer between the PCM and the external metal finishing layer can help improve the performance of sandwich panels using PCMs.

A PCM-facade panel for day-lighting and room heating was studied by Weinläder et al. [2005]. An experimental set-up in the outdoor test facility was established and the experimental data were used to validate a model developed for the PCM-facade panel. The thermal performance of the PCM-facade panel was then simulated using the model validated. Compared to a double glazing without the PCM, the PCM-facade panel can reduce the heat losses in south oriented façade by about 30% and solar heat gains by 50% in winter. The thermal comfort was improved while the PCM-façade panel can help increase the mean surface temperature by 2-3K. In summer, about 25% less energy gains can be achieved by using the PCM-façade panels as compared to the double glazing without sun protection. Since the PCM-façade panel can transmit enough light, it can be used as day-lighting elements.

Ibáñez et al. [2005] presented a methodology to evaluate thermal effects of the inclusion of PCMs in the elements of buildings using a building simulation program TRNSYS. This method was developed based on the multi-zone building component model (Type 56) of TRNSYS 15. The useful results for determining the PCMs in walls/ceiling/floor, storage capacities of panels with PCMs and optimal phase change temperatures of PCMs were summarized based on the simulation studies. With the help of this methodology, two real size concrete cubicles were designed to experimentally study the performance of concrete walls using PCMs under the weather condition of Puigverd. The results indicated that the use of PCMs in concrete walls can result in an improved thermal inertia and lower inner temperatures as compared with the conventional concrete.

The use of a PCM in walls and roofs as a thermal barrier was numerically and experimentally studied by Ismail and Castro [1997]. The results showed that the PCM wall was effective in maintaining the indoor temperature close to the established comfort limits. A case study for an existing building in Campinas, SP, Brazil indicated that at least 19% energy in case of window units and 31% energy in case of central air-conditioning units can be saved by using the PCM in roofs and walls as compared with the conventional construction without using PCMs.

Based on the results obtained in Ref. [Pasupathy A and Athanasius L et al. 2008], a passive system with a double layer PCM concept was introduced by Pasupathy and Velraj [2008]. The results from simulation and experimental studies showed that a double layer PCM incorporated in the roof can narrow the indoor air temperature swing and can satisfy all weather conditions of Chennai City, India.

The above research efforts have demonstrated that the passive use of PCMs in buildings can also help enhance indoor thermal comfort and reduce global energy consumption. The proper system designs play significant roles in the successful use of PCMs in buildings to maximize the overall performance.

2.6 Control strategies for the effective use of building thermal mass

The actual effect of the use of PCM in air-conditioned buildings increases the building thermal mass. The proper or optimal control of the system is essential for utilize the potential of PCM and reduce the energy consumption of building. However, there is no sufficient study on optimal control of air-conditioned SSPCM building.

There have been a number of simulation and experimental studies that have demonstrated significant potential for reducing peal cooling demand using building thermal mass through control of zone temperatures. Many researchers have also studied the impact of indoor temperature set point adjustment on load shifting and demand limiting [Braun JE, 1990, 2001. Lee KH and Braun JE, 2008 et al.]. These studies make very good contributions to the application of building thermal mass under an optimal zone temperature set point trajectory [Rabl A and Norford LK, 1991. Antonopoulos KA and Koronaki EP, 2001. et al.]. However, due to the heat capacitance of the normal building envelope, the energy stored in the building thermal mass is limited [Zhang YP and Lin KP et al. 2006]. Phase change materials have very large capacitance when place phase change taking place and can store large amount energy over a small melting temperature range. If cold is stored prior to the on-peak period and is released during the on-peak period, it can reduce the peak cooling load obviously. However, no sufficient quantitative study on the energy and electricity cost saving using SSPCM in air-conditioned buildings can be found, and particularly no study on the effects of control strategies has been reported.

Electrical demands vary significantly during day and night due to the changes of weather conditions and the demands by industrial, commercial and residential activities. In many countries, electrical demands and time-of-use (TOU) utility rates have been designed to encourage shifting of electrical loads from peak periods to off-peak periods. Since PCMs as TES systems in buildings can store “cold” by using night time cheap electricity or free one from nature environment, and use it with a time delay for space cooling in daytime. Therefore, significant economic benefits can be achieved for places where a differential pricing system is adopted. A reduction of sizes of HVAC systems is also possible [Kondo T and Ibamoto T, 2006]. Therefore, they can be used for peak cooling load shifting/reduction. In the meantime, they can be used for peak heating load shifting/reduction in cold climate conditions in winter [Roth K, Westphalen D et al. 2007. Stovall TK and Tomlinson JJ, 1995. et al.]. The use of PCMs in buildings can help shift considerable amount of building loads from peak periods to off-peak periods [Yamaha M and Misaki S, 2006].

2.7 Summary

This chapter provided a comprehensive overview on previous studies related to the investigation and evaluation of dynamic characteristics and energy performance of buildings due to the integration of phase change materials (PCMs). A summary of major results from a number of studies are listed in table 2.1.

The followings are the conclusive remarks and recommendations for further studies in this direction.

1) Most studies have demonstrated that thermal storage effects of PCMs have positive effects on building thermal and energy performance. The can help enhance indoor thermal comfort and reduce energy consumption of buildings. A down-size of HVAC equipment is also possible;
2) Most existing studies were carried out based on numerically simulations and/or prototype experiments. The dynamic characteristics of buildings using PCMs have been evaluated and analyzed in most of reviewed studies. However, the studies on

energy performance of buildings using PCMs, particularly air-conditioned buildings, are still insufficient;

3) The inadequate heat transfer of PCM storages might be a problem in some applications. Further research on enhancing the heat transfer performance of PCM wallboards and/or developing heat transfer enhancement materials are needed;
4) In most of reviewed active systems, the simple and conventional control strategies were used. To maximize the potential of using PCMs, the research on using supervisory and optimal control strategies are needed.
5) The application of PCMs for free cooling in buildings is subjected to local climate conditions. A large temperature difference between day and night is favorable for free cooling applications. The selection of PCMs is also essential for the successful applications of free cooling techniques in buildings.

To sum up, there is still a long way for building scientists and professionals to go in order to make the PCM technologies have desirable and satisfactory performance and be convenient to be used in practice to enhance indoor thermal comfort and building energy efficiency and sustainability.

Table 2.1 Summary of major results from previous studies

No	References	PCMs used	Locations of PCMs	Objects	Major results	Study method
1	Halford and Boehm [39]	A salt type PCM that is held in stasis by a perlite matrix	Between two layers of insulation in a configuration known as resistive, capacitive, resistive	A geometry, in which the wall or ceiling structure was assumed as a three-layer plane wall with PCM in the center layer	Can achieve a 19–57% maximum reduction in peak load as compared to a purely resistive R-19 wall	Simulation
2	Kondo and Ibamoto [41]	A mixture of n-paraffins with melting point 25°C.	The PCM ceiling board	An office building in Tokyo, Japan	The running cost is 96.6% lower than that of rock wool ceiling board	Simulation
3	Kissock and Limas [43]	K18 with an average melting temperature of 25.6°C	In walls and roofs	Concrete sandwich walls, low-mass steel roofs and gypsum wallboard in frame walls under the typical meteorological weather data in Dayton, Ohio	Can reduce peak loads by 19%, 30%, and 16% in concrete sandwich walls, steel roofs and gypsum wallboards, respectively	Simulation
4	Zhang et al. [44]	A highly crystalline, n-paraffin-based PCM	PCM frame walls	A full instrumented test house of 1.83m×1.83m×1.22m in Lawrence, Kansas, USA	The average wall peak heat flux and space cooling load were reduced about 15% and 8.6%, respectively.	Experiment
5	Medina et al. [45]	Paraffin-based PCM	The PCM is in thin-walled copper pipes, which were inserted into horizontal slots cut into the polystyrene foam	A full instrumented test house of 1.83m×1.83m×1.22m	Can reduce peak heat flux by 37% and 62% using a PCMSIP with 10% and 20% PCM concentrations	Experiment
6	Nagano et al.	The PCM was made from	The PCM was embedded directly	A small experimental	89% daily cooling load can be	Experiment

	[47]	foamed glass beads and paraffin waxes	below OA floor boards in the form of granules	system with a floor area of $0.5m^2$	stored in night using a 30mm thick packed bed of the granular PCM	
7	Stetiu and Feustel [19]	Paraffin-based PCM	The phase-change wallboard containing 20% by paraffin mass	A prototype IEA building located in California climate condition	The peak cooling load can be reduced by 28%	Simulation
8	Kaygusuz [48]	$CaCL_2.6H_2O$	The PCM was filled in cylindrical PVC containers in a storage tank	A solar-assisted heat pump with the PCM storage at the Karadeniz Technical University	Saved 9390~12056 kWh net energy during the heating season in 1992 with different systems	Experimental & simulation (SOLSIM)
9	Hammou and Lacroix [54]	Capric acid or n-octadecane	PCM walls comprising spherical capsules, 0.064m in diameter	A room of 5m×5m × 3m with a storage wall of 0.192m thick	Can save about 32% electricity consumption for space heating	Simulation
10	Hassan and Beliveau [55]	RUBITHERN RT 54	The PCM storage tank was linked to a concrete building envelope	A selected building in Blacksburg, VA with the propose integrated solar system	Can save 61.5% of the annual heating bill	Simulation
11	Zhou et al. [60]	The shape-stabilized PCM	The SSPCM plates as the inner linings of walls and the ceiling	A house (3.9m× 3.3m×2.7m) in Beijing, China	Can save 12% of the total energy use in winter in Beijing	Simulation
12	Wang et al. [67]	$C_{16}H_{34}$	The MPCM slurry storage	A system with a cooled ceiling system, a MPCM slurry storage and an evaporative cooling system under five cities in China	Can offer energy saving up to 80% under northwestern China and 10% under southeastern China	Simulation
13	Peippo et al. [70]	Fatty acids	PCM panels were in inside surfaces of a south-facing room except floor	A $120m^2$ passive solar house	Annual energy savings in Finland and Wisconsin were 6% and 15%	Simulation (FHOUSE)
14	Stovall and	Paraffin-based PCM	The external and interior partition	A house (17m×13m×3m) in Boston	Can save \$190 annual cost saving	Simulation

	Tomlinson [72]		walls were constructed using PCM wallboards		with a 3~5 year payback period	(TRNSYS)
15	Heim and Clarke [78]	Fatty acids	The PCM-gypsum plasterboard was used as an internal room lining	A multi-zone, highly glazed and naturally ventilated passive building	Can reduce heating energy demand up to 90% during the heating season	Simulation (ESP-r)
16	Athienitis et al. [98]	With 25% by weight of Butyl stearate	The PCM gypsum board as interior lining in the test room	An outdoor test-room (2.82m×2.22m×2.24m) in Montreal	Can save about 15% of the total heating load	Experiment & simulation
17	Chen et al. [99]	Paraffin-based PCM	The PCM gypsum board was in the inner surfaces of the north wall	A unit room in the middle floor in Beijing	The energy saving rate of heating season is about 10%	Experiment & simulation
18	Weinläder et al. [104]	RT25 (12mm) and S27(8.6mm)	PCMs were in transparent plastic containers placed behind a double glazing with an air gap of 10mm	A south façade panel in Würzburg, Germany	Can reduce 30% heat losses and 50% solar heat gains in winter, and 25% energy gains in summer	Experiment & Simulation
19	Ismail and Castro [107]	A mixture of commercial Glycol wax	In walls and roofs	An existing building in Campinas, SP, Brazil	Save 19% and 31% energy for cases using window and central AC units	Simulation & Experiment

CHAPTER 3 SIMPLIFIED MODELS OF SSPCM BUILDING STRUCTURE AND OPTIMAL NODAL PLACEMENT

The simplified building model is an important basis of the thermodynamic characteristic and energy performance analysis particularly for operational performance evaluation and control applications. This chapter mainly presents a simplified model of shape stabilized phase change material (SSPCM) buildings, the theoretic basis of optimal nodal placement of simplified models of building envelopes based on frequency response characteristic analysis, and a genetic algorithm (GA) estimator developed to identify the optimal parameters to match the frequency response characteristics of simplified models with theoretical frequency response characteristics. The validity of optimal nodal placement will be demonstrated with three typical constructions.

3.1 Introduction

Due to the ability to provide high energy storage density and the characteristics to store heat/cold at relatively constant temperatures, phase change materials (PCMs) as thermal energy storage (TES) media in buildings have attracted increasing attention for developing low energy or energy efficient buildings. Many scientists, environmentalists and international communities are now taking an interest on the applications of PCMs in buildings to enhance their thermal and energy performance. The use of PCMs in buildings can provide different functions for different applications. For instance, they can be used for enhancing the free cooling of buildings, building peak load shifting, solar energy utilization, waste heat recovery, etc. These functions can be achieved by passive or active means.

However, the successful use of PCMs in buildings depends on many factors, such as the type and amount of PCMs used, the encapsulation method used, the location of PCMs in building structures, building design and orientation, equipment design and selection, climate condition, utility rate policy, occupancy schedule, system control and operational algorithms, etc. To properly use PCMs in buildings, the accurate prediction of the dynamic characteristics and energy performance of buildings using PCMs is essential, which can help building practitioners to fully understand the building temperature response characteristics and potential energy savings due to the use of PCMs. They can therefore properly select and design the building and the use of PCMs and properly control the system to fully use the energy saving potential provided by the PCMs.

In building applications, PCMs can be integrated into building covering materials such as concrete, gypsum wallboard, plaster, etc., as part of building structures for lightweight or even heavyweight buildings to increase the thermal mass. In recent years, a kind of novel compound PCM, the so-called shape-stabilized PCM (SSPCM) has been attracting the interests of the researchers [Inaba H and Tu P, 1997. Ye H and Ge XS, 2000. Xiao M and Feng B et al. 2000, 2001]. It consists of paraffin as dispersed PCM and high-density polyethylene (HDPE) or other materials as supporting material. Since the mass percentage of paraffin can be as much as 80% or so, the total stored energy is comparable with that of traditional PCMs. As long as the operating temperature is below the melting point of the supporting material, the compound material can keep its shape even the PCM changes from solid to liquid [Ye H and Ge XS, 2000]. This reduces the liquid PCM leakage danger and PCM can be therefore used for thermal storage in buildings without encapsulation [Zhou GB and YP et al. 2008].

In order to predict the overall energy consumption, it is essential to have models to estimate the cooling or heating energy consumption needed for maintaining the air temperature and humidity in buildings [Braun JE and Montgomery KWet al. 2001. Henze G and Felsmann C et al. 2004. Yao Y and Lian ZW et al. 2004]. Over the last two or more decades, there were many mathematical models to analyze the thermal performance of building integrated with PCMs [Verma P and Varun et al. 2008, Zhang YP and Lin KP et al. 2008 et al.]. These mathematical models were mainly on the basis of first law and second law of thermodynamics. Zhang and Su et al. [2001] presented a general model which can be used to analyze the instantaneous temperature distribution, instantaneous heat transfer rate, and thermal storage capacity of a LHTES system. Halford and Boehm [2007] developed an idealized model for PCMs. This model uses the one-dimensional diffusion equation driven by time varying temperature functions imposed at the boundaries. Heim and Clarke [2004] presented a numerical model for PCMs encapsulated in porous building materials. Vakilaltojjar and Saman [2001] presented a semi-analytical model for PCMs using the finite elements method. A heat transfer model of SSPCM wall and ceiling was presented by Zhou and Yang et al. [2009]. Although these mathematical models can well describe the heat transfer processes of building envelopes integrated with PCMs, they were too complicated to apply in many practical applications concerning computation speed and program size particularly when involving large buildings or models are used for online applications.

This paper presents a method to simplify building model integrated with SSPCM and identify their parameters using easily available building physical properties. The simplified building model integrated with SSPCM consists of the simplified models of the external wall (3R2C model) and the SSPCM plate (4R2C). 3R2C wall model was developed to simulate the building envelopes [Braun JE and Chaturvedi N, 2002, Seem JE and Klein SA et al. 1989]. The nodal placement of the 3R2C model can be obtained by matching the theoretical frequency response characteristics of the building envelope with the frequency response characteristics of the simplified model using genetic algorithm [Mitchell JM, 1997]. A 4R2C model is developed to represent the SSPCM layer. The parameter identification of the 4R2C model is performed as follows. Given a typical weather profile, the heat transfer between the SSPCM wall and the indoor air (at controlled indoor temperature condition) and the indoor air temperature (in the condition without air-conditioning) are simulated by the theoretical model. A GA preprocessor is then used to find out the optimal 4R2C values of the 3R2C+4R2C model which give the best fitting with both heat transfer and indoor air temperature in time-domain.

3.2 Description on simplified dynamic model

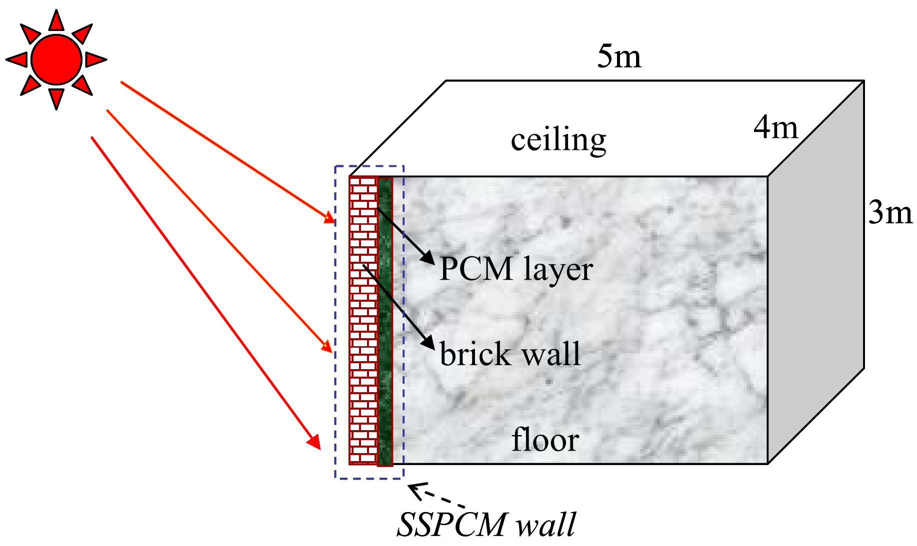

Figure 3.1 Schematic of SSPCM wall and the ideal model house

The SSPCM wall considered consists of a brick (or concrete) wall and a PCM layer as shown in Figure 3.1. Figure 3.2 illustrates the simplified dynamic model of an external wall integrated with SSPCM. The simplified SSPCM wall model predicts the dynamic heat transfer process of the wall, which can be used to simulate the effects of SSPCM on building dynamic characteristics and energy performance of building. The brick layer and the PCM layer are simplified as 3R2C and 4R2C models respectively. For the brick layer, the whole thermal capacitance is assumed as two lumped thermal capacitances (C_{w1}, C_{w2}) and the whole thermal resistance is assumed as three lumped thermal resistances (R_{w1}, R_{w2}, R_{w3}). The optimal distributions (optimal node placement) of the capacitances and the resistances are identified to best fit the theoretical dynamic heat transfer process as described in the next session. The PCM layer is divided into two sub-layers. The capacitance of each sub-layer is assumed a lumped capacitance (C_{p1}, C_{p2}). The heat transfer resistance of each sub-layer is assumed as two resistances on both side of its lumped capacitance (R_{p11}, R_{p12} and R_{p21}, R_{p22}). The optimal distributions of the sub-layers and the thermal resistances within the sub-layers are identified to best fit the theoretical dynamic heat transfer process of the PCM layer as described in the next session. Three further assumptions are made on the PCM sub-layers:

i. The PCM temperature of each sub-layer is uniform which determines the state of entire sub-layer;

ii. The specific heat and thermal conductivity of each PCM layer is a function of its temperature;

iii. The distributions of the sub-layers and the thermal resistances within the sub-layers remain unchanged while the actual values vary following the changes of the specific heat and thermal conductivity.

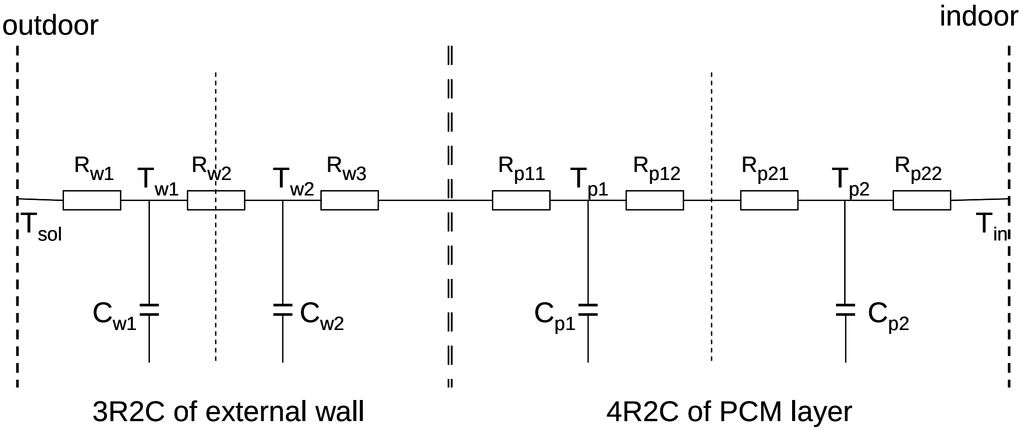

Figure 3.2 Schematic of the simplified dynamic building model

The heat transfer of the external wall integrated with SSPCM can be represented with the following differential equations:

$$C_{w1}\frac{dT_{w1}(t)}{dt}=\frac{T_{sol}(t)-T_{w1}(t)}{R_{w1}}-\frac{T_{w1}(t)-T_{w2}(t)}{R_{w2}} \tag{3.1}$$

$$C_{w2}\frac{dT_{w2}(t)}{dt}=\frac{T_{w1}(t)-T_{w2}(t)}{R_{w2}}-\frac{T_{w2}(t)-T_{p1}(t)}{R_{w3}+R_{p11}} \tag{3.2}$$

$$C_{p1}\frac{dT_{p1}(t)}{dt}=\frac{T_{w2}(t)-T_{p1}(t)}{R_{w3}+R_{p11}}-\frac{T_{p1}(t)-T_{p2}(t)}{R_{p12}+R_{p21}} \tag{3.3}$$

$$C_{p2}\frac{dT_{p2}(t)}{dt}=\frac{T_{p1}(t)-T_{p2}(t)}{R_{p12}+R_{p21}}-\frac{T_{p2}(t)-T_{in,a}(t)}{R_{p22}} \tag{3.4}$$

$$C_{air}\frac{dT_{in,a}(t)}{dt}=\frac{T_{p2}(t)-T_{in,a}(t)}{R_{p22}+R_{air}}+Q_{oe} \tag{3.5}$$

$$Q_{in,s}=\frac{T_{p2}(t)-T_{\mathrm{in,a}}(t)}{R_{p22}+R_{air}} \tag{3.6}$$

where, R and C are resistance and capacitance. T is temperature. Subscript w, p, in, indicate brick wall, PCM, indoor. Q_{oe} is the heat load generated by occupants and equipments. R_{air} is the convection heat transfer resistance between indoor air and wall (PCM) surface. The properties of the building envelopes and PCM layer are relatively easy to obtain which can be utilized to establish the simplified 3R2C and 4R2C models.

A simple south-facing brick chamber is considered as the ideal model house for SSPCM wall model validation, which has only one exterior wall integrated with SSPCM (the south wall), as shown in Figure 3.1. For the simplicity and reliability of validation, the other three walls, ceiling and floor are considered to be thermally isolated while the indoor air is considered to be perfectly mixed with lumped thermal capacitance. The dimension of the room is 5.0m (length)×4.0m (width)×3.0m (height). The SSPCM plate is attached to inner surfaces of south wall only.

3.3 Parameter identification of simplified model

The overall capacitances and resistances of the brick wall layer and the PCM layer are determined by the physical properties of the wall and PCM (including its temperature). The parameter identification of the 3R2C wall model and 4R2C PCM layer model is actually to find out the optimal distributions of the resistances and capacitance among the nodes of the models (optimal nodal placement). There are three independent parameters to be identified for each model respectively. The other parameters of the model can be determined simply by these independent parameters as described in the Session 3.4.

Parameter identification of simplified model includes identification of the parameters of the 3R2C model of external wall (R_{w1}, R_{w3}, C_{w2}) and the 4R2C model of SSPCM layer (β_p, β_{p1}, β_{p2}). Where, β_p, β_{p1} and β_{p2} are resistance ratios of the sub-layers of the SSPCM plate defined by Eq. (3.12)–(3.14). It is achieved by two GA-based estimators for the two models respectively as illustrated in Figure 3.3.

The parameters of 3R2C models of the wall (brick layer) are identified by finding the best matching between the frequency response characteristics of the simplified model and the theoretical frequency response characteristics of wall using the genetic algorithm.

The optimal nodal placement of the simplified model of the wall is based on the equivalent frequency characteristics of the simplified model and its relevant theoretical model. The process of the optimal nodal placement of the simplified model of a building envelope is to search the parameters of the models allowing the frequency characteristics of the simplified model match that of the theoretical model the best. First, the theoretical frequency characteristic of heat transfer of the building envelope is deduced. Second, the frequency characteristic of the simplified 3R2C model is deduced. Then the objective function for parameter optimization is given with the deduced frequency characteristics. The GA estimator is used for parameter optimization of 3R2C models of the building envelopes. The details of this method can be found in reference [Wang SW and Chen YM, 2001. Wang SW and Xu XH, 2006].

After the parameters of 3R2C model are identified, the heat transfer between the SSPCM wall and the indoor air (at controlled indoor temperature condition) and the indoor air temperature (in the condition without air-conditioning) are simulated by the theoretical models at the given weather condition. The second estimator is then used to find out the optimal parameters of the 4R2C PCM layer model which give the best fitting between the heat gain and indoor air temperature profiles predicted by theoretical model and that predicted by the simplified 4R2C model of the PCM layer (together with 3R2C wall model with optimized parameters).

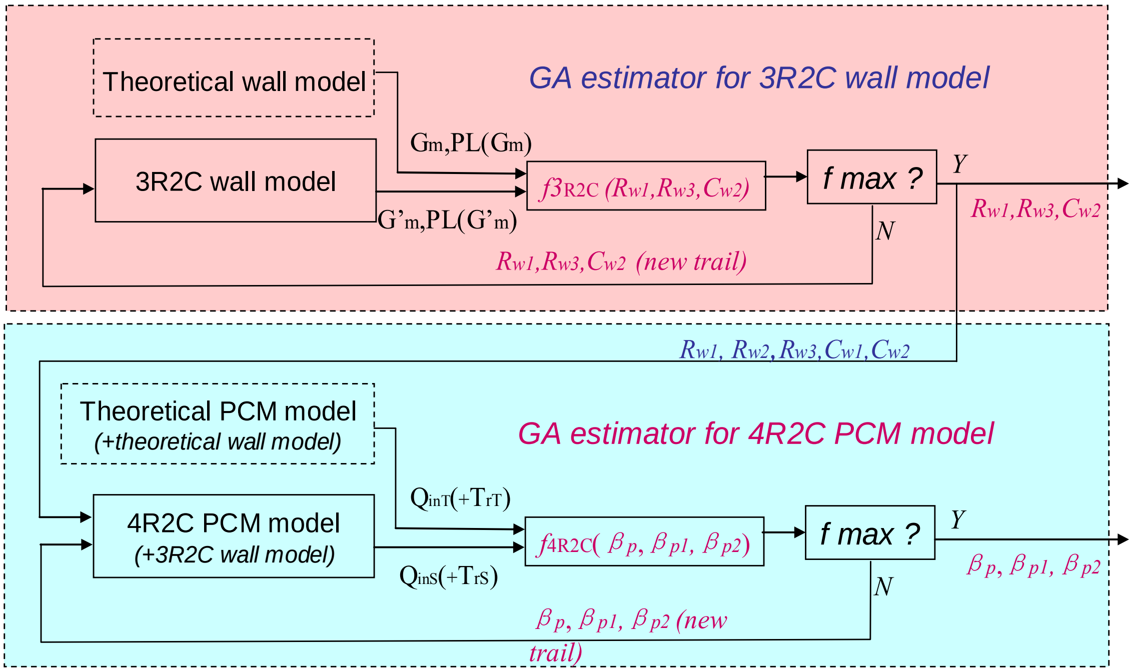

Figure 3.3 Flow chart of parameters identification

3.3.1 Parameters identification of 3R2C wall model

A brief on the parameter identification method of the external wall (3R2C) model is given here. The details can be found in the previous publication [Wang SW and Xu XH, 2006]. The objective function of such optimization is expressed in Eq. (3.7). The optimization process is actually searching the optimal values of the three model parameters, which allow the frequency response of the simplified model best fit the theoretical response.

$$J_{3R2C}(R_{w1},R_{w3},C_{w2})=\sum_{n=1}^{N}\sum_{m=X,Y,Z}(W_m^{AM}\left\|G_m(j\omega_n)\right|-\left|G'_m(j\omega_n)\right\|+W_m^{PL}\times\left|PL(G_m(j\omega_n))-PL(G'_m(j\omega_n))\right|) \tag{3.7}$$

where, J_{3R2C} is the objective function of the simplified model of the wall, PL is the phase lag (denoted as $PL(G(j\omega))$), N is the number of frequency points, W is the weighting factor associated with the amplitudes and phase lags of frequency characteristics of the external, cross and internal heat conductions, respectively. In this study all the weighting factors were set as 1 as it was found that such value works well. R_{w1} and R_{w3} are constrained between 0 and R_w, which is the total resistance of the external wall. C_{w2} is constrained between 0 and C_w, which is the total capacitance of the wall. The other two parameters can be obtained as follows:

$$R_{w2} = R - R_{w1} - R_{w3} \tag{3.8}$$

$$C_{w1} = C - C_{w2} \tag{3.9}$$

The number of frequency points N and the frequency range (10^{-n1}, 10^{-n2}) of concern are determined as follows. *n1, n2* and N are generally chosen as 8, 3 and $10(n_1-n_2)+1$, respectively. With the properties of individual layers of the calculated wall, the theoretical frequency characteristics can be calculated easily. With the assumed parameter values of the simplified models, the frequency characteristics can also be calculated conveniently as follow.

$$f_{3R2C}(R_{b1}, R_{b3}, C_{b2}) = \frac{1}{J_{3R2C}(R_{b1}, R_{b3}, C_{b2})} \tag{3.10}$$

3.3.2 Parameters identification of 4R2C SSPCM model

The objective function for the optimal node placement of the PCM layer is defined by Eq. (3.11).The parameters to be optimized are the distributions of the PCM sub-layers and the thermal resistances within the two sub-layers of the SSPCM plate 4R2C model, which allow the outputs of simplified model match the outputs of the theoretical model the best.

$$J_{4R2C}(\beta_p, \beta_{p1}, \beta_{p2}) = \sqrt{\frac{\sum_{k=1}^{n}(Q_{in,t,k} - Q_{in,s,k})^2}{n-1}} \tag{3.11}$$

$$\beta_p = \frac{R_{p11} + R_{p12}}{R_{pcm}} = \frac{C_{p1}}{C_{pcm}} \tag{3.12}$$

$$\beta_{p1} = \frac{R_{p11}}{R_{p11} + R_{p12}} \tag{3.13}$$

$$\beta_{p2} = \frac{R_{p21}}{R_{p21} + R_{p22}} \tag{3.14}$$

$$R_{pcm} = R_{p11} + R_{p12} + R_{p21} + R_{p22} \tag{3.15}$$

$$C_{pcm} = C_{p1} + C_{p2} \tag{3.16}$$

where, J_{4R2C} is the objective function of the simplified model of the SSPCM plate. $Q_{in,t}$ and $Q_{in,s}$ are the heat exchange between the internal face structure and indoor air of the theoretical model and simplified model respectively. β_p, β_{p1} and β_{p2} are resistances ratios of the sub-layers of the SSPCM plate.

The fitness function (f_{4R2C}) for the simplified model of the PCM plate, which is the reciprocal of the objective function of the minimization problem as Eq. (11), is represented by Eq. (3.17).

$$f_{4\mathrm{R2C}}(\beta_p, \beta_{p1}, \beta_{p2}) = \frac{1}{J_{4\mathrm{R2C}}(\beta_p, \beta_{p1}, \beta_{p2})} \tag{3.17}$$

Both GA estimators for parameters identification of these simplified models are developed based on the GA driver by Carroll [2001]. The parameters of the GA driver are important for convergence speed. They are selected according to Carroll's recommendation and determined by simulation tests.

3.4 Specifications of structures and working conditions

In this study, six combinations of wall and SSPCM structures were used including three types of walls (light wall, median wall and heavy wall) and two types of SSPCM (thickness of 10mm and 20mm respectively). The Hong Kong weather profile was used for parameter identification of the model. The Shenyang and Beijing weather profiles were used for the model validation.

The thermophysical properties of SSPCM and material of building envelope are shown in Table 3.1. The heat of fusion of SSPCM is 160kJ/kg and the melting temperature of the SSPCM is 26-27°C. The phase change temperature range of SSPCM was assumed to be 1K referring to typical PCM materials [Zhou GB and Yang YP et al. 2009].

Table 3.1 Envelope materials and their thermophysical properties

Materials	Density (kg/m^3)	Specific heat (kJ/kg·K)	Thermal conductivity (W/m·K)	Thickness (mm)
PCM	850	1.0	0.2	10/20
brick	1400	1.05	0.58	115/240/490

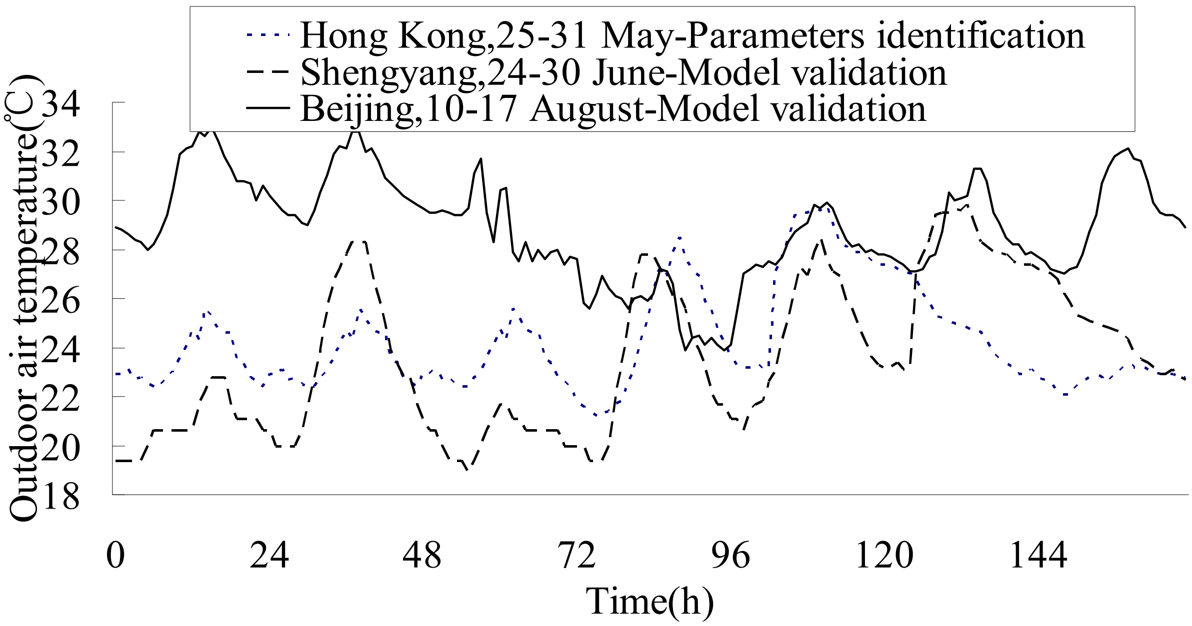

Figure 3.4 Outdoor air temperature profiles

Three weather data profiles used in this study are shown in Figure 3.4. In this study, the models were used to predict to calculate the heat transfer between the internal surface of the structure and the indoor air in case with air-conditioning (controlled condition) and the indoor air temperature in the case without air-conditioning (passive condition). The outputs of the simplified model were compared with the outputs of the theoretical model in two approaches. Approach I compares the indoor temperatures (T_{in}) predicted by the two models at given internal load (Q_{oe}), produced by the indoor equipments etc., under the passive condition. Approach II compares the indoor heat exchange between the internal surface of the structure and indoor air (Q_{in}) predicted by the two models at given indoor air temperature (T_{in}) under air-conditioned conditions.

At air-conditioned conditions, the indoor temperature was controlled at 26°C in office hour (8:00 AM-6:00 PM) and at 25°C in other period (6:00 PM-8:00 AM) respectively. At passive conditions, the total internal heat was 0.08 kW in office hour (8:00 AM-6:00 PM) and 0.02 kW in other period (6:00 PM-8:00 AM) respectively.

The theoretical models were solved numerically using the finite element method by dividing the wall and SSPCM into 20 layers and 10 layers respectively. In this study, three types of wall including light wall, median wall and heavy wall were tested. The tested thicknesses of the SSPCM were 10mm and 20mm. The heat of fusion of the PCM material is 160kJ/kg and the phase change range is 1K. The specific heat of PCM is 1 kJ/kg in both solid and liquid states. As the phase change range is 1K, the equivalent specific heat of PCM in the phase change region is 160 kJ/kg·K as shown in Figure 3.5. The melting temperature of PCM is 26°C and 28°C respectively in different tests. To ensure the numerical stability of the models, the specific heat of the PCM is assumed to change from one level to the other following a linear line over a range of 0.1 K as shown in Figure 3.5 instead of sharp step changes.

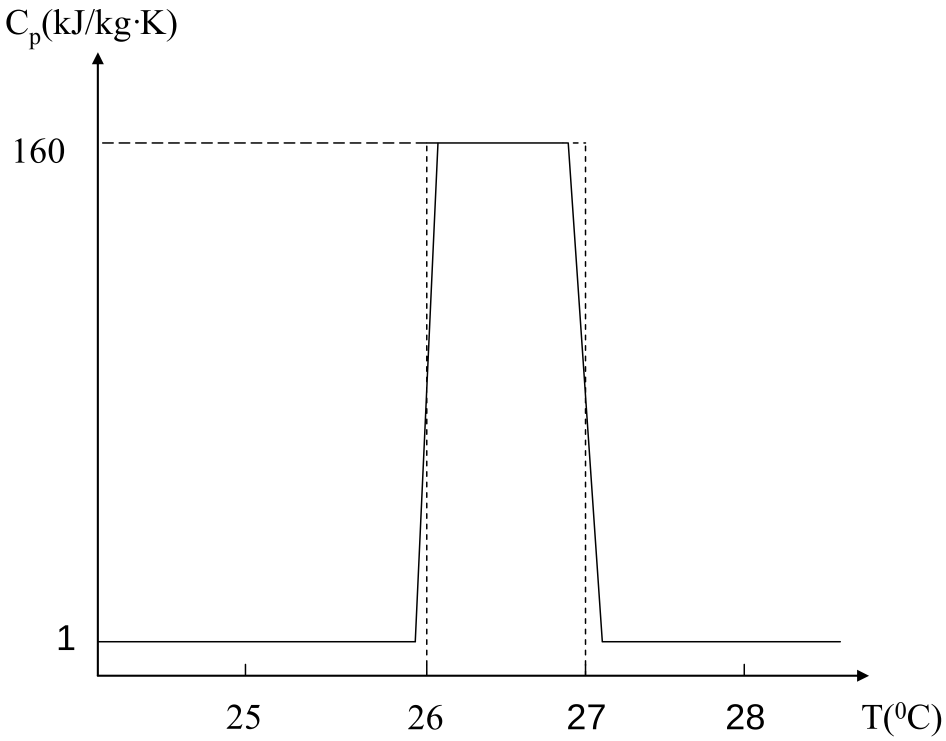

Figure 3.5 Equivalent specific heat of SSPCM

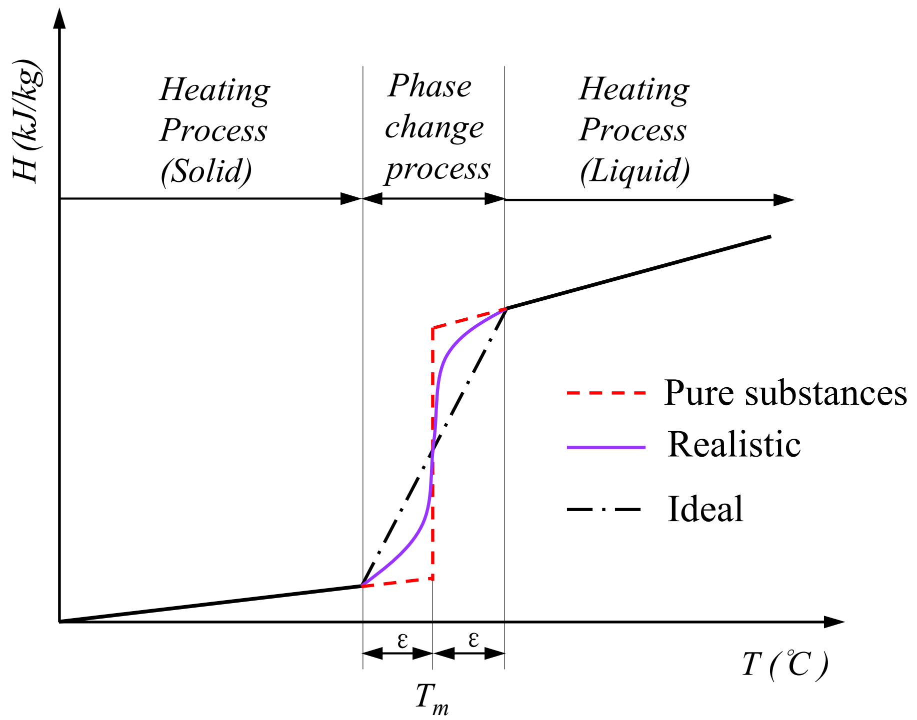

Figure 3.6 Relationship between the enthalpy and temperature by phase changes

For simplified modeling of PCMs used in buildings, two typical phase change curves, i.e. 'ideal' curve' and 'realistic' curve, as shown in Fig. 3.6, are assumed to represent the phase change processes of PCMs. According to this assumption, a layer of PCMs incorporated into buildings can be taken as a lumped capacitance (C_{pcm}) with two small resistances, which represent the heat exchanger between the PCM and its surroundings. It is worthy noticing that this lumped capacitance of PCMs varies with the changes of the temperature in the case the phase change processes of PCMs follows a 'realistic' curve. Based on this assumption, the generic simplified models for passive and active buildings integrated with PCMs can be developed.

3.5 Results of parameter identification

3.5.1 Parameters of 3R2C wall model

The values of resistances and capacitances of brick wall in different types of wall were obtained as shown in Table 3.2.

Table 3.2 Resistances and capacitances of brick in different types of walls

Wall type	Parameters identified	
	Resistances (K/kW)	Capacitances (kJ/K)
Light wall (115mm)	R_{w1}=3.14 R_{w2}=10.475 R_{w3}=2.91	C_{w1}=1117.69 C_{w2}=910.91
Median wall (240mm)	R_{w1}=4.17 R_{w2}=25.425 R_{w3}=4.94	C_{w1}=1599.21 C_{w2}=2634.39
Heavy wall (490mm)	R_{w1}=3.29 R_{w2}=60.09 R_{w3}=7.02	C_{w1}=1132.03 C_{w2}=7511.57

3.5.2 Parameters of 4R2C SSPCM model

The objective function of the 4R2C model parameter identification was formulated in two different means. Method One: considering both Q_{in} and T_{in}, the relative deviations of Q_{in} and T_{in} were minimized. Method Two: considering the Q_{in} only, the relative deviations of Q_{in} was minimized. The resistances and capacitances of SSPCM in different types of wall are presented in Table 3.3.

Table 3.3 Resistances and capacitances of 4R2C SSPCM model of different types of structures

Wall Type	Thickness of SSPCM layer	Total R_{pcm} and C_{pcm} with phase change	Total R_{pcm} and C_{pcm} without phase change	4R2C model parameters identified by minimizing ΔQ_{in} and ΔT_{in}		4R2C model parameters identified by minimizing ΔQ_{in}	
Light wall (115mm)	D_{SSPCM}=10mm	R_{pcm}=0.415K/kW C_{pcm}=16320kJ/K	R_{pcm}=4.15K/kW C_{pcm}=102kJ/K	$R_{p11}=0.53R_{pcm}$ $R_{p12}=0.13R_{pcm}$ $R_{p21}=0.32R_{pcm}$ $R_{p22}=0.02R_{pcm}$	$C_{p1}=0.53C_{pcm}$ $C_{p2}=0.47C_{pcm}$	$R_{p11}=0.20R_{pcm}$ $R_{p12}=0.27R_{pcm}$ $R_{p21}=0.30R_{pcm}$ $R_{p22}=0.23R_{pcm}$	$C_{p1}=0.20C_{pcm}$ $C_{p2}=0.80C_{pcm}$
	D_{SSPCM}=20mm	R_{pcm}=0.83K/kW C_{pcm}=32640kJ/K	R_{pcm}=8.3K/kW C_{pcm}=204kJ/K	$R_{p11}=0.65R_{pcm}$ $R_{p12}=0.05R_{pcm}$ $R_{p21}=0.21R_{pcm}$ $R_{p22}=0.09R_{pcm}$	$C_{p1}=0.65C_{pcm}$ $C_{p2}=0.35C_{pcm}$	$R_{p11}=0.35R_{pcm}$ $R_{p12}=0.28R_{pcm}$ $R_{p21}=0.26R_{pcm}$ $R_{p22}=0.11R_{pcm}$	$C_{p1}=0.35C_{pcm}$ $C_{p2}=0.65C_{pcm}$
Median wall (240mm)	D_{SSPCM}=10mm	R_{pcm}=0.415K/kW C_{pcm}=16320kJ/K	R_{pcm}=4.15K/kW C_{pcm}=102kJ/K	$R_{p11}=0.17R_{pcm}$ $R_{p12}=0.08R_{pcm}$	$C_{p1}=0.17C_{pcm}$ $C_{p2}=0.83C_{pcm}$	$R_{p11}=0.52R_{pcm}$ $R_{p12}=0.15R_{pcm}$	$C_{p1}=0.52C_{pcm}$ $C_{p2}=0.48C_{pcm}$

				$R_{p21}=0.69R_{pcm}$ $R_{p22}=0.06R_{pcm}$		$R_{p21}=0.31R_{pcm}$ $R_{p22}=0.02R_{pcm}$	
	D_{SSPCM}=20mm	R_{pcm}=0.83K/kW C_{pcm}=32640kJ/K	R_{pcm}=8.3K/kW C_{pcm}=204kJ/K	$R_{p11}=0.57R_{pcm}$ $R_{p12}=0.12R_{pcm}$ $R_{p21}=0.29R_{pcm}$ $R_{p22}=0.02R_{pcm}$	$C_{p1}=0.57C_{pcm}$ $C_{p2}=0.43C_{pcm}$	$R_{p11}=0.50R_{pcm}$ $R_{p12}=0.14R_{pcm}$ $R_{p21}=0.30R_{pcm}$ $R_{p22}=0.06R_{pcm}$	$C_{p1}=0.50C_{pcm}$ $C_{p2}=0.50C_{pcm}$
Heavy wall (490mm)	D_{SSPCM}=10mm	R_{pcm}=0.415K/kW C_{pcm}=16320kJ/K	R_{pcm}=4.15K/kW C_{pcm}=102kJ/K	$R_{p11}=0.16R_{pcm}$ $R_{p12}=0.09R_{pcm}$ $R_{p21}=0.68R_{pcm}$ $R_{p22}=0.07R_{pcm}$	$C_{p1}=0.16C_{pcm}$ $C_{p2}=0.84C_{pcm}$	$R_{p11}=0.21R_{pcm}$ $R_{p12}=0.04R_{pcm}$ $R_{p21}=0.69R_{pcm}$ $R_{p22}=0.06R_{pcm}$	$C_{p1}=0.21C_{pcm}$ $C_{p2}=0.79C_{pcm}$
	D_{SSPCM}=20mm	R_{pcm}=0.83K/kW C_{pcm}=32640kJ/K	R_{pcm}=8.3K/kW C_{pcm}=204kJ/K	$R_{p11}=0.74R_{pcm}$ $R_{p12}=0.04R_{pcm}$ $R_{p21}=0.20R_{pcm}$ $R_{p22}=0.02R_{pcm}$	$C_{p1}=0.74C_{pcm}$ $C_{p2}=0.26C_{pcm}$	$R_{p11}=0.71R_{pcm}$ $R_{p12}=0.11R_{pcm}$ $R_{p21}=0.16R_{pcm}$ $R_{p22}=0.02R_{pcm}$	$C_{p1}=0.71C_{pcm}$ $C_{p2}=0.29C_{pcm}$

3.5.2.1 Parameter identification by minimizing indoor heat exchange relative deviation (ΔQ_{in}) and indoor air temperature relative deviation (ΔT_{in})

With the Hong Kong weather profile, the parameters of the 4R2C model were identified using the objective function as in equation (3.18).

$$J_{4R2C}(\beta_p,\beta_{p1},\beta_{p2}) = \sqrt{\frac{\sum_{k=1}^{N}(Q_{in,t,k}-Q_{in,s,k})^2}{N-1}} + \frac{1}{R_{equ}} \bullet \sqrt{\frac{\sum_{k=1}^{N}(T_{in,t,k}-T_{in,s,k})^2}{N-1}} \tag{3.18}$$

$T_{in,t}$ and $T_{in,s}$ are indoor temperature of the theoretical model and simplified model respectively. The resistances and capacitance of 4R2C PCM model for light wall, median wall and heavy with different thickness of PCM layer are presented in Table 3.3.

Comparison between indoor temperatures predicted by simplified and theoretical models

Figure 3.6 to Figure 3.8 present the predicted indoor temperature (T_{in}) profiles under passive condition in the parameter identification cases using different structures respectively.

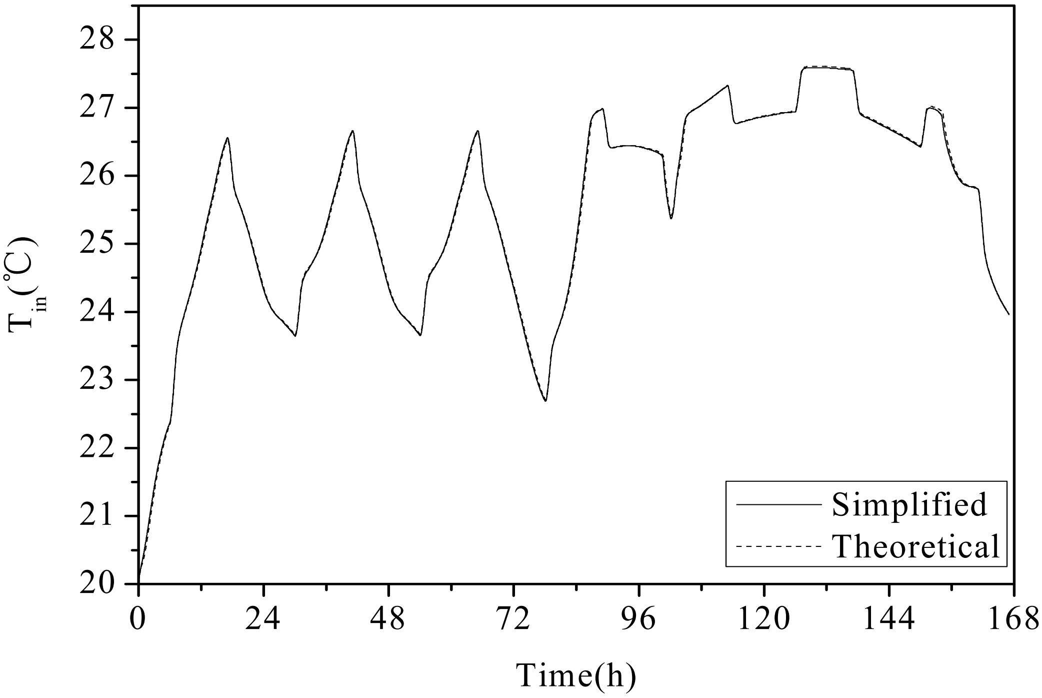

Figure 3.6 Indoor air temperatures (T_{in}) of SSPCM building with light wall

(D_{SSPCM} = 10mm) (parameters identification case)

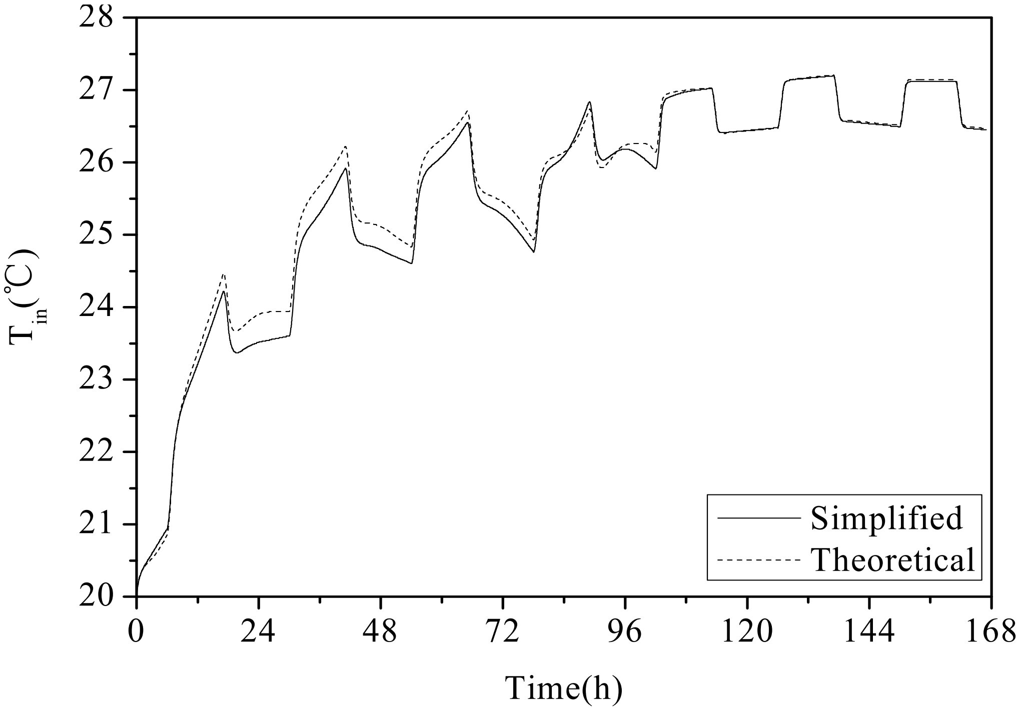

Figure 3.7 Indoor air temperatures (T_{in}) of SSPCM building with median wall

(D_{SSPCM} = 20mm) (parameters identification case)

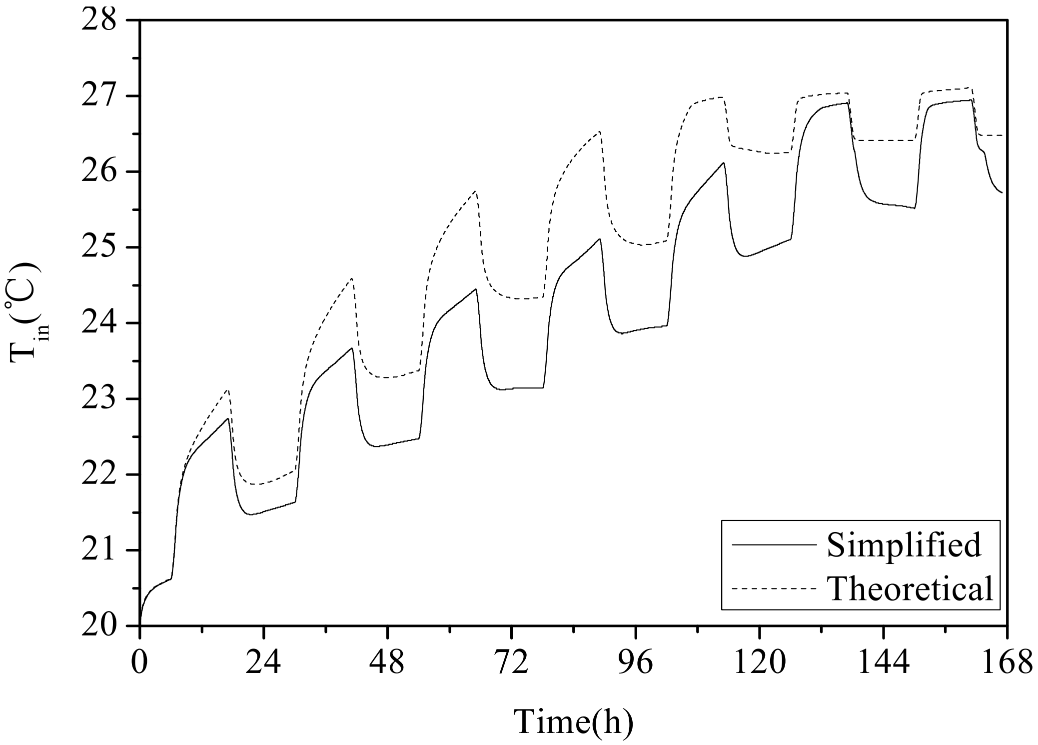

Figure 3.8 Indoor air temperatures (T_{in}) of SSPCM building with heavy wall (D_{SSPCM} = 20mm) (parameters identification case)

It can be seen that the indoor temperature (T_{in}) profiles predicted by the theoretical model and simplified model were nearly the same for structures with light wall and very close for structures with median wall. The indoor temperature profiles wall predicted by two models for structures with heavy wall had significant discrepancy, indicating that the simplified model does not suitable to simulate structure of heavy walls.

Comparison between heat exchanges predicted by simplified and theoretical models

Figure 3.9 present the predicted profiles of the indoor heat exchange between the internal face structure and indoor air (Q_{in}) predicted by two models in parameter identification cases for structures with light wall.

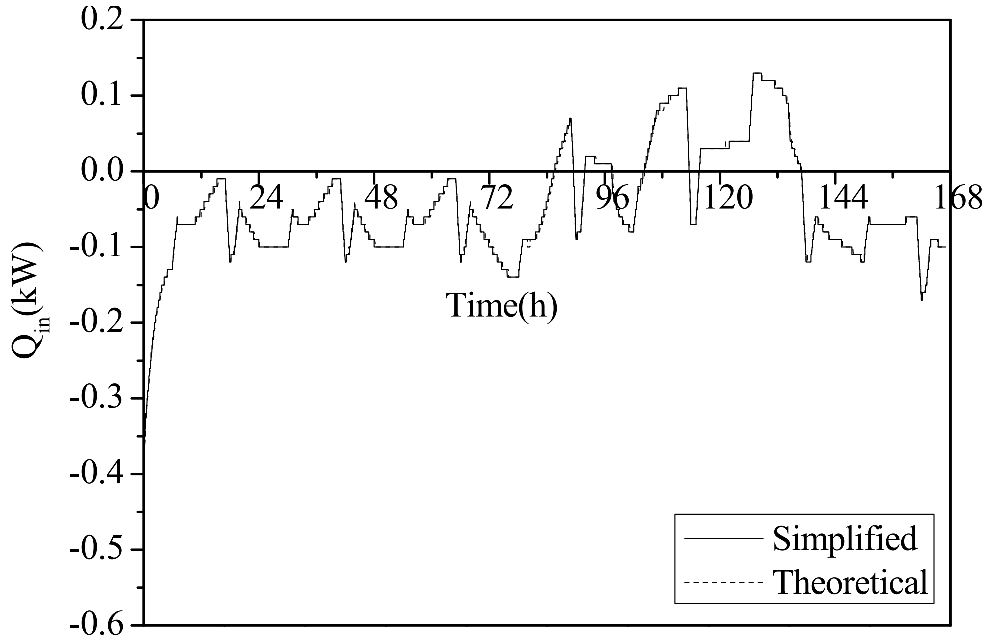

Figure 3.9 Indoor heat exchange (Q_{in}) of SSPCM building with light wall (D_{SSPCM} = 10mm) (parameters identification case)

It can be found that the discrepancy of Q_{in} in two models was very small for structures with light wall. The discrepancy is also very small for median wall, but obvious for structures with heavy wall.

3.5.2.2 Parameter identification by minimizing indoor heat exchange relative deviation (ΔQ_{in}) only

With the same Hong Kong weather profile, a different objective function, equation (11), was used to study the impact when only the heat exchange is used for parameter identification. The parameters of the simplified model for the structures of light wall, median wall and heavy wall with different thickness of PCM layer are presented in Table 3.5. Figure 3.10 and Figure 3.11 present the comparison between the temperatures and heat exchanges predicted by the two models for light wall with D_{SSPCM}=10mm.

Figure 3.10 presents the comparison between the indoor temperatures predicted by the simplified model and the theoretical model. Figure 3.11 presents the comparison between the heat transfer rates predicted by simplified model and theoretical model. It can be seen that T_{in} and Q_{in} predicted simplified model matched well with that predicted by the theoretical model for the structures with light wall, which is the same as observed in the case when parameter identification was conducted by minimizing both ΔQ_{in} and ΔT_{in}. The results were also satisfactory for median wall but not satisfactory for heavy wall.

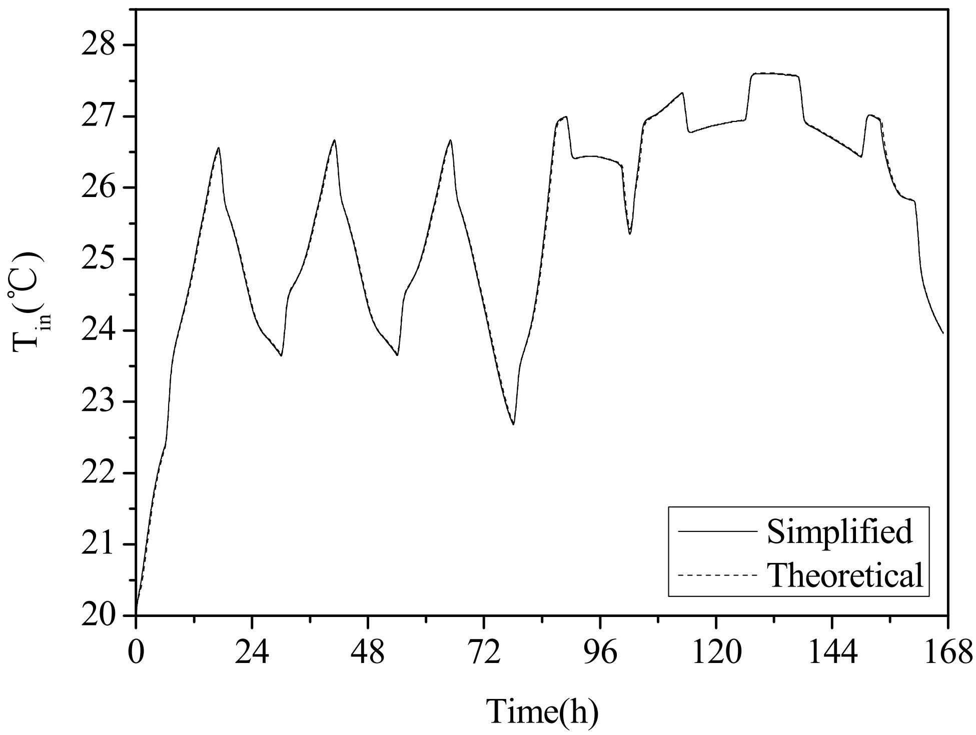

Figure 3.10 Indoor air temperatures (T_{in}) of SSPCM building with light wall (D_{SSPCM} = 10mm) (parameters identification case)

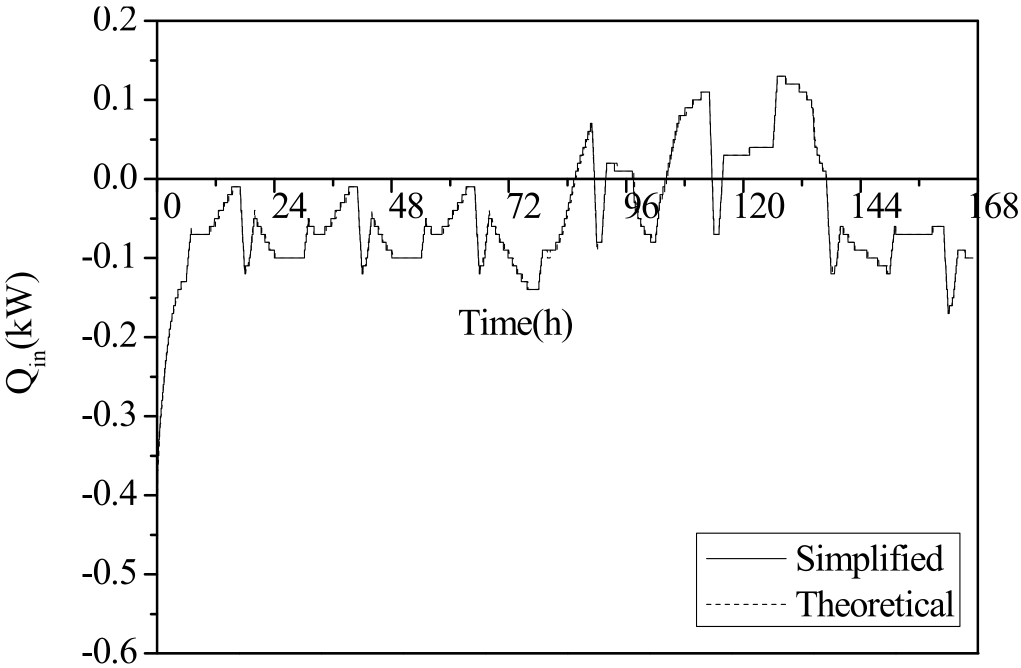

Figure 3.11 Indoor heat exchange (Q_{in}) of SSPCM building with light wall (D_{SSPCM} = 10mm) (parameters identification case)

3.5.2.3 Summary of prediction errors in parameter identification cases

Table 3.4 presents a summary of deviations of Q_{in} and T_{in} of simplified models compared with theoretical model for different types of walls in all parameter identification cases. For the light wall with D_{SSPCM}=10mm, the deviation of ΔQ_{in} is 0.0017 kW and 0.0016 kW when the parameters were identified by minimizing ΔQ_{in} and ΔT_{in} and minimizing ΔQ_{in} respectively, the deviation of ΔT_{in} is 0.0266 K and 0.028 K when the parameters were identified by minimizing ΔQ_{in} and ΔT_{in} and minimizing ΔQ_{in} respectively. The deviation of ΔQ_{in} was smaller when identified by minimizing ΔQ_{in} only, but the deviation of ΔT_{in} was larger in this case. The maximum deviations of ΔQ_{in} and ΔT_{in} are both slightly larger when parameters were identified by minimizing ΔQ_{in} only.

From this table, it can be observed that the deviations of Q_{in} and T_{in} for different types of structures with light wall and medium walls were very small and the errors for different types of structures with heavy wall were obvious. It is worth noticing that the Bi number can be used as the criteria to determine if the lumped parameters can be used for transient heat transfer calculation [Incropera FP and DeWitt DP, 1996]. When checking the Bi numbers of the walls in this study, it was observed that Bi numbers of the light and medium wall structures are 0.0093 and 0.0594, well below the suggested threshold (0.1) and the Bi number of the heavy wall structure is 0.26, well above 0.1. It indicates that the conclusion made from study matches the criteria based on Bi number. The thickness of the wall corresponding to the Bi number of 0.1 is 330mm. From the comparison, it can be found also that the deviations of the model using the parameters identified by minimizing both ΔQ_{in} and ΔT_{in} and by minimizing ΔQ_{in} only had not obvious difference. Therefore, the results of this study suggest parameter identification of 4R2C model to be performed by minimizing ΔQ_{in} only as it is simpler and gives similar fitness.

Table 3.4 Summary of deviations of Q_{in} and T_{in} of simplified models compared with theoretical for different types of structures

		$\frac{\sum_{k=1}^{n} \lvert Q_{in,t,k} - Q_{in,s,k} \rvert}{n}$ (kW)	$\max \lvert Q_{in,t,k} - Q_{in,s,k} \rvert$ (kW)	$\frac{\sum_{k=1}^{n} \lvert T_{in,t,k} - T_{in,s,k} \rvert}{n}$ (K)	$\max \lvert T_{in,t,k} - T_{in,s,k} \rvert$ (K)
Identification by minimizing ΔQ_{in} and ΔT_{in}					
Light wall	D_{SSPCM}=10mm	0.0017	0.0278	0.0266	0.18
	D_{SSPCM}=20mm	0.0021	0.0303	0.0213	0.34
Median wall	D_{SSPCM}=10mm	0.0082	0.0461	0.1458	0.41
	D_{SSPCM}=20mm	0.006	0.0352	0.1344	0.4
Heavy wall	D_{SSPCM}=10mm	0.0208	0.0615	0.862	1.49
	D_{SSPCM}=20mm	0.0188	0.0432	0.7915	1.44
Identification by minimizing ΔQ_{in}					
Light wall	D_{SSPCM}=10mm	0.0016	0.0366	0.028	0.19
	D_{SSPCM}=20mm	0.0017	0.0309	0.0216	0.17

Median wall	D_{SSPCM}=10mm	0.0082	0.0486	0.1451	0.41
	D_{SSPCM}=20mm	0.006	0.0261	0.1331	0.4
Heavy wall	D_{SSPCM}=10mm	0.0208	0.0615	0.8621	1.48
	D_{SSPCM}=20mm	0.0186	0.0432	0.7898	1.43

3.6 Summary

This chapter presented the simplified physical model for building structure integrated with SSPCM, and particularly a method to identify the parameters of the model, including the wall model and the SSPCM model.

The simplified 3R2C+4R2C model can provide accurate and reliable prediction of the thermodynamic performance of the building structures integrated with SSPCM layer. It was also found that the 2R1C SSPCM model cannot provide the prediction with sufficient accuracy and the deviations of temperature and heat transfer rate predictions were larger than that of the 4R2C SSPCM model in the scale of at least one order of magnitude. The nodal placement (distribution of the resistances and capacitances among the nodes) affects the outputs of the simplified model significantly and the proper nodal placement is essential to ensure that the simplified model can provide accurate and reliable outputs.

Two genetic algorithm-based preprocessors were developed to identify and optimize the parameters on resistances and capacitances of the 3R2C wall model and 4R2C SSPCM model. It was found that GA is an effective tool for optimize the nodal placement of the two models in frequency domain and time domain respectively.

The prediction errors of the model using parameters identified by minimizing both the heat transfers between the internal surface of the structure and indoor air (ΔQ_{in}) and indoor temperature (ΔT_{in}) and by minimizing ΔQ_{in} only had not obvious difference. Therefore, it is suggested that parameter identification of 4R2C model to be performed by minimizing ΔQ_{in} only as it is simpler and gives similar fitness.

CHAPTER 4 VALIDATION OF THE SIMPLIFIED MODEL OF SSPCM BUILDING

This chapter presents the validation of the simplified SSPCM building model. There are twelve test cases, including structures of different thicknesses of wall and SSPCM under different weather conditions. The parameters of the 4R2C of SSPCM model are that identified using the Hong Kong weather profile and listed in Chapter 3, which were identified by minimizing ΔQ_{in} only. Examples of test data and a summary of the accuracy of the model in the Shenyang and Beijing case studies are presented in this chapter.

4.1 Introduction

Prior to adopting the 4R2C model, a 2R1C model for the SSPCM layer was studied and tested. Results of tests show that proper distribution of the resistances might allow indoor temperature and heat transfer predicted by the simplified 2R1C model very close to that given by the theoretical model at some test conditions. But it was hard to find one set of parameters allowing both indoor temperature and heat transfer rate close to that given by the theoretical model at different conditions. For instance, in the case of light wall with 20mm PCM, the average and maximum heat transfer rate deviations were over fifty times of the deviations given by 4R2C model. The average and maximum temperature deviations were over twenty times of the deviations given by 4R2C model.

4.2 Shenyang validation case

The Shenyang weather profile is the temperature profile during 24-30 June. The phase change temperature of SSPCM was 26-27°C. The Q_{in} and T_{in} curves predicted by the simplified model and theoretical model nearly overlapped for light wall and median wall with D_{SSPCM}=10mm and D_{SSPCM}=20mm.

Figure 4.1 presents the comparison between the indoor temperatures predicted by the simplified model and the theoretical model. Figure 4.2 presents the comparison between the heat transfer rates predicted by simplified model and theoretical model. It can be seen that T_{in} and Q_{in} predicted simplified model matched well with that predicted by the theoretical model for the structures with light walls, which is the same as observed in the case when parameter identification was conducted by minimizing both ΔQ_{in} and ΔT_{in}. The results were also satisfactory for median walls but not satisfactory for heavy walls.

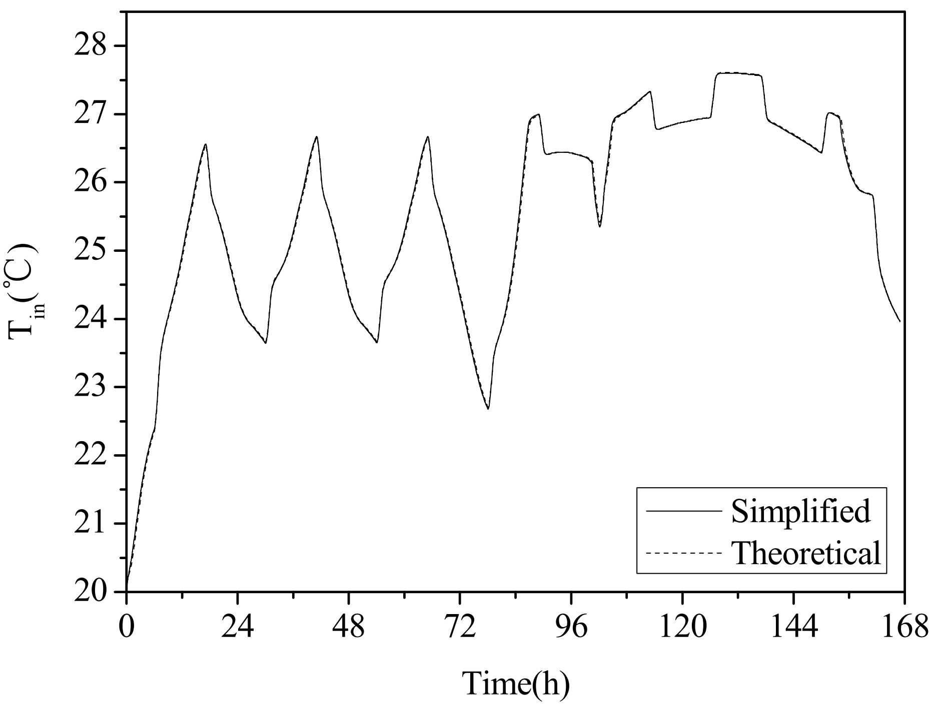

Figure 4.1 Indoor air temperatures (T_{in}) of SSPCM building with light wall (D_{SSPCM} = 10mm) (Shenyang validation case)

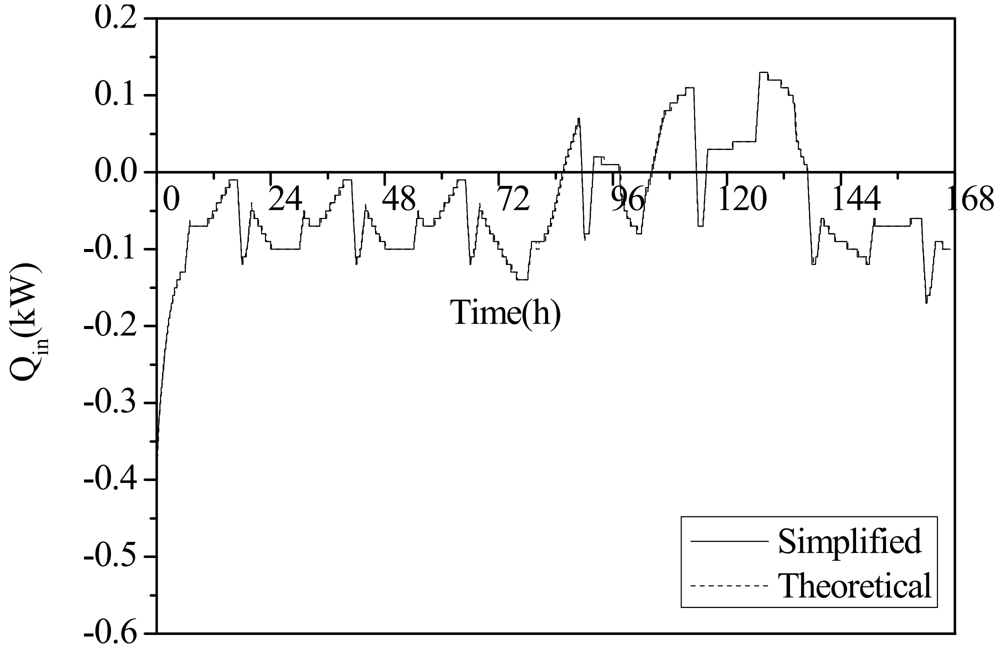

Figure 4.2 Indoor heat exchange (Q_{in}) of SSPCM building with light wall

(D_{SSPCM} = 10mm) (Shenyang validation case)

The deviations of indoor heat exchange (Q_{in}) and indoor air temperature (T_{in}) in the cases of light wall and median wall are listed in Table 4.1.

From this table, it can be found that the deviations of Q_{in} and T_{in} were very small for the light wall with both type of SSPCM structures, and a little bigger for the median wall. The maximum discrepancy of ΔQ_{in} and ΔT_{in} were not large for light wall and median wall.

Table 4.1 Deviations of indoor heat exchange (Q_{in}) and indoor air temperature (T_{in}) for different types of walls (Shenyang validation case)

	$\frac{\sum_{k=1}^{n}\left\|Q_{in,t,k}-Q_{in,s,k}\right\|}{n}$ (kW)		$\max\left\|Q_{in,t,k}-Q_{in,s,k}\right\|$ (kW)	
	D_{SSPCM} =10mm	D_{SSPCM}=20mm	D_{SSPCM}=10mm	D_{SSPCM}=20mm
Light wall	0.0025	0.0026	0.0366	0.036
Median wall	0.0105	0.0078	0.0486	0.0261
	$\frac{\sum_{k=1}^{n}\left\|T_{in,t,k}-T_{in,s,k}\right\|}{n}$ (K)		$\max\left\|T_{in,t,k}-T_{in,s,k}\right\|$ (K)	
	D_{SSPCM}=10mm	D_{SSPCM}=20mm	D_{SSPCM}=10mm	D_{SSPCM}=20mm
Light wall	0.0366	0.0278	0.24	0.18
Median wall	0.1555	0.1473	0.58	0.56

4.3 Beijing validation case

The tests were conducted using the Beijing weather condition in the period between August 10 and August 17. The phase change temperature of SSPCM was 28-29°C in this case study. The Q_{in} and T_{in} curves of simplified model and theoretical model nearly overlapped for light wall and median wall with both D_{SSPCM}=10mm and D_{SSPCM}=20mm.

Figure 4.3 presents the comparison between the indoor temperatures predicted by the simplified model and the theoretical model. Figure 4.4 presents the comparison between the heat transfer rates predicted by simplified model and theoretical model. It can be seen that T_{in} and Q_{in} predicted simplified model matched well with that predicted by the theoretical model for the structures with light wall, which is the same as observed in the case when parameter identification was conducted by minimizing both ΔQ_{in} and ΔT_{in}. The results were also satisfactory for median wall but not satisfactory for heavy wall.

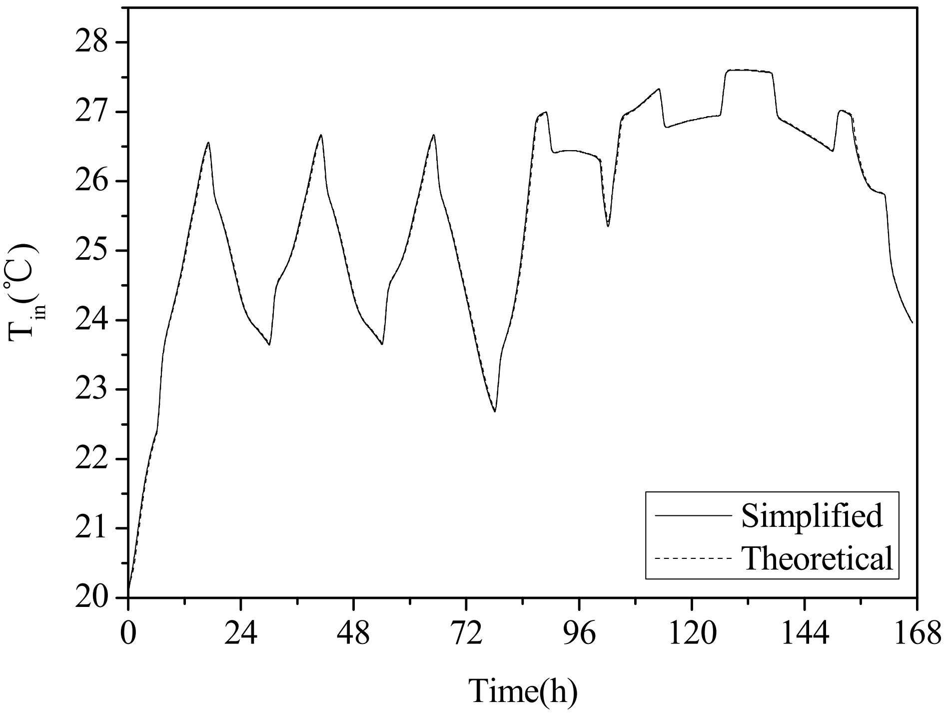

Figure 4.3 Indoor air temperatures (T_{in}) of SSPCM building with light wall (D_{SSPCM} = 10mm) (Beijing validation case)

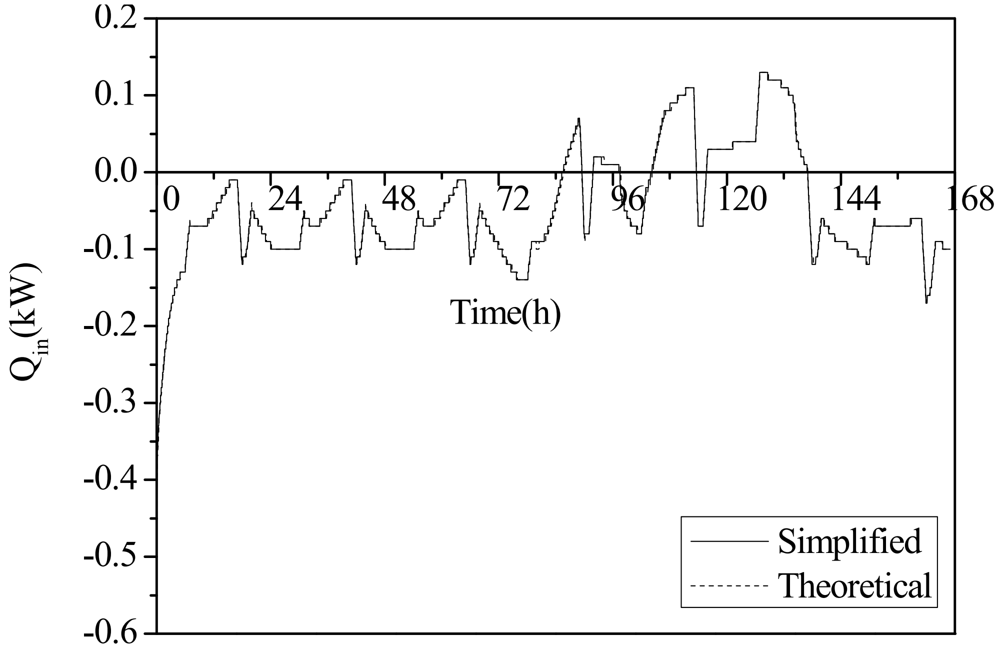

Figure 4.4 Indoor heat exchange (Q_{in}) of SSPCM building with light wall (D_{SSPCM} = 10mm) (Beijing validation case)

The deviations of indoor heat exchange (Q_{in}) and indoor air temperature (T_{in}) for light wall and median wall are listed in Table 4.2. The results were similar to the Shenyang validation case.

From the Shenyang and Beijing validation case studies, it can be found that the simplified model can produce rather accurate predictions which are close to that predicted by the theoretical model for both light walls and median walls. For one type of wall of certain wall and PCM layers, a set of parameters can allow the simplified model suitable for the applications in different conditions including different weather conditions and different phase change temperatures.

Table 4.2 Deviations of indoor heat exchange (Q_{in}) and indoor air temperature (T_{in}) for different types of walls (Beijing validation case)

	$\frac{\sum_{k=1}^{n}\left\|Q_{in,t,k}-Q_{in,s,k}\right\|}{n}$ (kW)		$\max\left\|Q_{in,t,k}-Q_{in,s,k}\right\|$ (kW)	
	D_{SSPCM}=10mm	D_{SSPCM}=20mm	D_{SSPCM}=10mm	D_{SSPCM}=20mm
Light wall	0.0014	0.0018	0.0489	0.0332
Median wall	0.0071	0.0056	0.065	0.0441
	$\frac{\sum_{k=1}^{n}\left\|T_{in,t,k}-T_{in,s,k}\right\|}{n}$ (K)		$\max\left\|T_{in,t,k}-T_{in,s,k}\right\|$ (K)	
	D_{SSPCM}=10mm	D_{SSPCM}=20mm	D_{SSPCM}=10mm	D_{SSPCM}=20mm
Light wall	0.0262	0.0309	0.35	0.48
Median wall	0.2766	0.1024	1.39	0.71

4.4 Application issues of the simplified model

The simplified dynamic model of building structure integrated with SSPCM is validated above, and it shows that the simplified model can work well for the light and median wall structures. An actual building was chosen for application tests and some of the results are provided below. The set-point of indoor temperature was 24°C for the office hour between 8:00 AM and 8:00 PM, the phase change temperature was 23.5-24.5°C. In the same condition, the comparisons between the indoor temperatures of

SSPCM building and reference building in Beijing and Hong Kong are presented in Figure 4.5 and Figure 4.6, respectively.

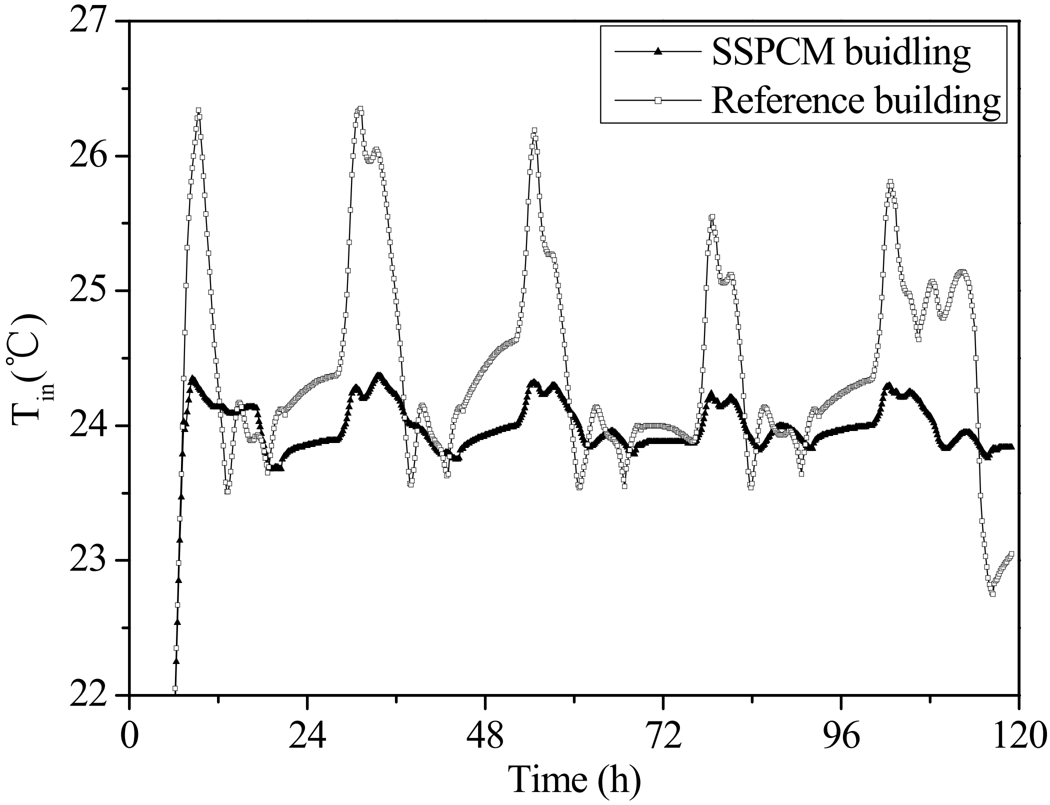

Figure 4.5 Indoor air temperatures (T_{in}) of SSPCM and reference building in Beijing

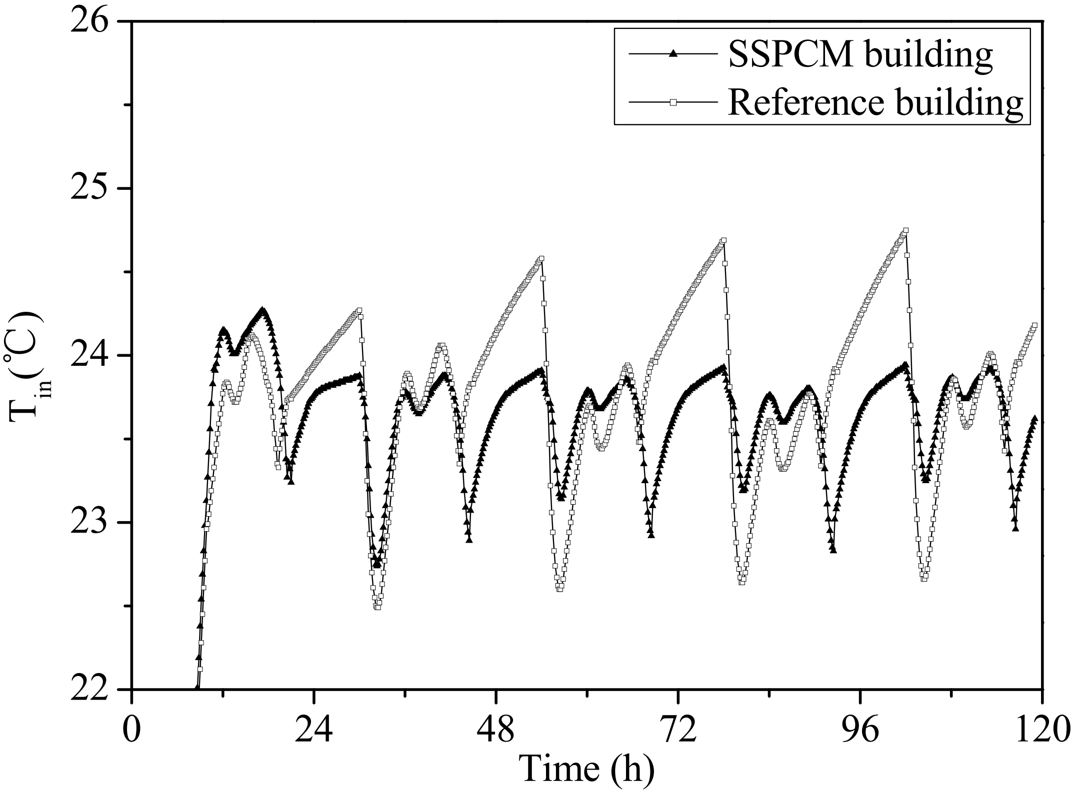

Figure 4.6 Indoor air temperatures (T_{in}) of SSPCM and reference building in Hong Kong

In the Beijing weather condition, the indoor air temperature of the SSPCM building was around 24°C in the office hour, and the temperature had a little swing, but the indoor air temperature was nearly 2°C higher for the reference building. In the Hong Kong weather condition, the indoor air temperature of the SSPCM building was a little below 24°C in the office hour, but the indoor air temperature was nearly 1°C higher for the reference building.

As mentioned in the literature review chapter, there were a few mathematical models [Zhang YP, Su Y et al. 2001. Halford CK and Boehm RF, 2007. Heim D and Clarke JA, 2004 et al.] had been developed to analysis the thermodynamic process of PCM when it is used in buildings. Most of them were proven having satisfactory accuracy in predicting the thermal dynamic and heat transfer process of PCM structures. These models provide good basis to study the behavior and potential energy benefits of using PCM materials in buildings. However, concerning the complexity of the computing programs for solving the equations of models and the computing speeds of the programs, they have obvious limitations in engineering applications. Some of the models were actually based on the finite elements method. The others are in the format of partial differential equations or need iterative processes for solving the equations. To obtain accurate solutions, finite elements methods or other numerical methods are needed. These limitations may not be a problem for the scientific studies concerning the use of PCMs. However, when the PCM materials are adopted as an engineering option in industrial practice, these models are too complicated concerning the programming efforts needed, program size and computation speed in many applications. For instance, the design evaluation of full scale buildings or large buildings, and the online control applications, complex models of large program sizes and long computation time will not be applicable.

There are no details on program sizes and computation speed available for the above models. However, one such type of TRNSYS models can be found. It is the TRNSYS model developed by Juha Jokisalo, Piia Lamberg, Kai Sirén [2005]. The FORTRAN code of this model has over 270 lines while of FORTRAN code of the simplified model developed in this study has 20 lines only. To simulate a single zone with air conditioning systems, the computation time when using this TRNSYS PCM wall model is 11 times of the computation time using the normal TRNSYS wall model without PCM. To simulate the same single zone system, the computation time when using this TRNSYS PCM wall model was over 250 times of the computation time when using the simplified model developed in this study (also in TRNSYS platform running in the same personal computer).

4.5 Summary

The simplified building model can well represent thermodynamic performance (heat transfer to indoor space) of the building envelopes integrated with SSPCM for walls of normal thickness (not more than 300mm approximately) including light wall and median wall. The simplified building model can't work well for heavy wall because the node placement is too little and 3R2C can't provide the same veracity.

The Bi number (<0.1) can be also used to check if the simplified model is valid to the strictures, which matches the observation in this study. Test results also show that model is suitable the SSPCM layer of normal thickness in practical applications (not significantly more than 20mm). The simplified model is very simply in programming and has very high peed in computation. It is therefore very suitable to the applications of system performance evaluation, optimal control, diagnosis, etc.

CHAPTER 5 BUILIDNG SYSTEMS AND TEST PLATFORM

This chapter presents the reference and SSPCM buildings, the air-conditioning system, dynamic models of building and VAV air-conditioning systems, the test conditions and control strategies used in the following studies. The models incorporate the thermal, hydraulic, environmental and mechanic characteristics and energy performance, to simulate the system controlled by strategies implemented in Energy Management and Control Systems (EMCS).

5.1 Introduction

Dynamic simulation of HVAC system provides a convenient and low cost tool in testing, commissioning and evaluating HVAC system control strategies or the control programs implemented in Energy Management and Control Systems (EMCS) [Lebrun J, Wang SW, 1993. Wang SW, 1997]. Dynamic models, which are convenient to use and well represent the dynamic characteristics in all the aspects of concern, are the basis for practical applications.

Recently, many researchers have focused on dynamic modeling and simulation of HVAC systems. Studies on the VAV air-conditioning system dynamic modeling and simulation for control applications are also being conducted. However, those models focus on simulating the thermal dynamic and energy characteristics.

When the on-line control performance of supervisory and local control strategies are of concern in order to test, evaluate and commission the strategies under simulated ‘real-life’ conditions, the realistic characteristics of air flow-pressure balance needs to be incorporated into the system simulation. The real-life environmental behavior of the system also needs to be incorporated into the system simulation due to the increasing concern on the effects of control strategies on indoor environment. This was not sufficiently addressed in the past although there are studies conducted to study the environmental control strategies using simulation method. The simulation test of on-line supervisory strategies implemented in integrated digital stations of EMCS also requires the simulation of the integrated VAV system of large scale.

5.2 Buildings and VAV air-condition system

The building used as the reference in this study refers to an existing forty-six storey commercial building in Hong Kong. The floor under study is an office floor of about 2400m^2 floor areas. The offices and the associated air-conditioning system in half of the floor selected are simulated, which have a total floor area of about 1200m^2. The external walls are concrete walls with the thickness of 115mm. The internal walls are brick walls. The area of the window is 20% of the external wall. The total areas of external walls (excluding window area) are 76.44m^2, 37.44m^2, 37.44m^2, 76.44m^2, 34.32m^2, 34.32m^2 for Zone 1 to Zone 6, respectively. The SSPCM consists of paraffin as dispersed PCM and high-density polyethylene (HDPE) as supporting material. The SSPCM plates are attached to the inner surfaces of all external walls. The thickness of SSPCM is 20mm. The total area of SSPCM plates on studied floor area (half a floor) is 296.4m^2, and the volume of the SSPCM plates is 5.928m^3.

The air-conditioning systems used for both reference building and SSPCM building are exactly the same. Two central air handling units (AHU) serve the floor. Each serves half of the floor. One AHU serving the offices under study consists of a VAV system and a constant air volume (CAV) system (for perimeter offices only). The design air flow rates of the VAV system and CAV system are 6.0m^3/s and 1.4m^3/s, respectively.

The AHU/VAV system and their associated offices are simulated to test the control, energy performances and indoor thermal environment of the air-conditioning system under different control strategies implemented in EMCS. The perimeter offices orientating north are equipped with CAV terminals beside VAV terminals, and the others are equipped with VAV terminals only.

The floor area simulated consists of eight open plan offices (zones). The floor areas of the offices are shown in Figure 5.1. The north, west and east walls are external walls connecting to the outside. The south and other walls are internal walls connecting different offices.

A schematic of the air-conditioning system serving the office floor is presented in Figure 5.2. The chilled water flow rates through cooling coils are modulated to control the coil outlet air temperature at the desired set-point. Two variable speed fans are used as the VAV supply fan and return fan respectively. The CAV supply fan is a constant speed fan. The speed of the VAV supply fan is modulated to control the supply air static pressure in the main supply duct at the predetermined set-point. The return fan speed is modulated to control the exfiltration flow rate in order to maintain certain positive pressure in the building. It is achieved by controlling the difference between the total supply and return air flow rates within the upper and lower limits.

The CAV system is used when the cooling load of the perimeter zones is high.

Pressure-independent VAV terminals are used, which employ the cascade control logic based on PI control. The indoor air temperature (PI) controller of each zone determines the set-point of air flow rate of the zone VAV terminal. The flow controller of the VAV terminal modulates the damper of the terminal to control the air flow rate at its set-point. The outdoor air controller is used to control the outdoor air flow by modulating the dampers. The minimum outdoor air flow rate set-point is determined by the DCV strategy. The set-point is optimized by making a compromise between two control strategies, i.e. combining the enthalpy control and demanded ventilation [Wang SW, 1999].

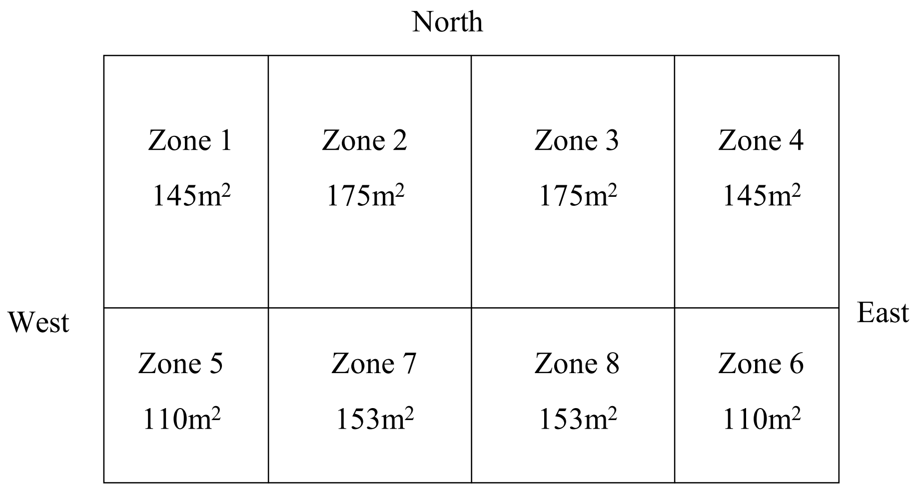

Figure 5.1 Selection of zones of simulated floor

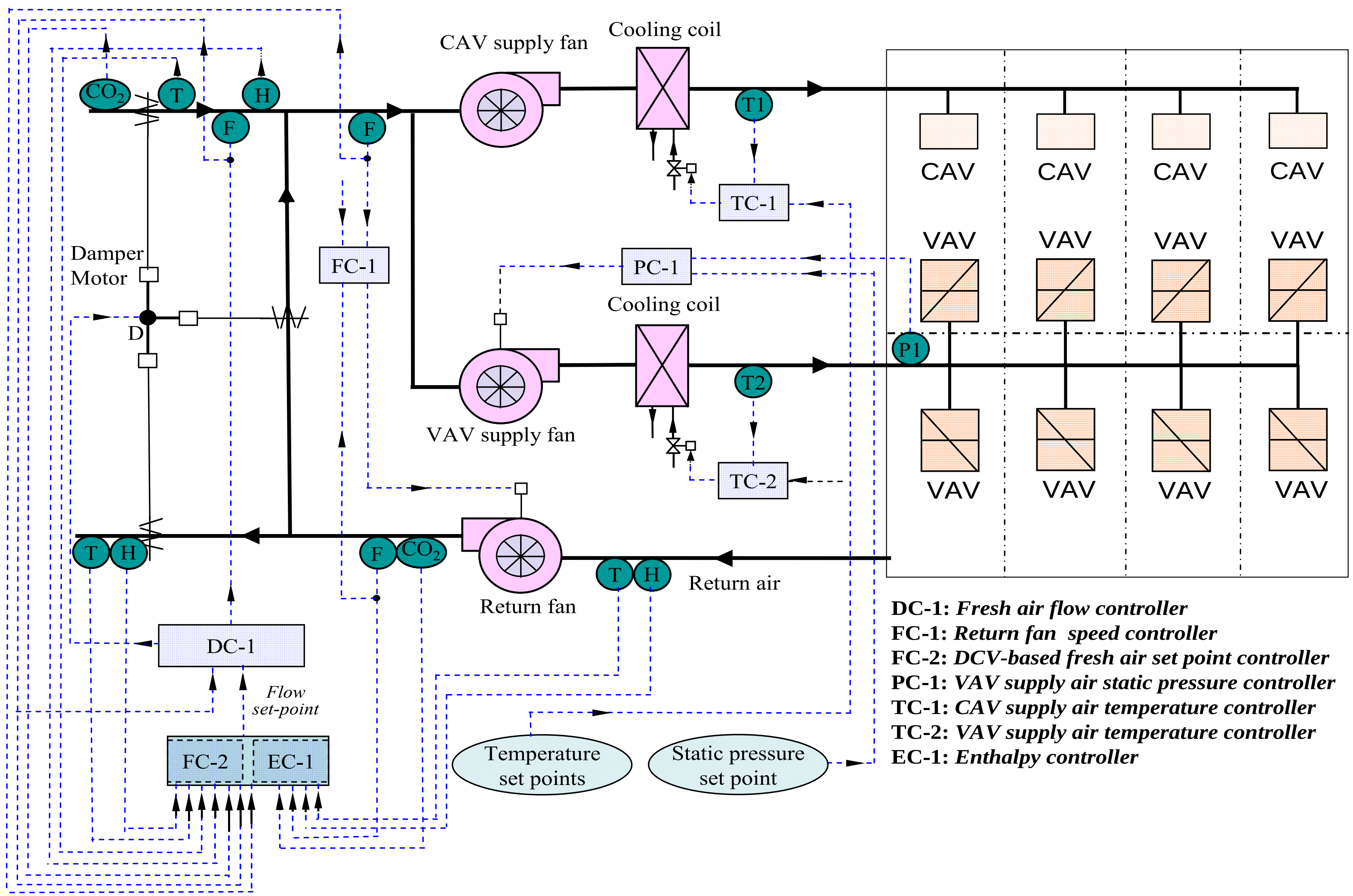

Figure 5.2 Schematic of Air-conditioning system

5.3 Simplified building models

A simplified building model simulates the dynamic balance of energy, moisture, CO_2 and a pollutant, which is suitable for testing the control, energy and environmental performances of on-line local and supervisory control strategies. It is developed on the basis of improving the conceptual building model developed in the IEA Annex 10 and 17 [Wang SW, 1999]. The modeling of CO_2 and another pollutant aims at simulating the occupant and non-occupant generated pollutants although both can be used to simulate any type of pollutants if the relevant generation sources are properly modified.

The model represents the open plan office floor by a network of thermal resistance, thermal capacitance and air volume. Each space is considered as a node of well mixed air volume with uniform temperature, moisture, CO, and pollutant concentration. The connections between zones are the air mass exchanges caused by air flow. For the SSPCM building, the external wall of each zone is represented by 3 resistances and 2 capacitances, and the shape stabilized phase change material (SSPCM) plate as inner surface of each external wall is represent by 4 resistances and 2 capacitances. For the reference building, the external wall of each zone is the same with the SSPCM building except without the SSPCM layer.

The internal structure and furniture in each zone are represented by a node of thermal capacitance connected to the zone through a thermal resistance. The model uses a simplified method to compute the heat load of solar radiation absorbed by the external walls by means of an equivalent ‘sol-air’ temperature. The ‘sol-air’ temperature is defined here as an equivalent temperature, which takes account of the effect of the solar radiation absorbed by building external walls (including absorbency and emission) as the effect of increment of outside air temperature to building. The solar heat gain transmitted through the windows is added directly to the node of the internal structure and furniture of a relevant zone. It is firstly absorbed by internal structures and furniture, and then released to the zone air due to the temperature difference. It is modified from the conventional definition of the 'sol-air' temperature [Laret L and Liebecq G et al. 1987], which is used in the building model of IEA Annex 10 and 17.

The dynamic heat transfer characteristics of the buildings are simulated using the simplified R/C models [Kaygusuz K, 1999]. The simplified model of the SSPCM building is shown in Figure 5.4. According to the best matching between the heat transfers of the simplified model and theoretical model, all the resistances and capacitances can be identified by the GA (genetic algorithm)-based scheme as presented previously in detail in Chapter 3.

The heat transfer of the external wall integrated with SSPCM can be represented with the following differential equations:

$$C_{w1}\frac{dT_{w1}(t)}{dt}=\frac{T_{sol}(t)-T_{w1}(t)}{R_{w1}}-\frac{T_{w1}(t)-T_{w2}(t)}{R_{w2}} \tag{5.1}$$

$$C_{w2}\frac{dT_{w2}(t)}{dt}=\frac{T_{w1}(t)-T_{w2}(t)}{R_{w2}}-\frac{T_{w2}(t)-T_{p1}(t)}{R_{w3}+R_{p11}} \tag{5.2}$$

$$C_{p1}\frac{dT_{p1}(t)}{dt}=\frac{T_{w2}(t)-T_{p1}(t)}{R_{w3}+R_{p11}}-\frac{T_{p1}(t)-T_{p2}(t)}{R_{p12}+R_{p21}} \tag{5.3}$$

$$C_{p2}\frac{dT_{p2}(t)}{dt}=\frac{T_{p1}(t)-T_{p2}(t)}{R_{p12}+R_{p21}}-\frac{T_{p2}(t)-T_{in,a}(t)}{R_{p22}} \tag{5.4}$$

$$C_{air}\frac{dT_{in,a}(t)}{dt}=\frac{T_{p2}(t)-T_{in,a}(t)}{R_{p22}+R_{air}}+Q_{oe} \tag{5.5}$$

where, R and C are resistance and capacitance. T is temperature. Subscripts *w, p, in*, indicate brick wall, PCM, indoor air. Q_{oe} is the heat load generated by occupants and equipments. R_{air} is the convection heat transfer resistance between indoor air and wall (PCM) surface. The properties of the building envelopes and PCM layer are relatively easy to obtain which can be utilized to establish the simplified 3R2C and 4R2C models. To maximize the benefit from the energy storage using SSPCM plates in the air-conditioned building, the melting temperature and heat of fusion are 23-24°C and 160kJ/kg, respectively.

The configuration of the reference building is the same as the SSPCM building except without the SSPCM layer. The dynamic heat transfer processes of the envelopes are simulated by the similar equations after eliminating Equation (5.3) and (5.4).

5.4 Air-conditioning system models

The components of the air-conditioning system and its control system to be simulated include: cooling coil, variable and constant speed fans, duct, sensors, VAV terminal, control actuators, water valves and air dampers, air pressure-flow balance of the system, and local PI controllers. To simulate the control characteristics of the system, the models of the cooling coil, duct, sensors, and control actuators are dynamic models and the realistic operation process of the digital controller is simulated. A brief on the main models of the system components is provided here below and more details can be found in the reference [Wang SW, 1999]

A model is developed to simulate the pressure-flow balance of the building and air-conditioning system. The effect of air velocity and wind effect on the system pressure-flow balance is neglected. The flow resistances of the VAV and CAV filters and cooling coils are considered to be constant. The constant flow resistance before VAV pressure sensor represents the resistance of the air attenuator and duct before the sensor. The resistance of the air duct after the VAV pressure sensor is considered to be constant. The constant CAV duct flow resistance represents the flow resistance of the CAV air attenuator and duct. The flow resistances of the CAV terminals and diffusers are considered to be constant. The resistances of VAV terminals and diffusers are variables, which depend on the positions of the VAV dampers. The pressure in the entire occupied space is considered to be uniform when simulating the system pressure-flow balance. The air leakage through the building envelop is computed by assuming a constant flow resistance linking the occupied space to outside. The flow resistance of return duct is considered to be constant. The resistances of the outdoor air, recycle air and exhaust air dampers vary according to the positions of the dampers.

The static pressure-flow characteristics of the VAV supply fan, CAV supply fan and return fan are simulated by separate models. The pressure flow balance computation is based on the air mass conservation and pressure balance.

A duct model is developed to simulate the heat loss through duct wall, dynamic effects of the duct wall and the effects of transfer delay on temperature, moisture, CO, and the pollutant. A duct is divided into a number of sections considering the duct length and the velocity range of the air flowing inside. The process of the air flowing in the duct at a simulation step is assumed consisting of three separate 'sub-processes': moving of the air segments; mixing of air within individual sections and the heat exchange with outside through duct wall.

To simulate an axial fan, the state of the fan is represented by three variables (φ, ζ, λ) the air volume flow rate, fan total pressure rise and fan absorbed power, respectively, as shown in equations (5.6)-(5.8).

$$\varphi = \frac{4 \cdot v_a}{\pi^2 \cdot D^3 \cdot N} \tag{5.6}$$

$$\zeta = \frac{2 \cdot PT_{fan}}{\rho_u \cdot (\pi \cdot D \cdot N)^2} \tag{5.7}$$

$$\lambda = \frac{800 \cdot W_{fan}}{\pi^4 \cdot D^5 \cdot N^3 \cdot \rho_a} \tag{5.8}$$

A dynamic model is developed to simulate the cooling coil. The model includes a steady-state approach and a dynamic approach. The model includes a steady-state approach and a dynamic approach. A first order differential equation is used to represent the dynamics of a coil with lumped thermal mass. The dynamic equation on the basis of energy balance ensures that the energy is conserved.

$$C_c \frac{dt_{c1}}{d\tau} = \frac{t_{a,in} - t_c}{R_1} - \frac{t_c - t_{w,in}}{R_2} \tag{5.9}$$

where, t_c is the mean temperature of coil, $t_{a,in}$ and $t_{w,in}$ are the inlet air and water temperatures. C_c is the overall thermal capacity of the coil, R_1 and R_2 are the overall heat transfer resistances at the air and water sides.

The air and water temperatures at the outlet ($t_{a,ex}$, $t_{w,ex}$) therefore can be computed by the heat balances of both sides:

$$t_{a,ex} = t_{a,in} - \frac{SHR \cdot (t_{a,in} - t_c)}{R_1 \cdot C_u} \tag{5.10}$$

$$t_{w,ex} = t_{w,in} - \frac{t_c - t_{w,in}}{R_2 \cdot C_w} \tag{5.11}$$

where, C_a and C_w are the capacity flow rates of air and water, *SHR* is the sensible heat ratio. *SHR* uses the same value calculated in the same inlet condition in the steady state case using the by-pass factor method.

A 'realistic' controller model is developed to simulate the DDC controllers. The model represents the following functions of the DDC (Direct Digital Control) functions, discrete-time operation of digital controllers and supervisory control strategies. The time scheduling of a sampling cycle is considered to be four steps: process variable sampling, control outputs computation, control signal output, and waiting time for the next sampling cycle. The PID control function used in DDC loops uses the ISA algorithm. Its discrete form is used in the models.

An actuator model is used to represent the characteristics of actuators. The actuator is assumed to accelerate very quickly and then turn at constant speed. A minimum change (e.g. the sensitivity of the actuator defined as a parameter of the model) in demanded position is required to restart the actuator. The model includes the hysteresis in the linkage between actuators and valves or dampers. If a valve stem is driven by a rotary actuator, the speed of the valve stem varies with the position of the crank.

The dynamics sensor model is used to simulate the temperature, pressure, flow and CO_2 sensors using the time constant method. Different time constants are used for different sensors depending on the characteristics of the sensors and the measured variables and the locations of the sensors.

5.5 Test conditions and control strategies

5.5.1 Weather profiles

The buildings with the air-conditioning system were tested in selected days in Beijing and Hong Kong, which represent the typical northern and southern weather characteristics in China. The selected days in the tests are July 21 to July 25 in Beijing and Hong Kong respectively. The solar radiation is below 600W/m^2 and 1000W/m^2 in Beijing and Hong Kong, respectively. The daily solar radiation in Beijing is lower than of Hong Kong in most time of the days. The outdoor temperature in Beijing is between 17.5°C to 31.5°C in the five test days, and the outdoor temperature in Hong Kong is between 25.5°C to 31.5°C in the five test days. The maximum daily temperature variation is 14.0°C in Beijing test days, which is much higher than that (6.0°C) in the Hong Kong test days. The hourly outdoor temperature and solar radiation in the selected days are show in Figure 5.3 and Figure 5.4, respectively.

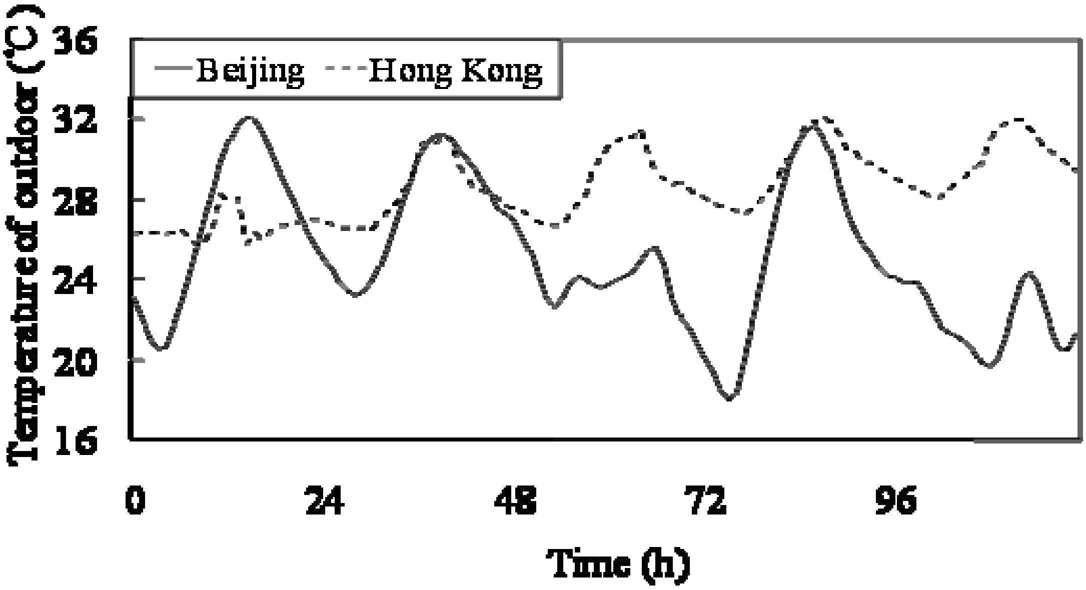

Figure 5.3 Hourly outdoor air temperatures

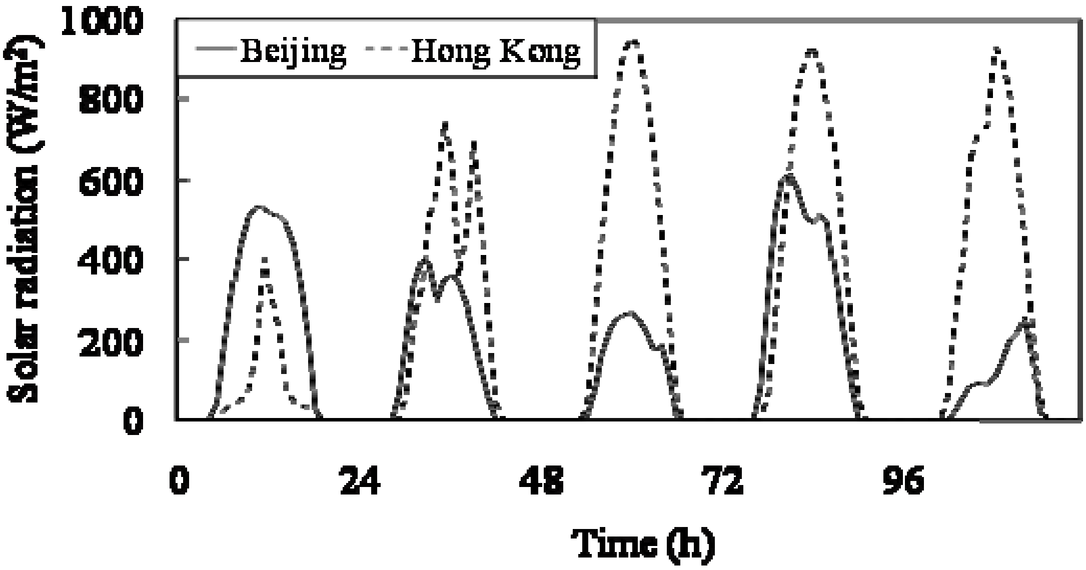

Figure 5.4 Hourly solar radiations

According to the electricity pricing policy of the Beijing Electric Power Company, the hourly electricity price of commercial building in Beijing is shown in Table 5.1.

Where the “time-based pricing” policy is adopted. Three different prices are applied during different five periods in a day. The periods of 8:00 AM-11:00 AM and 6:00 PM-11:00 PM are peak period while the electricity price is 1.2 CNY/kWh. The period over night (11:00 PM-7:00 AM) is off-peak period while the electricity price is 0.3 CNY/kWh. During the rest of the day, the electricity price is 0.8 CNY/kWh.

The electricity pricing policy in Hong Kong is different from Beijing. There are four tariffs offered by the major power company in Hong Kong, China Light and Power Company (CLP), which could be selected by users. The demand limiting period is between 9:00 AM and 9:00 PM. The actual peak demand (kVA) is an average over half hour period which represents the highest electricity consumption of a user. According to the tariff of China Light and Power Company (CLP), the electricity tariff suitable to commercial buildings of the scale used in this study is shown in Table 5.1 also. The electricity bill of a user consists of two parts, the peak demand charge and energy consumption charge.

Table 5.1 Details of time-based pricing and energy-plus-demand-based pricing

<table>
<tr><th colspan="3">Time-base Pricing (Beijing)</th><th colspan="4">Energy-plus-demand-based Pricing (Hong Kong)</th></tr>
<tr><td colspan="3">Energy consumption Part (CNY/kWh)</td><td colspan="2">Peak Demand
Part (HKD/kVA)</td><td colspan="2">Energy Consumption
Part (HKD/kWh)</td></tr>
<tr><td>8AM-11AM
6PM-11PM</td><td>7AM-8AM
11AM-6PM</td><td>11PM-7AM</td><td>On-peak
Period</td><td>Off-peak
Period</td><td>On-peak
Period</td><td>Off-peak
Period</td></tr>
<tr><td rowspan="2">1.2</td><td rowspan="2">0.8</td><td rowspan="2">0.3</td><td>61.9
(first 650)</td><td>0.0
(less than the
on-peak peak)</td><td>0.632
(first
200,000)</td><td rowspan="2">0.562</td></tr>
<tr><td>59.1
(exceeding
part)</td><td>24.2
(lager than the
on-peak peak)</td><td>0.618
(exceeding
part)</td></tr>
</table>

In the manipulating the test data for comparison studies, the overall COP of the chilling system used was 3 and the power factor of the electrical systems used was 0.9. The energy consumption when using the energy-plus-demand-based-pricing was calculated on the basis of the following assumptions. The energy consumptions of all the 31 days in July are the same as that in the selected test day. The peak demand of the month is the peak demand in the test day. The electricity consumption profiles of all other floors in the building flows are the same with the profile of the floor area studied (i.e. the electricity consumption profile is 92 times of that in the studied floor area). The electricity cost of the studied air-conditioning system in the test day is its contribution to the overall monthly electricity bill of the building.

5.5.2 Introduction of control strategies

Two control strategies, namely load shifting control strategy and demand limiting control strategy are developed and used in the cases of time-base pricing policy and energy-plus-demand-based pricing respectively. The *load shifting control strategy* attempts to maximize the reduction of the energy consumption during the peak period by using the lower electricity to store the cooling energy during the off-peak period. The *demand limiting control strategy* attempts to maximize the reduction of the peak demand during the demand-limiting period by resetting the zone temperature set-point. These two control strategies aims at saving daily electricity cost in time-based pricing and energy-plus-demand-based pricing policies respectively.

The phase change materials can discharge or charge “cold” during melting and freezing respectively. In this study, the SSPCM is used for cooling during the on-peak time in the occupied hours. For the conventional night ventilation, the phase change materials might not melt/freeze completely and make the full use of them.

The load shifting control and demand limiting control strategies are effective methods to some extent. If the SSPCM can be frozen to charge cold mostly using pre-cooling during the off-peak time and melt to discharge cold during the on-peak time, the peak cooling load will be reduced effectively so that to reduce the on-peak electrical charge. The zone temperature set-point for load shifting (LS), demand-limiting (DL) and normal control strategy are shown in Figure 5.5.

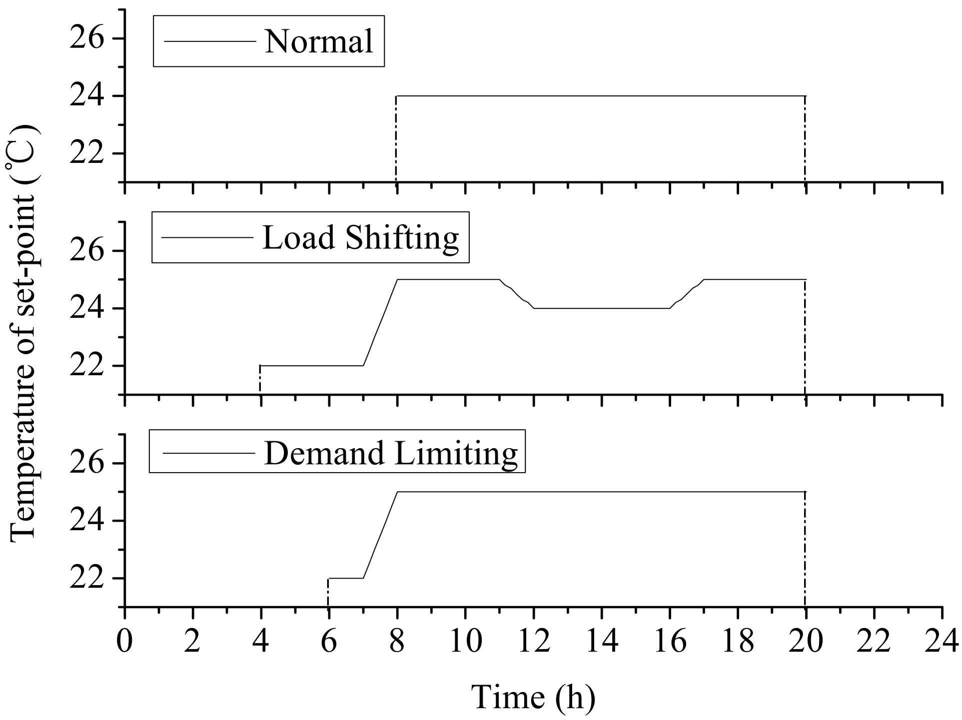

Figure 5.5 Zone temperature set-point for normal, load shifting and demand-limiting control

The occupied period is from 8:00 AM to 8:00 PM. Under the normal control, the set-point of indoor is fixed at 24.0°C during the occupied period and the system operates between 7:00 AM and 8:00 PM.

Under the load shifting control, the pre-cooling period is from 4:00 AM to 7:00 AM, the zone temperature set-point of pre-cooling is 22.0°C, the temperature set-point is raised from 22.0°C to 25.0°C from 7:00 AM to 8:00 AM, and then fixed at 25.0°C last to 11:00 AM, and then falls to 24.0°C at 12:00 AM, fixed at 24.0°C before 4:00 PM and raised to 25.0°C at 5:00 PM, then fixed at 25.0°C until 8:00 PM. Between 8:00 PM and 4:00 AM, the air-condition system is turned off.

Under the demand limiting control strategy, the pre-cooling period is from 6:00 AM to 7:00 AM which the indoor air temperature is set at 22.0°C, and then is raised to 25.0°C at 8:00 AM, the temperature set-point is fixed at 25.0°C until 8:00 PM. Between 6:00 AM and 8:00 PM, the air-condition system is turned off. .

5.6 Summary

In this study, there are two types of building constructions used, including SSPCM building and reference building. Three different control strategies were implemented, including normal control, load shifting control and demand limiting control. Two cities of typical climates, Beijing and Hong Kong, are chosen as the test locations.

The major performances data concerned in the test cases include the electricity consumption/cost and indoor thermal environment of SSPCM building and reference building under three different control strategies in Beijing and Hong Kong climates and electricity pricing policies. The results of only one test day in each case are presented in this thesis.

CHAPTER 6 INDOOR THERMAL ENVIRONMENT IN AIR-CONDITIONED SSPCM BUILDING

This chapter presents the indoor thermal environment of air-conditioned building integrated with SSPCM. The air-conditioned building is an office building introduced in Chapter 5. The indoor thermal environment concerned is mainly the indoor temperatures of zones in the selected floor. The indoor environment of the reference building is also presented for comparison, which is very similar with the SSPCM building except without the SSPCM layer.

6.1 Introduction

The thermal performance enhancement of a building due to the use of PCMs depends on many factors, including climate, design, orientation of the construction, and the amounts and types of PCMs used. In this air-conditioned building, the design, orientation of the construction is decided. The amounts and types of PCMs are selected based on the optimal characteristic of the light construction in using PCM. Therefore, the climate is a variable, including typical northern city (Beijing) and southern city (Hong Kong) in this study.

6.2 Indoor temperatures of zones

In this office building, the occupied hour was between 8:00 AM and 8:00 PM. The HVAC units were turned on during this period, and turned off after the office hour. The set-point of indoor temperature was maintained at 24.0°C during the occupied hours. The selective floor is divided into eight zones, the zone 1 to zone 6 connects to the outside, and zone 7 and zone 8 connects to the inside. Due to the different orientation and solar radiation on each external wall, the eight zone temperatures are also different during the same time. The phase change temperature of PCM is between 23.0°C and 24.0°C in this study.

Figure 6.1 and Figure 6.2 present the indoor air temperatures of reference building and SSPCM building in Beijing, respectively. Figure 6.3 and Figure 6.4 present the temperature of zone 1 and zone 4 in Beijing, respectively.

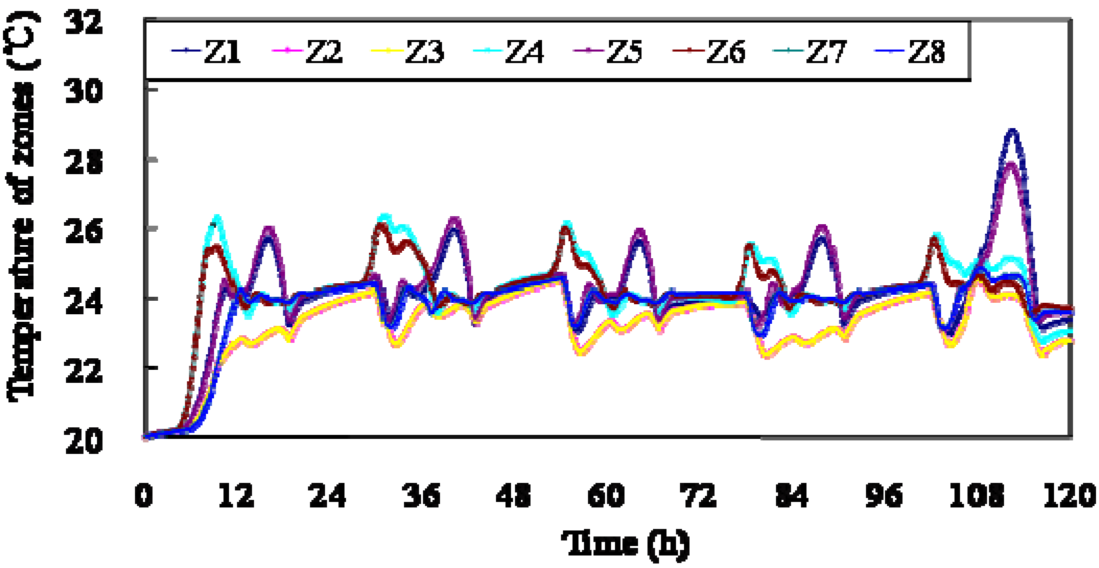

Figure 6.1 Indoor air temperatures of reference building (Beijing test case)

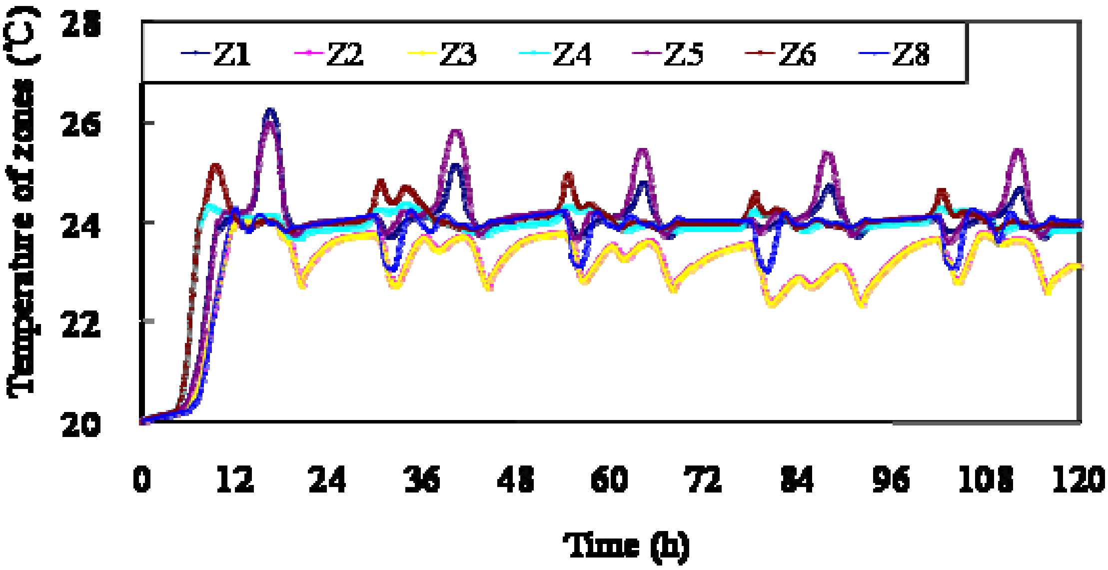

Figure 6.2 Indoor air temperatures of SSPCM building (Beijing test case)

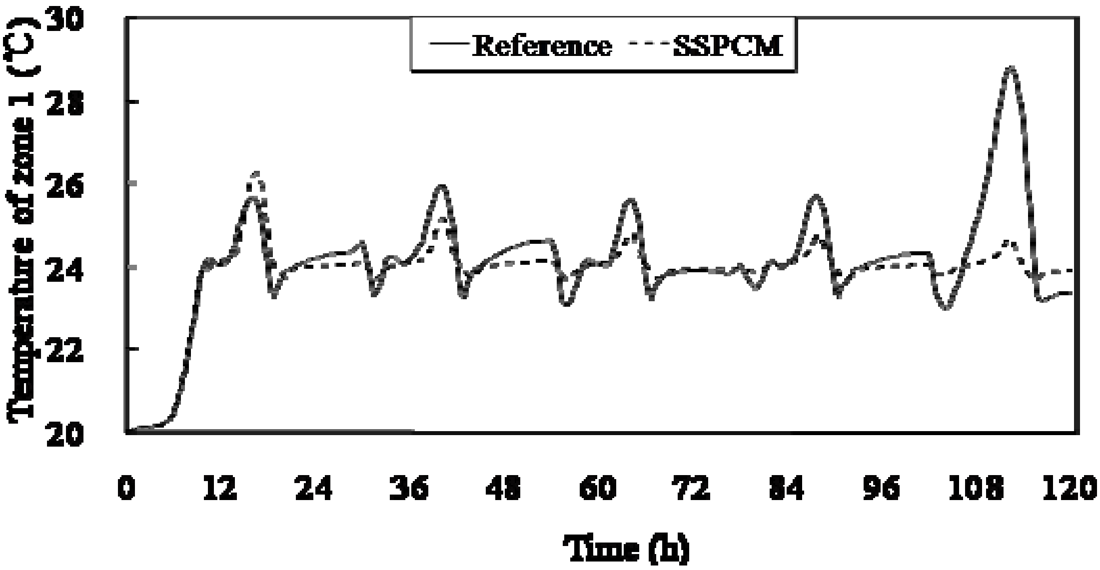

Figure 6.3 Indoor air temperature of zone 1 (Beijing test case)

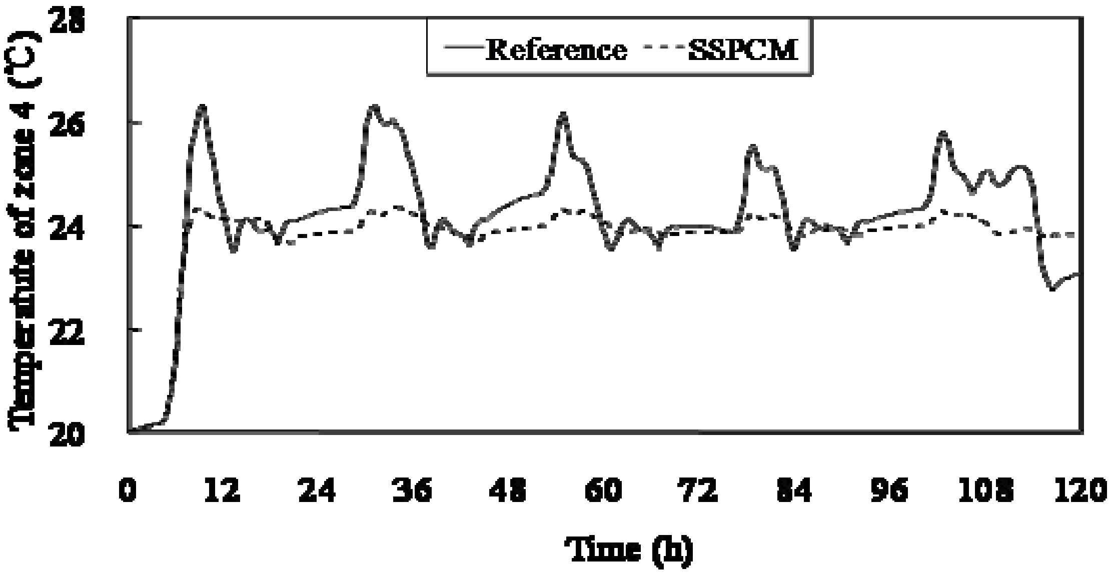

Figure 6.4 Indoor air temperature of zone 4 (Beijing test case)

Figure 6.5 and Figure 6.6 present the indoor air temperature of reference building and SSPCM building in Hong Kong, respectively. Figure 6.7 and Figure 6.8 present the temperature of zone 1 and zone 4 in Hong Kong, respectively.

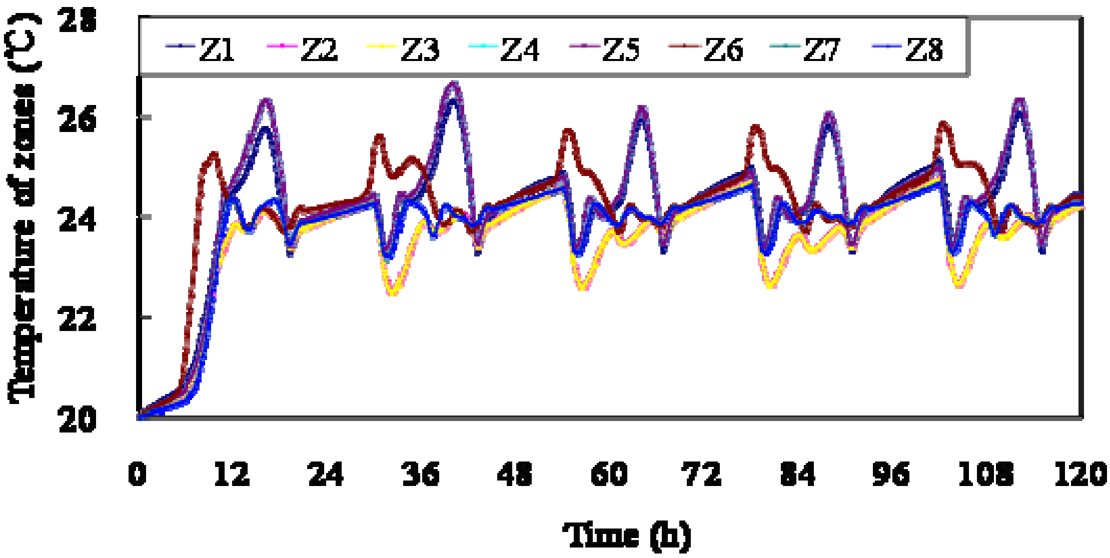

Figure 6.5 Indoor air temperature of reference building (Hong Kong test case)

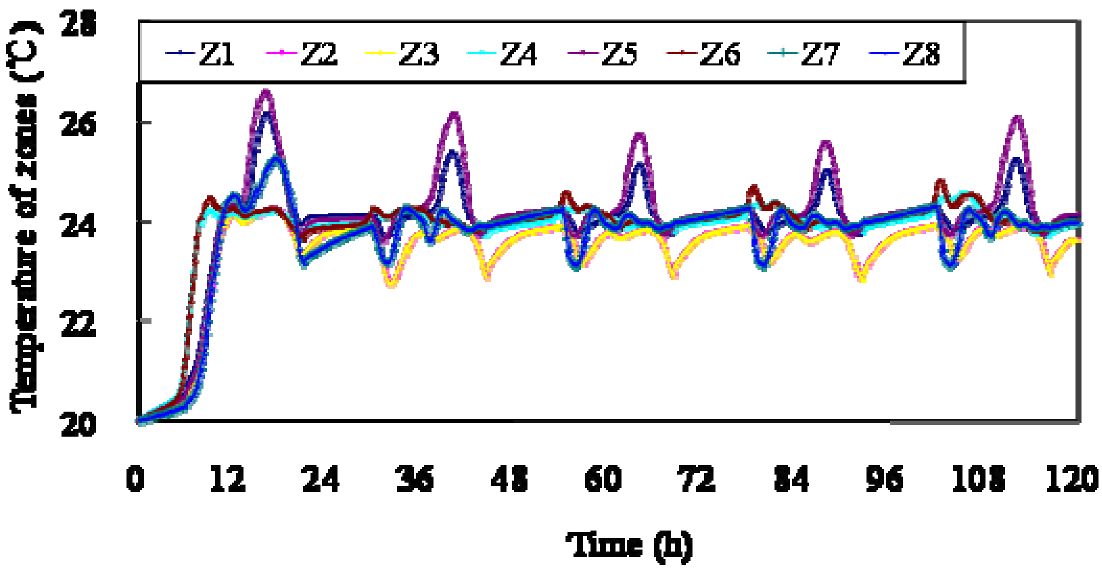

Figure 6.6 Indoor air temperature of SSPCM building (Hong Kong test case)

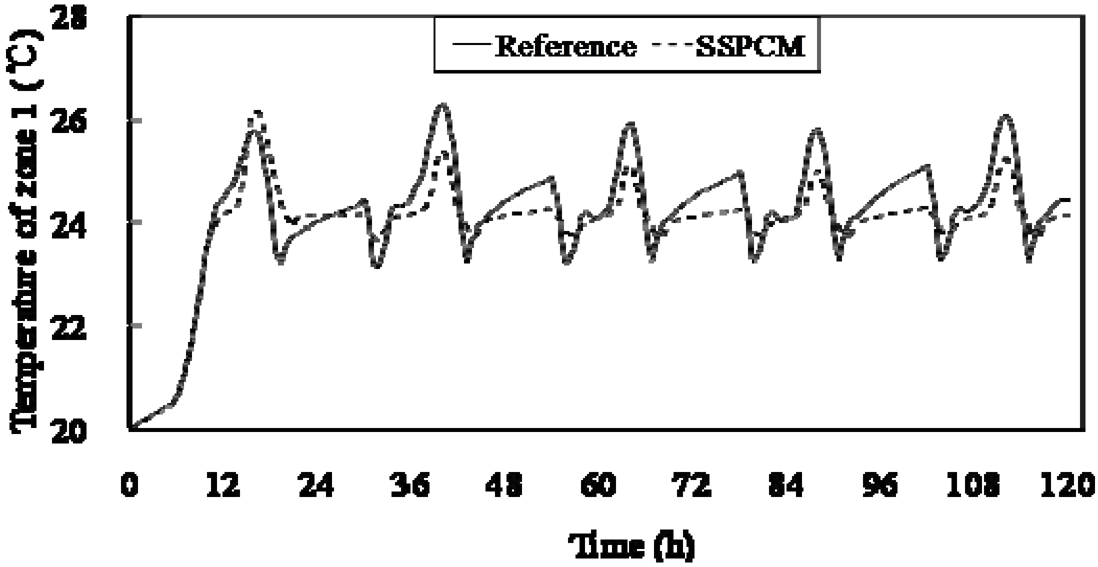

Figure 6.7 Indoor air temperature of zone 1 (Hong Kong test case)

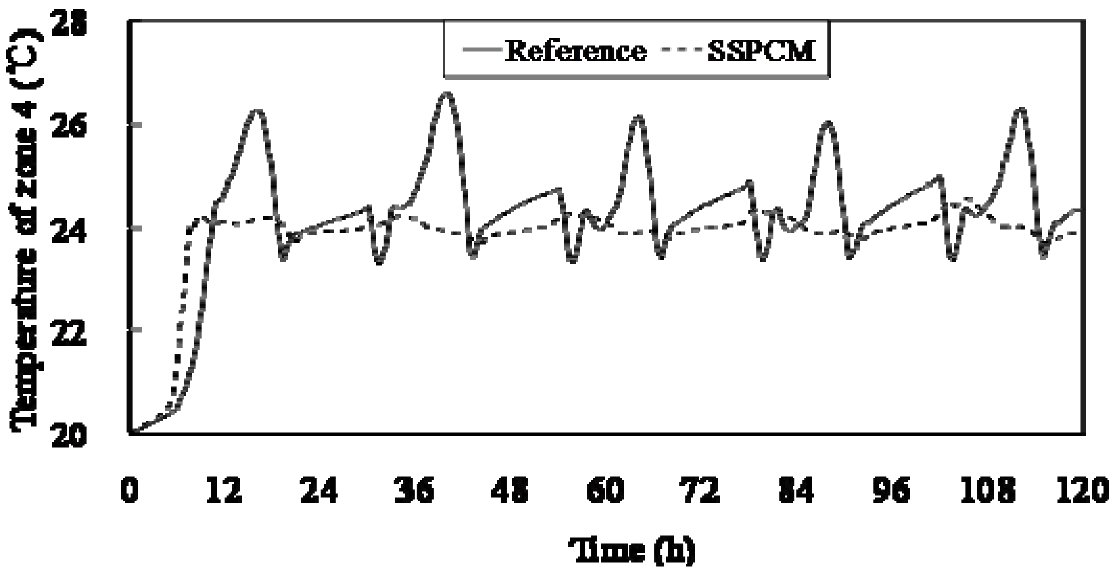

Figure 6.8 Indoor air temperature of zone 4 (Hong Kong test case)

From the above figures, it can be observed that the indoor air temperatures of reference building and SSPCM building were in the comfortable range during the occupied period most of the time, but the zone temperatures of the SSPCM building were lower than that of the reference building, and the zone temperatures swing less most of the time. Therefore the occupants could feel much more comfortable in the SSPCM building than in the reference building under the same condition. The SSPCM building shows some advantages over the reference building concerning the thermal dynamic performance.

6.3 Charge/discharge progress of PCM

The SSPCM plates are placed on the inside surface of the external wall. The south wall is connected to indoor, and there is no any SSPCM plate on it. The distribution of the SSPCM plates is shown in Figure 6.9.

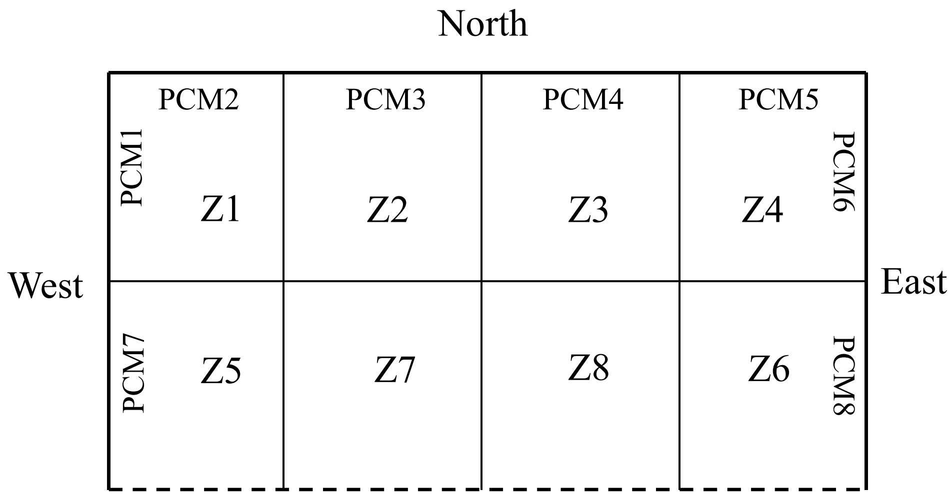

Figure 6.9 Distribution of SSPCM plates on each zone

The results in the daily average in four test day is presented to demonstrate the charge/discharge processes of SSPCM plates in Beijing and Hong Kong as shown in Figure 6.10, Figure 6.11 and Figure 6.12, Figure 6.13, respectively.

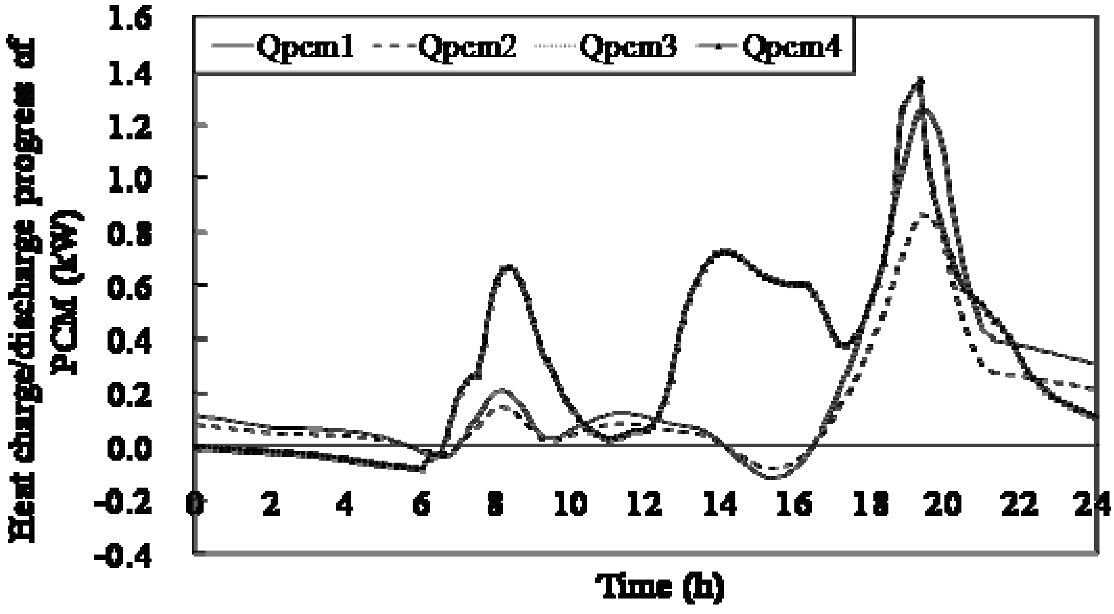

Figure 6.10 Charge/discharge progress of PCM1 to PCM4 (Beijing test case)

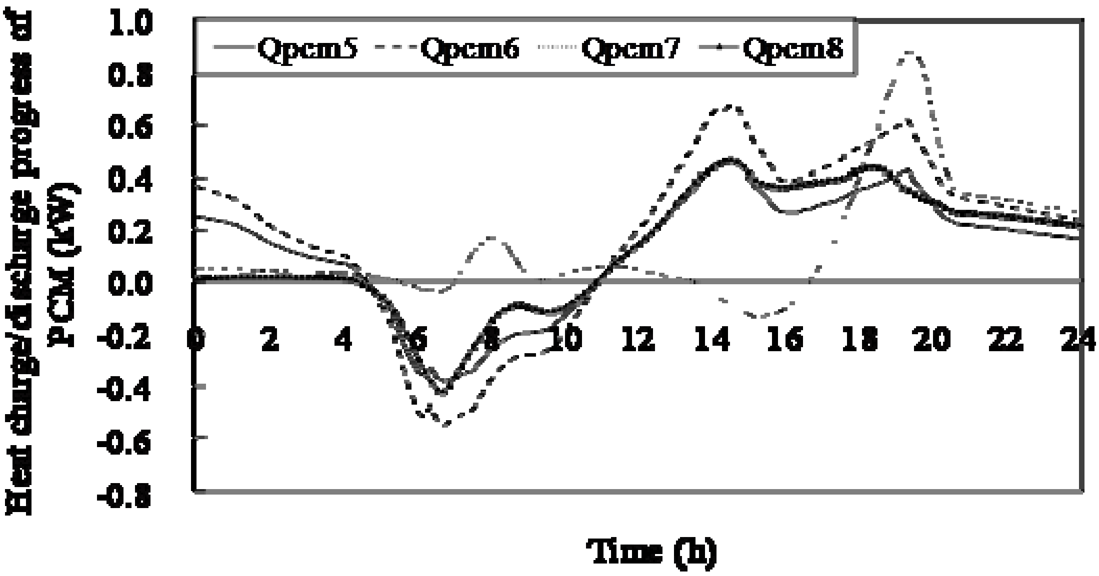

Figure 6.11 Charge/discharge progress of PCM5 to PCM8 (Beijing test case)

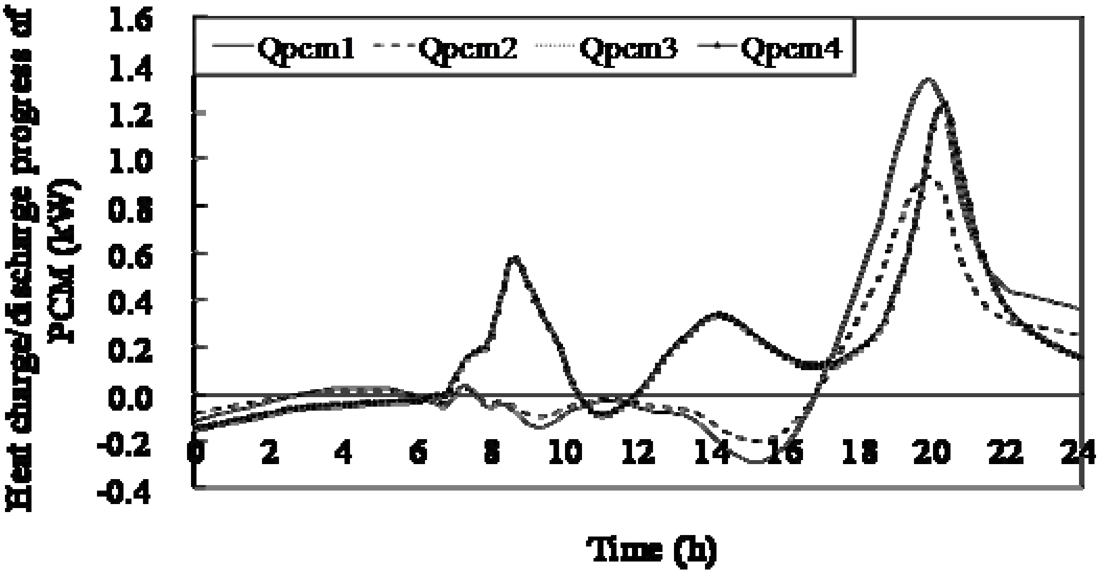

Figure 6.12 Charge/discharge progress of PCM1 to PCM4 (Hong Kong test case)

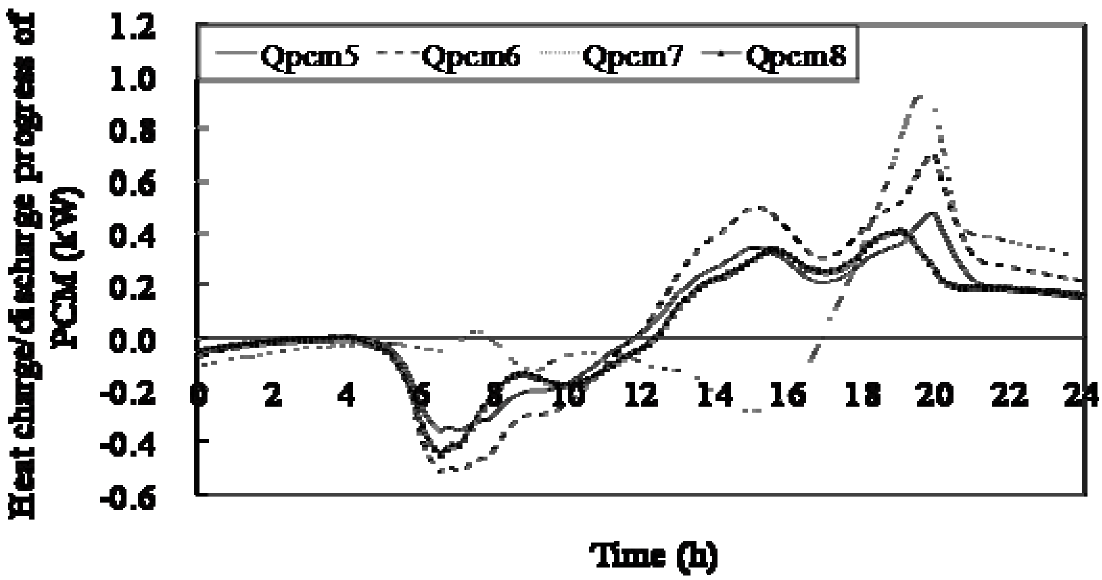

Figure 6.13 Heat charge/discharge progress of PCM5 to PCM8 (Hong Kong test case)

From Figure 6.10 and Figure 6.11, it can be observed that the SSPCM plates were charging cold in most of the time, even during the occupied period. From Figure 6.10 and Figure 6.13, is can be seen that the PCM5, PCM6 and PCM8 were discharging cold from about 5:00 AM to 12:00 AM and charging cold from 12:00 AM to 12:00 PM. The SSPCM plates are useful for cooling in the morning and not useful in the afternoon. Due to the PCM5 is placed on the north wall, which is near the east wall, and PCM6 and PCM8 are placed on the east wall, , the SSPCM plates could melt and discharge cold due to effect of solar radiation in the morning. The efficiency of using SSPCM is very low, and this is the reason why the total energy consumption of SSPCM building is nearly the same with that of the reference building.

6.4 Energy performance

Figure 6.14 and Figure 6.15 present the total energy consumption of SSPCM and reference buildings in Beijing and Hong Kong test case, respectively.

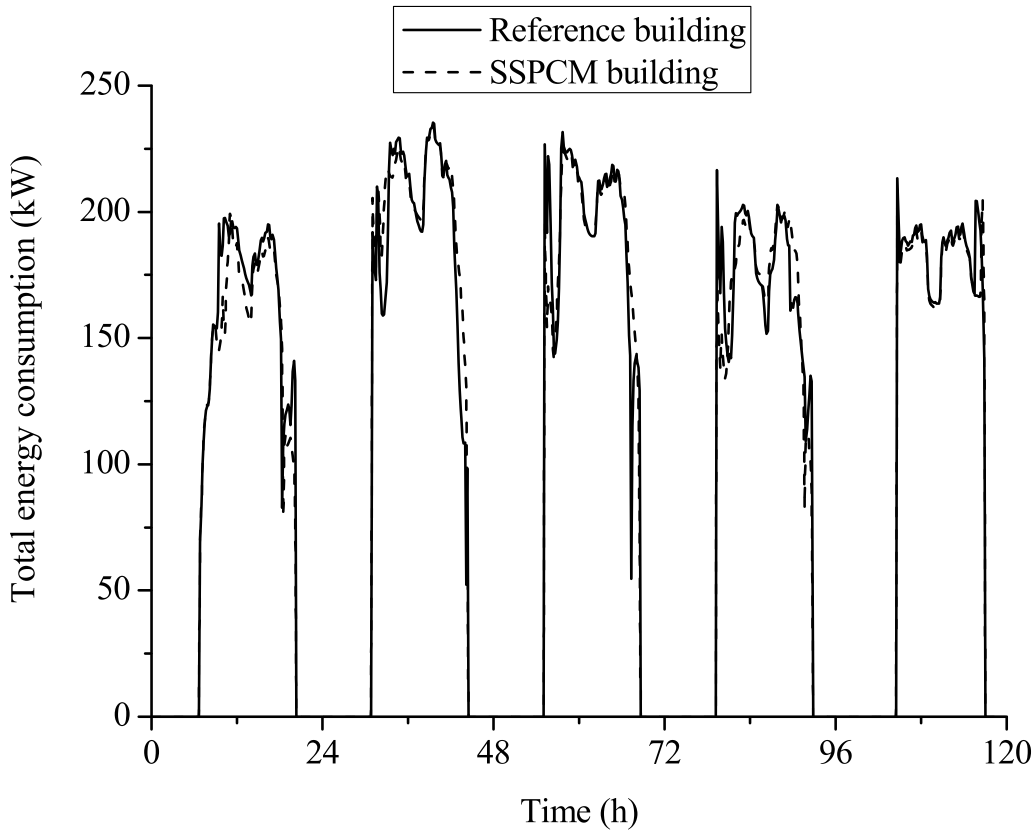

Figure 6.14 Total energy consumptions of SSPCM and reference building

(Beijing test case)

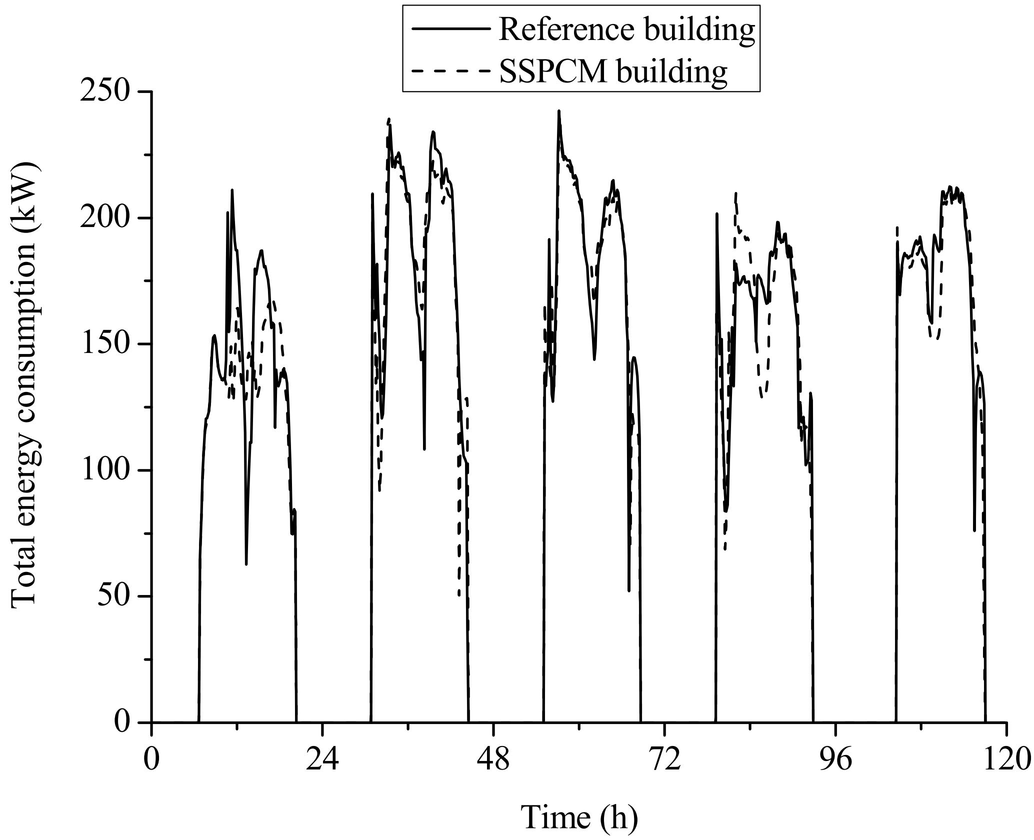

Figure 6.15 Total energy consumptions of SSPCM and reference buildings

(Hong Kong test case)

The above two figures show that the energy consumption of SSPCM building was nearly the same with that of the reference building in the five test days. It means that the SSPCM building did not save energy significantly, thought the indoor comfort was improved. Table 6.1 shows the detailed electricity consumption saving percentage of the SSPCM building compare with that of the reference building.

Table 6.1 Total electricity consumption saving comparison

	SSPCM building			Reference building			
City	W_{fan} (kWh)	Q_{coil} (kJ)	E_{total} (kWh)	W_{fan} (kWh)	Q_{coil} (kJ)	E_{total} (kWh)	Electricity saving
Beijing	1480	40332000	5214	1680	40982000	5475	4.76%
Hong Kong	2013	43512000	6042	2023	43775000	6076	0.57%

In the five test days, the electricity saving was 4.76% and 0.57% in Beijing and Hong Kong, respectively. Because the outdoor night temperature in Beijing was lower than that in Hong Kong, the phase change material could be frozen and store some cooling energy effectively. But the SSPCM plates did not show advantage fully. Considering the investment on SSPCM, the payback period was very long. So, we need some more effective method to use the SSPCM plate in the building for cooling.

6.5 Summary

The SSPCM plates have positive effect on the indoor comfort, and they reduce the indoor temperature swing during the occupied periods and maintain it in the comfortable range. The indoor temperature of SSPCM building is lower than that of the reference building. The energy consumption of SSPCM building is 4.76% and 0.57% less than that of the reference building in Beijing and Hong Kong, respectively. But the SSPCM plates are useless most of the period, and only third of eight SSPCM plates are useful and discharge cold in the morning. We need some more effective methods to use the SSPCM and make it to discharge cold during the occupied period. The optimal control strategies are needed in SSPCM commercial buildings.

CHAPTER 7 PERFORMANCE OF SSPCM BUILDING WITH NIGHT VENTILATION

In Chapter 6, it was concluded that some more effective methods are needed for using the SSPCM to charge/discharge cold. The night ventilation for free cooling in PCM building was studied by many researchers. The results obtained from those studies have primarily demonstrated that the free cooling technique by using PCMs in buildings can provide better indoor thermal comfort, and help reduce the need of air-conditioning use and sizes of air-conditioning systems. Therefore, the night ventilation was tested in this study to analyze the indoor environment performance and energy performance of the SSPCM building.

7.1 Introduction

The use of nature resources plays an important role in energy conservation. The night ventilation technique has been developed to cool down the surrounding of the buildings. Night ventilation can be either natural or mechanical. The night ventilation can really improve the indoor comfort and save energy consumption of air-conditioning system. Traditional building materials store cold in heavy material mass. By comparison, latent heat storage has the advantages of large energy store density and nearly isothermal nature of the storage progress.

Free cooling is a technique defined as “that amount of cooling which can be obtained from existing, additional or modified system components during low ambient conditions and used to partly or fully offset the load on mechanical refrigeration plant”.

The air side free cooling is to use fresh air and/or re-circulated indoor air to cool a building. It is often understood to store outdoor cool during low ambient conditions in night and supply it with a time delay for space cooling during daytime. According to this principle, the SSPCM can be cooled and store cold energy by the fresh cool air during night, and release the cold during the occupied periods when approaching the melting temperature. Numerical simulations of Arkar C et al. [2007] showed that free cooling can help reduce the size of the mechanical ventilation system and provide better thermal comfort conditions. A PCM with a melting temperature between 20.0°C and 22.0°C is the most suitable for free cooling in the case of a continental climate. The air change per hour (ACH) at night needs to be as high as possible but the ACH at daytime should be controlled properly. An experimental installation was also introduced by Kang et al. [2003] to test the thermal performance including the effects on decreasing the room temperature and energy consumption. The results showed that the night ventilation system integrated with a PCM packed bed storage (NVP) system can improve the thermal comfort level of indoor environment obviously. However, the energy saving due to the use of this system was not addressed.

PCMs used for free cooling have great effect on indoor environment performance of the building. However, this concept is only feasible in climate conditions with relatively large temperature differences between day and night in summer. It is also worthy noticing that the selection of PCMs plays significant roles in the successful use of the free cooing technique in buildings. The selected PCMs should have capability to ensure that the cooled air temperature is within the acceptable comfort levels of occupants. The usage efficiency of the SSPCM depends on the charge/discharge proportion in a cycle.

Many researchers investigated the indoor environment performance and energy consumption of PCM buildings combined with night ventilation in passive buildings. Little research work has done on the performance of PCM buildings combined with night ventilation in air-conditioned buildings. Therefore, the purpose of this study is to analyze the indoor environment performance and energy consumption of shape-stabilized PCM plates as inner linings under night ventilation condition in the air-conditioned building in summer.

7.2 Night ventilation for cold storage in SSPCM building

In this study, the buildings are air-conditioned using the same VAV and CAV systems presented earlier. The perimeter zones orientating north are equipped with CAV terminals beside VAV terminals, and the others are equipped with VAV terminals only. During night ventilation, all the VAV systems are turned on to bring in fresh air from 5:00 AM to 7:00 AM, the HVAC systems are turned on as usual after 7:00 AM. The set-point of indoor in office hour was 24.0°C.

The night ventilation technology was also used in SSPCM building and reference buildings to study its effects on the indoor environment performance and energy performance. The precondition of using night ventilation is that the daily temperature difference should higher than 15.0°C, base on this condition, only Beijing is appropriate to use night ventilation due to the daily temperature is about 15.0°C in the test days.

7.3 Dynamic performance of SSPCM building

Figure 7.1 and Figure 7.2 present the indoor air temperatures of reference and

SSPCM buildings using the night ventilation in Beijing, respectively. Figure 7.3 and Figure 7.4 present the indoor air temperature comparisons of reference and SSPCM buildings using the night ventilation of zone 1 and zone 4 in Beijing, respectively.

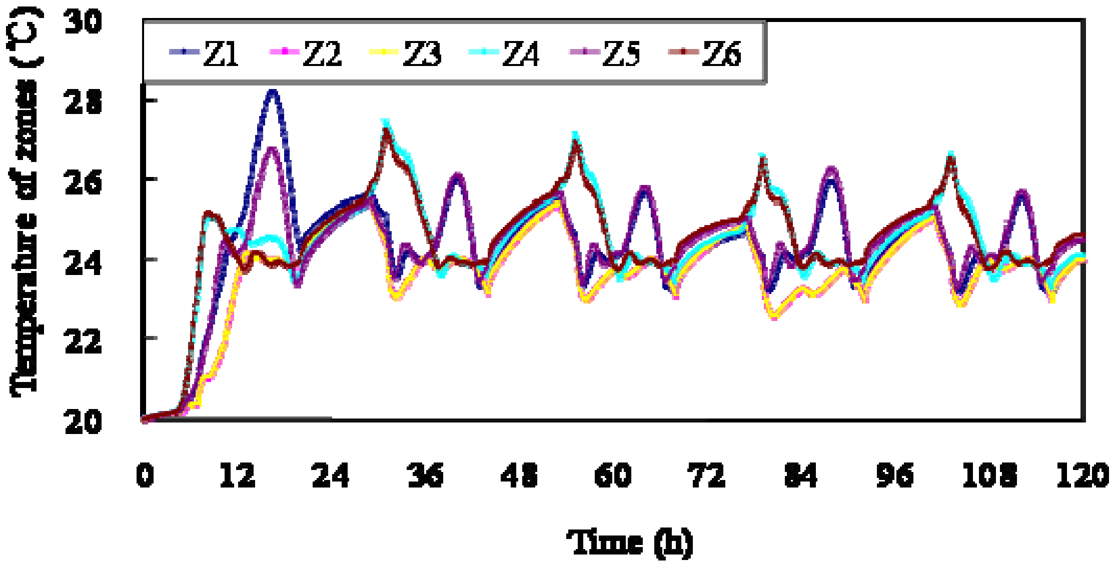

Figure 7.1 Indoor air temperature of reference building (Beijing test case)

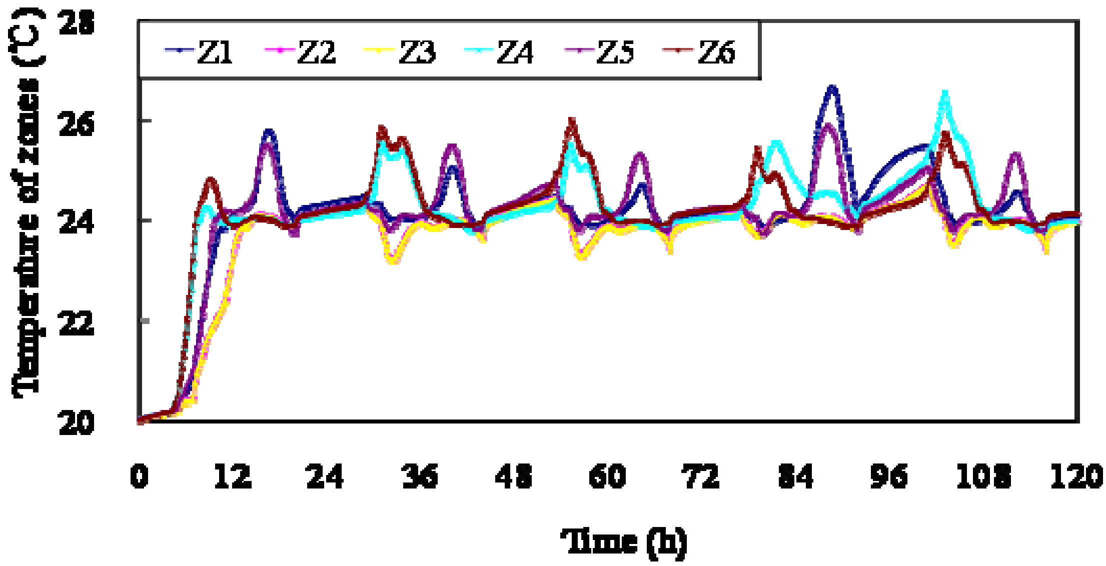

Figure 7.2 Indoor air temperature of SSPCM building (Beijing test case)

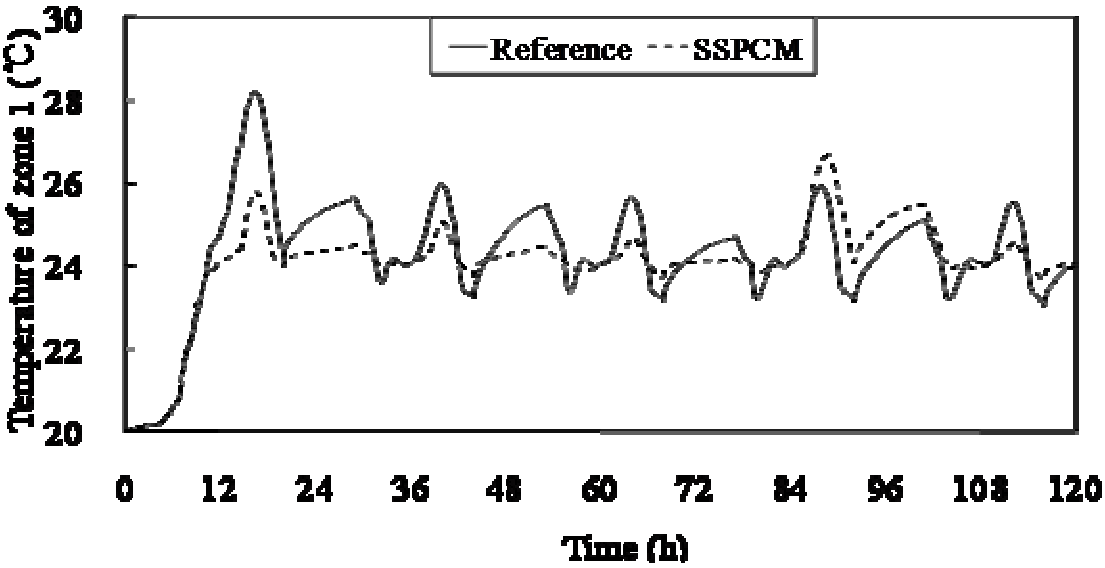

Figure 7.3 Indoor air temperature of zone 1 under night ventilation (Beijing test case)

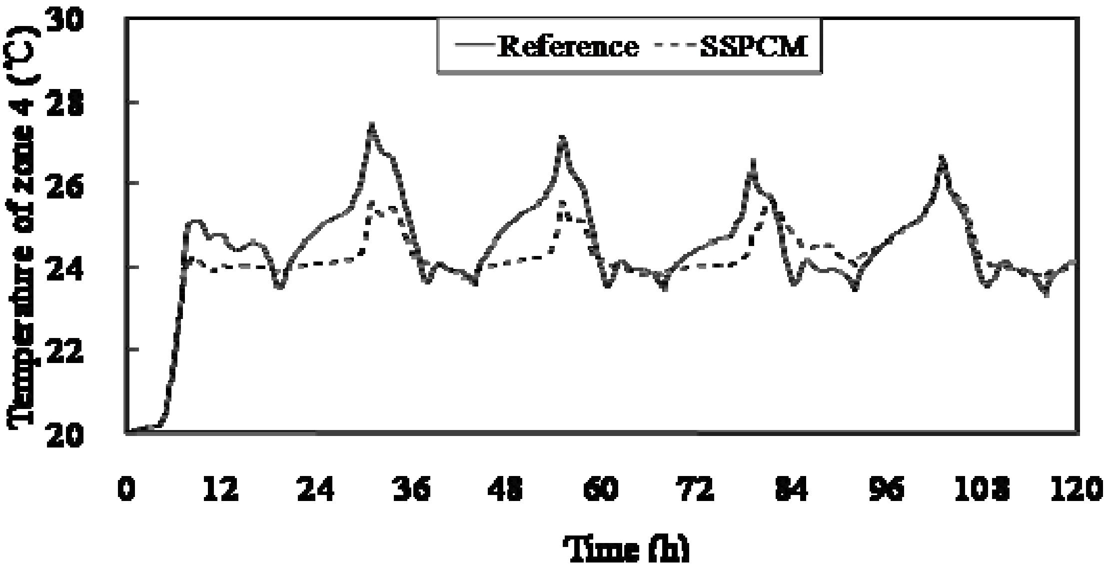

Figure 7.4 Indoor air temperature of zone 4 under night ventilation (Beijing test case)

It can be found that the zones temperature of SSPCM building were lower and swing less than that of the reference building with night ventilation. Therefore, the indoor comfort was improved when using the night ventilation for the SSPCM building.

7.4 Energy performance of SSPCM building

Figure 7.5 shows the total energy consumption of SSPCM and reference buildings under night ventilation in the five test days in Beijing. Table 7.1 presents a comparison between energy savings of the SSPCM and reference buildings using the night ventilation.

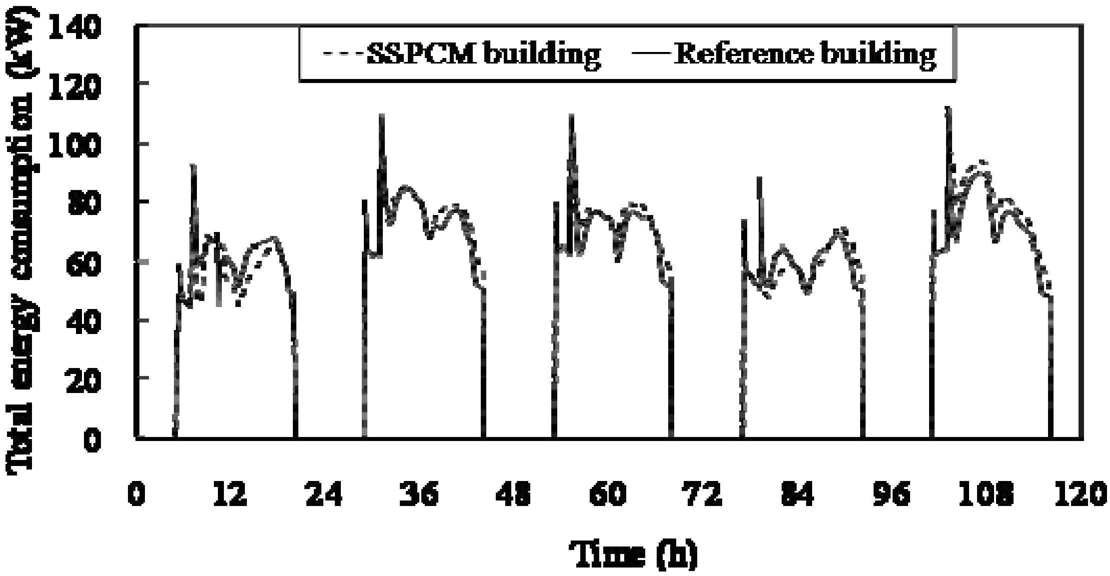

Figure 7.5 Total energy consumptions of SSPCM and reference building under night ventilation (Beijing test case)

Table 7.1 Total energy consumption saving comparison under night ventilation

	SSPCM building			Reference building			
City	W_{fan} (kWh)	Q_{coil} (kJ)	E_{total} (kWh)	W_{fan} (kWh)	Q_{coil} (kJ)	E_{total} (kWh)	Energy saving
Beijing	1204	42867500	5073	1160	42385500	5085	0.23%

From Figure 7.5 and table 7.1, it can be observed that the SSPCM building saved a little air-conditioning energy when using the night ventilation in the five test days in

Beijing. The SSPCM building did not show any advantage on energy saving.

PCM3 and PCM8 are chosen to investigate the heat charge/discharge processes of SSPCM plates in the building using night ventilation in Beijing. PCM3 is on the north external wall of zone 2, and PCM8 is on the east external wall of zone 8. Figure 7.6 shows the charging/discharging processes of PCM plates on the daily average in four test day.

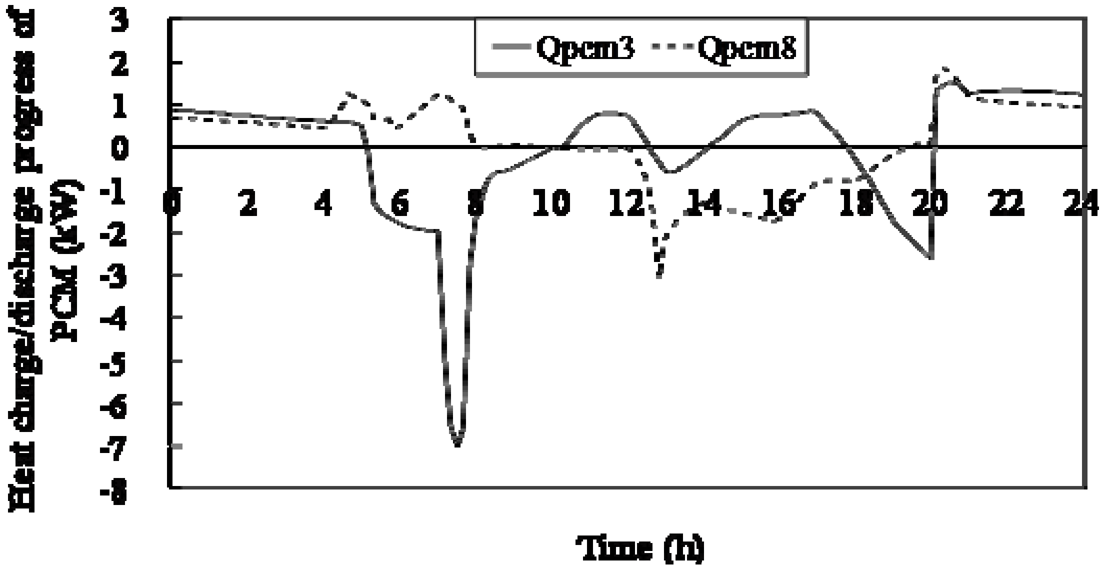

Fig7.6 Heat charge/discharge of PCM using night ventilation (Beijing test case)

From Figure 7.6, it can be found that the usage efficiency of SSPCM plates was very low. The PCM3 layer charges cold from 10:00 AM to 12:00 AM and 2:00 PM to 6:00 PM during the occupied hours, it was a waste of air-conditioning energy. The PCM8 layer discharged cold from 12:00 AM to 6:00 PM, it charged cold before 12:00 AM. This was the reason why the energy consumption of SSPCM building was nearly the same as that of the reference building. Another reason was the outdoor night temperature in the selective five days in Beijing was not cold enough to freeze the phase change material and store cold in the SSPCM plates during the night ventilation hour (5:00 AM-7:00 AM).

7.5 Summary

In this chapter, the dynamic characteristic and energy performance of SSPCM building using night ventilation was analyzed in the selected five test days in Beijing. The SSPCM building still had advantage on reducing the indoor temperature and temperature swing during the occupied periods. The indoor temperature of SSPCM building and reference building were all in the comfortable range in the occupied time. But the usage efficiency of SSPCM layers was very low, the total energy consumption of SSPCM building was only 0.23% less than the reference building when using the night ventilation technology in this study.

The night ventilation could really improve the daytime comfort inside the room and save energy consumption of air-conditioning. But it was not useful for any day in summer for cooling purpose. The precondition is that the outdoor night temperature is low enough and last longer, and the minimum temperature difference during a day in summer is 15.0°C.

In the normal weather condition, in order to save energy on using PCM for cooling, some optimal control strategies are needed to make full use of PCM in commercial buildings in summer.

CHAPTER 8 OPTIMAL CONTROL OF SSPCM BUILDINGS FOR PEAK DEMAND REDUCTION

This chapter presents the quantitative studies on the energy performance and the optimal control strategy of air-conditioned commercial buildings with envelopes enhanced by phase change materials when energy-plus-demand-based electricity pricing policy is used. The effects of SSPCM and demand limiting control are studied under different weather conditions and energy-plus-demand-based pricing policy. The test results under demand limiting control are presented.

8.1 Introduction

There have been a number of simulation and experimental studies that have demonstrated significant potential for reducing peak cooling demand using building thermal mass through controlling zone temperatures. However, due to the heat capacitance of the normal building envelope, the energy stored in the building thermal mass is limited. Phase change materials have very large capacitance when place phase change taking place and can store large amount energy over a small melting temperature range. If cold is stored prior to the on-peak period and is released during the on-peak period, it can reduce the peak cooling load significantly. However, no sufficient quantitative study on the energy and daily electricity cost saving using SSPCM in air-conditioned buildings can be found, and particularly no study on the effects of control strategies has been reported.

8.2 Demand limiting control strategy

With the demand limiting control, the building is precooled prior to an on-peak or critical peak-pricing period and then set-points are adjusted in an optimal way so that the absorbed energy into the building thermal mass is controlled and the peak cooling load is minimized. This type of strategy is appropriate for minimizing on-peak demand charges or for the use in a utility program where the utility takes active control for the end-user during periods of critical demand. The details can be found in session 5.5.

8.3 Energy performance of SSPCM building

The energy effects of the SSPCM building and demand limiting control were tested in Beijing and Hong Kong climate conditions under energy-plus-demand-based electricity pricing. Table 8.1 presents a summary of electricity costs of reference and SSPCM buildings under normal and demand limiting controls under different climate cases (daily average in four test day in both cases).

From Table 8.1, it can be found that, under the normal control, the daily electricity cost of the SSPCM building in Hong Kong test case was 5.31% lower than that of the reference building. For the reference building, the daily electricity cost in Hong Kong test case under the demand limiting control was slightly lower (0.07%) than that under the normal control. These results show that the saving when using demand limiting control or SSPCM alone was almost not effective or not significant. The daily electricity cost of the SSPCM building under the load shifting control was 10.61% lower than that of the reference building under the normal control. Similarly, it can be concluded that the advantage of SSPCM building can be fully utilized with the support of proper control, and the demand limiting control can achieve much significant energy saving when

SSPCM is used in the building.

Table 8.1 Summary of daily electricity cost of reference/SSPCM buildings under normal/demand limiting controls under different weather cases

	Hong Kong Test Case (HKD)			**Beijing Test Case (CNY)**		
	Reference Building	SSPCM Building	Overall Cost Saving	Reference Building	SSPCM Building	Overall Cost Saving
Normal Control	1083.5	1026	5.31%	1025.5	976	4.83%
Demand Limiting Control	1082.7	968.5	10.55%	1003.1	894.6	10.82%
Overall Cost Saving	0.07%	5.6%	10.61%	2.18%	8.34%	12.76%

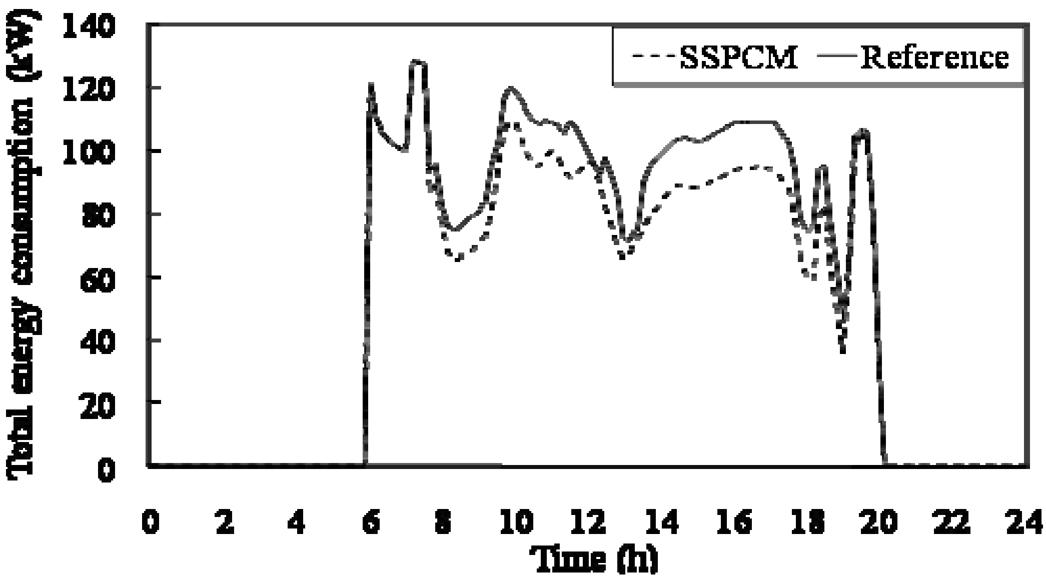

Figure 8.1 Energy consumptions of SSPCM and reference buildings under demand limiting control (Hong Kong test case)

Figure 8.1 presents a detailed comparison between the energy consumptions of the reference building and SSPCM building under the demand limiting control in Hong Kong test case (the second day). The energy consumption of the SSPCM building was lower than that of the reference building most of the time. From Table 8.1, it shows that the peak electricity demand and overall electricity consumption of the SSPCM building was reduced by 12.4% and 10.14% respectively compared with that of the reference building. The daily electricity cost of the SSPCM building was reduced by 10.55% compared with that of the reference building.

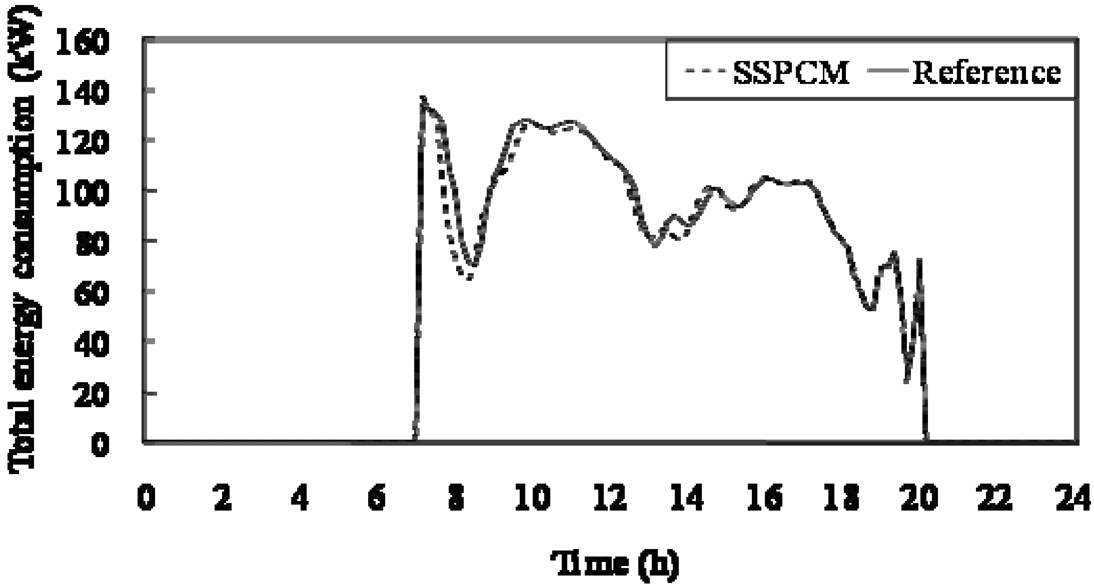

Figure 8.2 Energy consumptions of SSPCM and reference buildings under normal control (Hong Kong test case)

Figure 8.2 presents a detailed comparison between the energy consumptions of the reference building and SSPCM building under the normal control in Hong Kong test case (the second day). The energy consumption of the SSPCM building was lower than that of the reference building most of the time. With the similar calculation from Table 8.1, it shows that the peak electricity demand and overall electricity consumption of the SSPCM building was reduced by 0.2% and 1.77% respectively compared with that of the reference building. The daily electricity cost of the SSPCM building was reduced by 1.29% compared with that of the reference building.

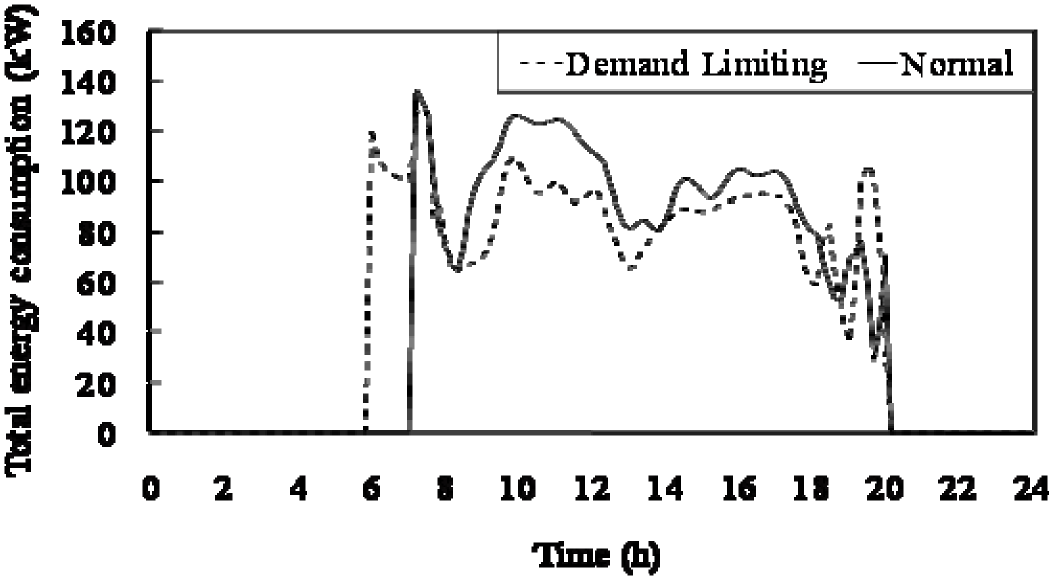

Figure 8.3 Energy consumptions of SSPCM building under demand limiting and normal control (Hong Kong test case)

Figure 8.3 presents a comparison between the energy consumptions under demand limiting control and normal control (SSPCM building) in Hong Kong test case. Table 7 shows that the overall electricity consumption of SSPCM building under demand limiting control strategy was reduced by 0.72% compared with that in the normal control case. The peak electricity demand of SSPCM building was reduced by 17.36% under the demand limiting control. The daily electricity cost of SSPCM building under demand limiting control reduced by 5.6% compared with that of normal control.

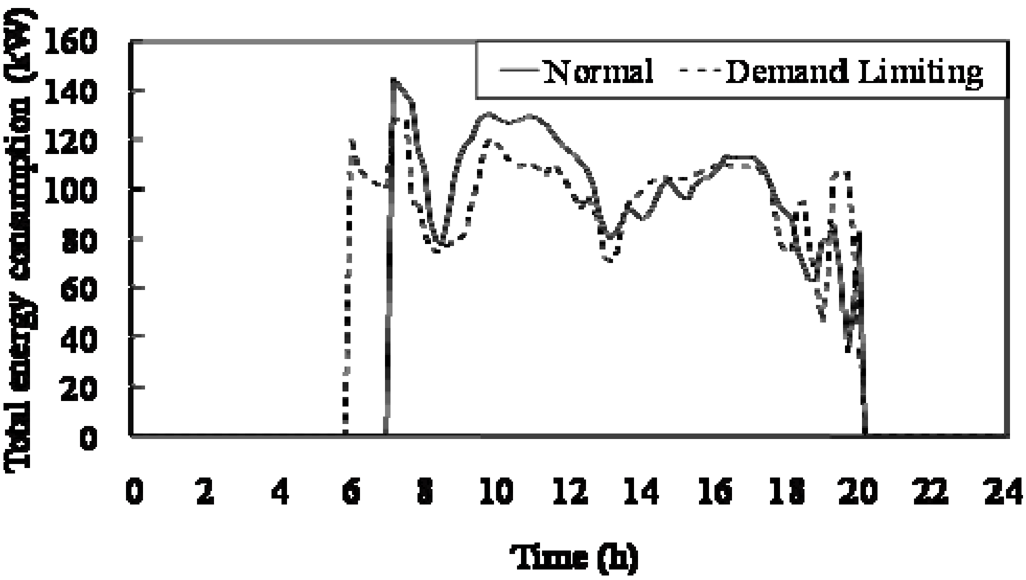

Figure 8.4 Energy consumptions of reference building under demand limiting and normal control (Hong Kong test case)

Figure 8.4 presents a comparison between the energy consumptions under demand limiting control and normal control (reference building) in Hong Kong test case. It can be found that the overall electricity consumption of reference building under demand limiting control strategy was increased by 3.28% compared with that in the normal control case. The peak electricity demand of SSPCM building was reduced by 8.30% under the demand limiting control. The daily electricity cost of SSPCM building under demand limiting control reduced by 0.07% compared with that of normal control.

Figure 8.5 presents a detailed comparison between the energy consumptions of the reference and SSPCM buildings under the demand limiting control in Beijing test case (the second day). Figure 8.6 presents a comparison between the energy consumptions under demand limiting control and normal control (SSPCM building) in Beijing test case.

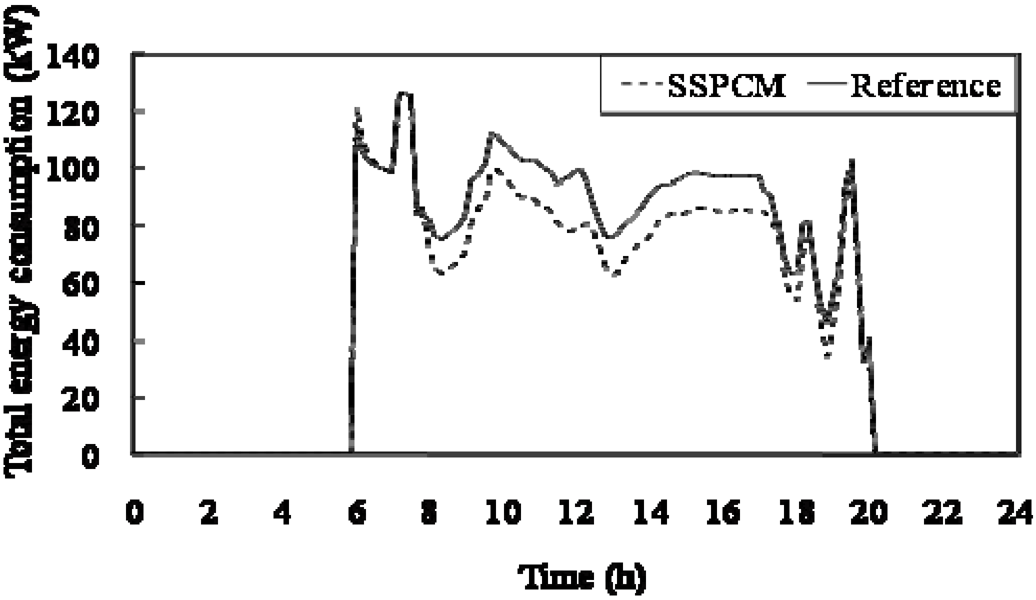

Figure 8.5 Energy consumptions of SSPCM and reference buildings under demand limiting control (Beijing test case)

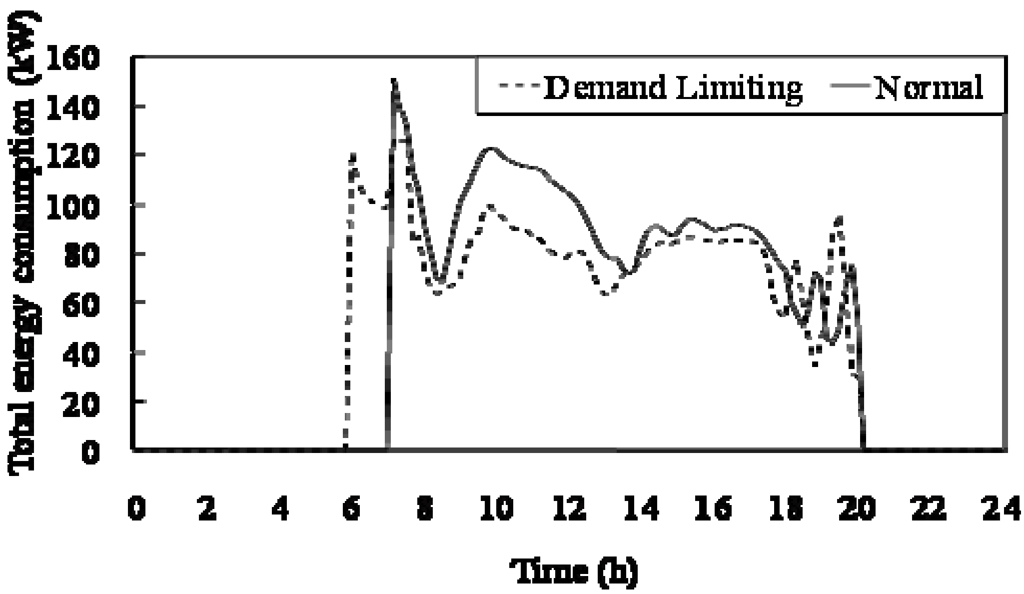

Figure 8.6 Energy consumptions of SSPCM building under demand limiting and normal control (Beijing test case)

The daily electricity cost of the SSPCM building under normal control was 4.83%

lower than that of the reference building. The daily electricity cost of the reference building under the demand limiting control was 2.18% lower than that of the same building under the normal control. The peak electricity demand of SSPCM building was reduced by 20.28% under the demand limiting control. The daily electricity cost of the SSPCM building under the demand limiting control was reduced by 12.76% compared with that of the reference building under the normal control in Beijing test case. Very significant saving can achieved when SSPCM and demand limiting control were used in the building at the same time.

Table 8.2 presents the detailed comparison between energy/electricity consumptions and indoor thermal environment of SSPCM and reference buildings when using demand limiting control under two climate cases. Table 8.3 presents a detailed comparison between energy/electricity consumptions and indoor thermal environment when using demand limiting control and normal control respectively to SSPCM building under two climate cases. The results in other test days in both climate cases are slight different but well support the same conclusions made based on the results presented.

8.4 Dynamic characteristics of SSPCM building

Figure 8.7 presents the comparison between the indoor air (Zone 2) temperatures of SSPCM and reference buildings under demand limiting control in Hong Kong test case. The indoor air temperatures of SSPCM building and reference building were very close with each other and within the comfortable range during the occupied period under demand limiting control. During the occupied period, the indoor air temperatures of reference building and SSPCM building were maintained at 23.4-25.1°C and 23.6-25.1°C respectively. The indoor air temperatures of SSPCM and reference buildings were also in the comfortable range during the occupied period under normal control and demand limiting control in Beijing test case. More details can be found in Table 8.2 and 8.3.

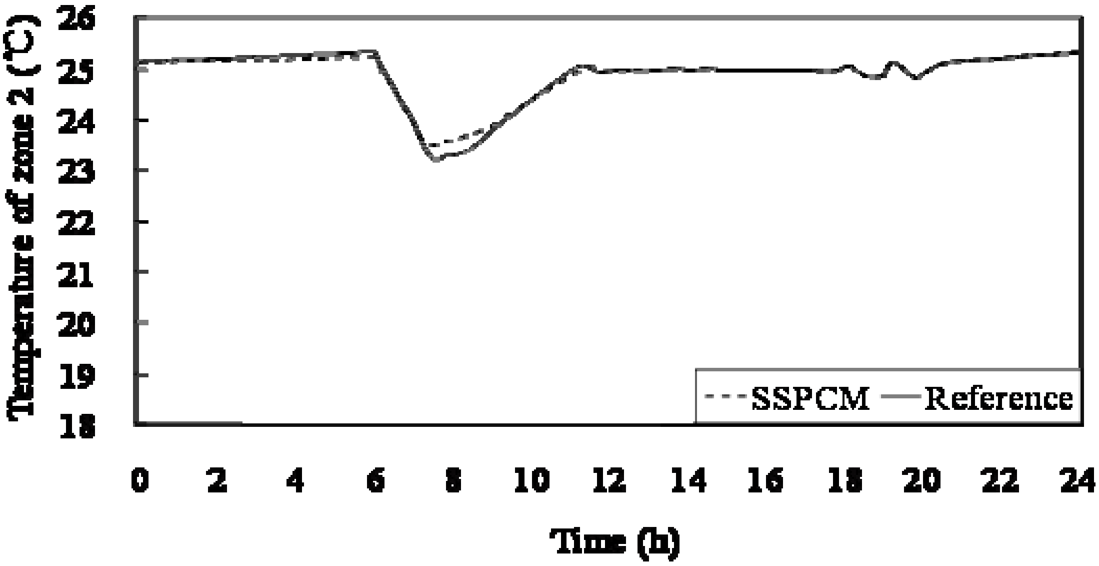

Figure 8.7 Indoor air temperatures of SSPCM and reference buildings under demand limiting control (Hong Kong test case)

Figure 8.8 presents the comparison between the indoor air (Zone 2) temperatures of SSPCM under demand limiting and normal control in Hong Kong test case. The indoor temperature of SSPCM building under the demand limiting control was nearly 1.0°C higher than that under the normal control. The indoor temperature of the SSPCM building under the two control strategies are all in the comfortable range during the occupied period in Hong Kong test case. The indoor air temperatures of SSPCM were also in the comfortable range during the occupied period under normal control and demand limiting control in Beijing test case. More details can be also found in Table 8.2 and 8.3.

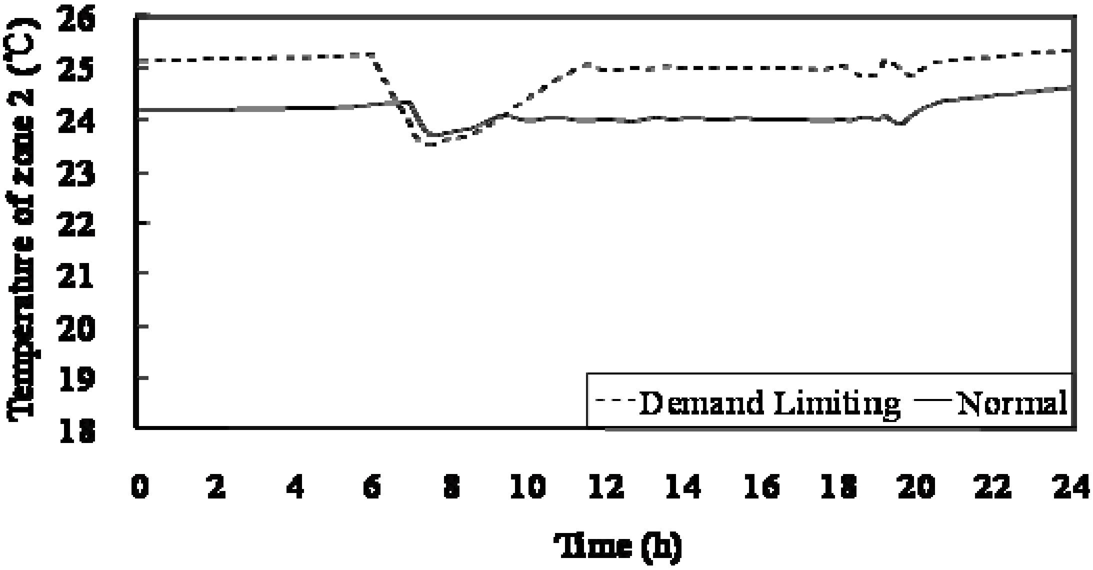

Figure 8.8 Indoor air temperatures of SSPCM building under demand limiting and normal control (Hong Kong test case)

Figure 8.9 presents the comparison between the indoor air (Zone 2) temperatures of SSPCM and reference buildings under demand limiting control in Beijing test case. It was very similar with that of the Hong Kong test case. The indoor air temperatures of SSPCM and reference buildings were also within the comfortable range during the occupied period under normal control and demand limiting control in Beijing test case. More details can be found in Table 8.2 and 8.3.

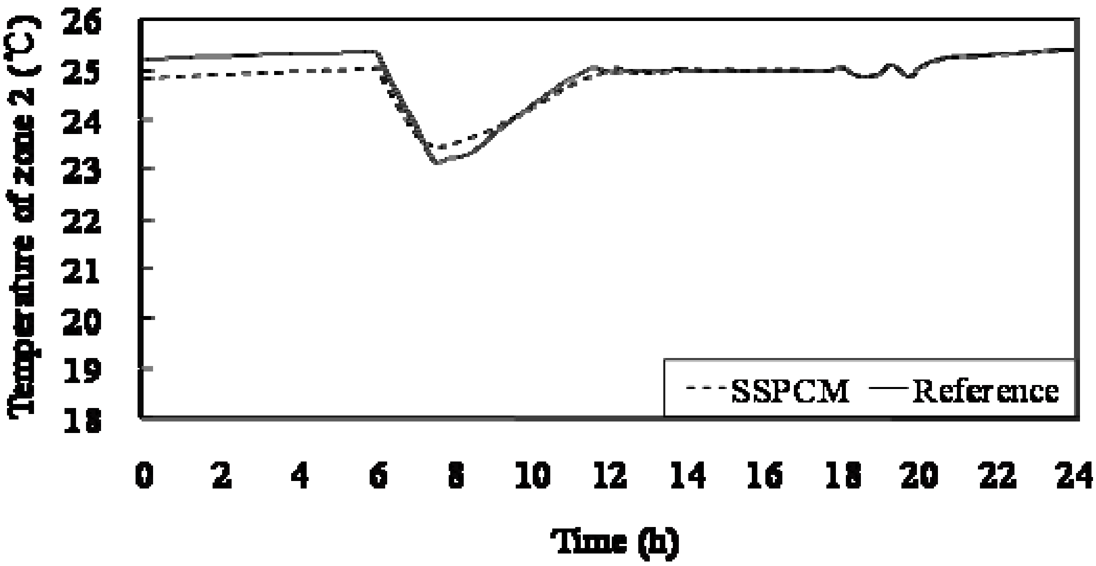

Figure 8.9 Indoor air temperatures of SSPCM and reference buildings under demand limiting control (Beijing test case)

Table 8.2 Daily energy/electricity consumptions and indoor thermal environment of SSPCM and reference buildings - demand limiting control

		Hong Kong			Beijing		
		Reference Building	SSPCM Building	Difference	Reference Building	SSPCM Building	Difference
Day Fan electricity consumption (kWh)		435	359	-76	392	331	-61
Day Coil cooling load (kJ)		10,314,000	9,481,854	-832,146	9,558,000	8,774,958	-783,042
Energy consumption part (kWh)	On-peak period	1071	939	-132	973	850	-123
	Off-peak period	311	297	-14	304	293	-11
Demand part (kVA)	On-peak period	128.2	115.2	-13 (-12.4%)	120.3	106.5	-13.8 (-11.47%)
Overall electricity consumption (kWh)		1,382	1,236	-154 (-10.14%)	1,277	1,143	-134 (-10.43%)
Daily electricity cost (Hong Kong Case: HKD, Beijing Case: CNY)		1,082.7	968.5	-114.2 (-10.55%)	1,003.1	894.6	-108.5 (-10.82%)
Indoor air Temp. (°C)	Average	24.9	24.8	-0.1	25.0	24.7	-0.3
	Minimum	23.4	23.6	0.2	23.3	23.5	0.2
	Maximum	25.1	25.1	0	25.1	25.1	0

Table 8.3 Daily electricity consumptions/costs and indoor thermal environment under demand limiting and normal control - SSPCM building

		Hong Kong			Beijing		
		Normal Control	Demand Limiting Control	Difference	Normal Control	Demand Limiting Control	Difference
Day Fan electricity consumption (kWh)		420	359	-61	398	331	-67
Day Coil cooling load (kJ)		8,908,458	9,481,854	573,396	8,474,928	8,774,958	300,030
Energy consumption part (kWh)	On-peak period	1053	939	-114	979	850	-129
	Off-peak period	192	297	105	204	293	89
Demand part (kVA)	On-peak period	139.4	115.2	-24.2 (-17.36%)	133.6	106.5	-27.1 (-20.28%)
Overall electricity consumption (kWh)		1,245	1,236	-9 (-0.72%)	1,183	1,143	-40 (-3.38%)
Daily electricity cost (Hong Kong Case: HKD, Beijing Case: CNY)		1,026	9,68.5	-57.5 (-5.6%)	976	894.6	-81.4 (-8.34%)
Indoor air Temp. (°C)	Average	24.0	24.8	0.8	24.0	24.7	0.7
	Minimum	23.8	23.6	-0.2	23.7	23.5	-0.2
	Maximum	24.1	25.1	1.0	24.1	25.1	1.0

8.5 Summary

Test results show that, under energy-plus-demand-based pricing policy and demand limiting control, the use of SSPCM in the building could reduce the overall building electricity cost significantly compared with that of the reference building. The daily electricity cost of the SSPCM building under demand limiting control was reduced also significantly compared with that under normal control. More significant saving on the daily electricity cost of the building could be achieved when it was enhanced by SSPCM and controlled by demand limiting strategy (10.61% and 12.76% in Hong Kong and Beijing climate cases respectively). The use of demand limiting control can contribute significant reduction on the peak electricity demand of the SSPCM building (17.36% and 20.28% in Hong Kong and Beijing test cases respectively compared with normal control).

CHAPTER 9 OPTIMAL CONTROL OF SSPCM BUILDINGS FOR LAOD SHIFTING

This chapter presents the quantitative studies on the energy performance and the optimal control strategy of air-conditioned commercial buildings with envelopes enhanced by phase change materials when time-based pricing policy is used. The effects of SSPCM and load shifting control are studied under different weather conditions and time-based electricity pricing policy. Test results under load shifting control are presented.

9.1 Introduction

Electrical demands vary significantly during day and night due to the changes of weather conditions and the demands by industrial, commercial and residential activities. In many countries, electrical demands and time-of-use (TOU) utility rates have been designed to encourage shifting of electrical loads from peak periods to off-peak periods. Since PCMs as TES systems in buildings can store “cold” by using night time cheap electricity or free one from nature environment, and use it with a time delay for space cooling in daytime. Therefore, significant economic benefits can be achieved for places where a differential pricing system is adopted.

9.2 Load shifting control strategy

Load shifting control uses precooling with a fixed set-point near the lower end of the comfort range prior to a fixed set-point near a higher end of comfort during the on-peak period. As a result of the cooled thermal mass, less heat gain occurs to the air during the hours following the rise in set-point than that occurs in normal control. As the temperature of the building thermal mass increases, the effects of heat absorption decreases resulting in an increased effect in cooling load. This control strategy maximizes the use of stored energy in building mass and is appropriate for minimizing on-peak period electricity energy charges.

9.3 Energy performance of SSPCM building

The energy effects of the SSPCM building and load shifting control were tested in Beijing and Hong Kong climate conditions under time-based electricity pricing. Table 9.1 summarizes the daily electricity cost of reference and SSPCM buildings under normal and load shifting controls under different climate cases (the daily average in four test day in both cases).

From Table 9.1, it can be found that, under the normal control, the daily electricity cost of the SSPCM building in Beijing test case was 2.66% lower than that of the reference building. For the reference building, the daily electricity cost in Beijing test case under the load shifting control was 2.80% lower than that under the normal control. These results show that the saving when using load shifting control or SSPCM alone was not very significant. Under the load shifting control, the daily electricity cost of the SSPCM building was 8.74% lower than that of the reference building. The daily electricity cost of the SSPCM building under the load shifting control was 8.87% lower than that of the same building under the normal control. The daily electricity cost of the SSPCM building under the load shifting control was 11.44% lower than that of the reference building under the normal control. It can be concluded that the advantage of the

SSPCM building can be effectively utilized with the support of proper control, and the load shifting control can achieve much significant energy saving when SSPCM is used.

Table 9.1 Summary of daily electricity cost of reference and SSPCM buildings under normal and load shifting controls in different climate cases

	Hong Kong test case (HKD)			Beijing test case (CNY)		
	Reference Building	SSPCM Building	Overall Cost Saving	Reference Building	SSPCM Building	Overall Cost Saving
Normal Control	1235.4	1174.2	4.95%	1149.2	1118.6	2.66%
Load Shifting Control	1204.9	1094.1	9.20%	1117.0	1019.4	8.74%
Overall Cost Saving	2.47%	6.82%	11.44%	2.80%	8.87%	11.29%

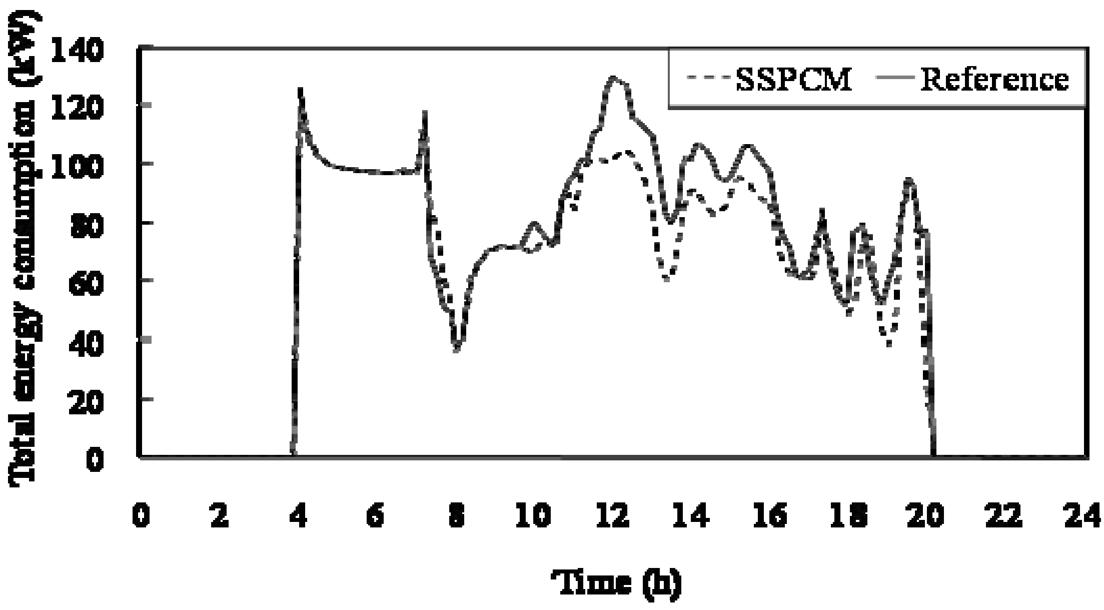

Figure 9.1 Energy consumptions of SSPCM and reference buildings under load shifting control (Beijing test case)

Figure 9.1 presents a detailed comparison between the energy consumptions of the reference and SSPCM buildings under the load shifting control in Beijing test case. The overall electricity consumption of the SSPCM building was 7.51% lower than that of the reference building, and the daily electricity cost of the SSPCM building was 8.74% lower than that of the reference building as shown in Table 9.2.

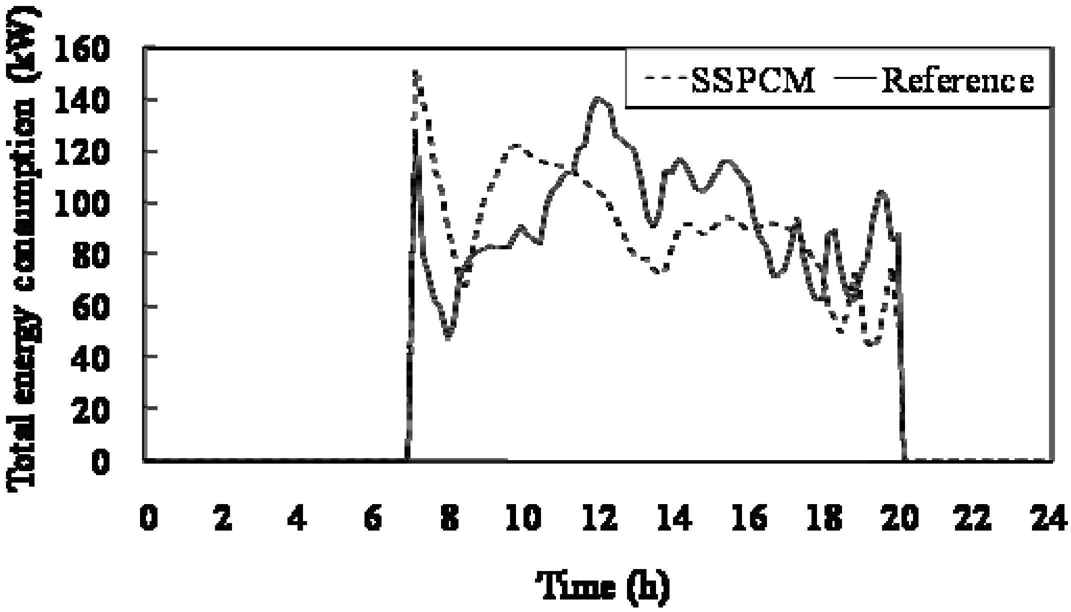

Figure 9.2 Energy consumptions of SSPCM and reference buildings under normal control (Beijing test case)

Figure 9.2 presents a detailed comparison between the energy consumptions of the reference and SSPCM buildings under the normal control in Beijing test case. The overall electricity consumption of the SSPCM building was 4.07% lower than that of the reference building, and the daily electricity cost of the SSPCM building was 2.66% lower than that of the reference building.

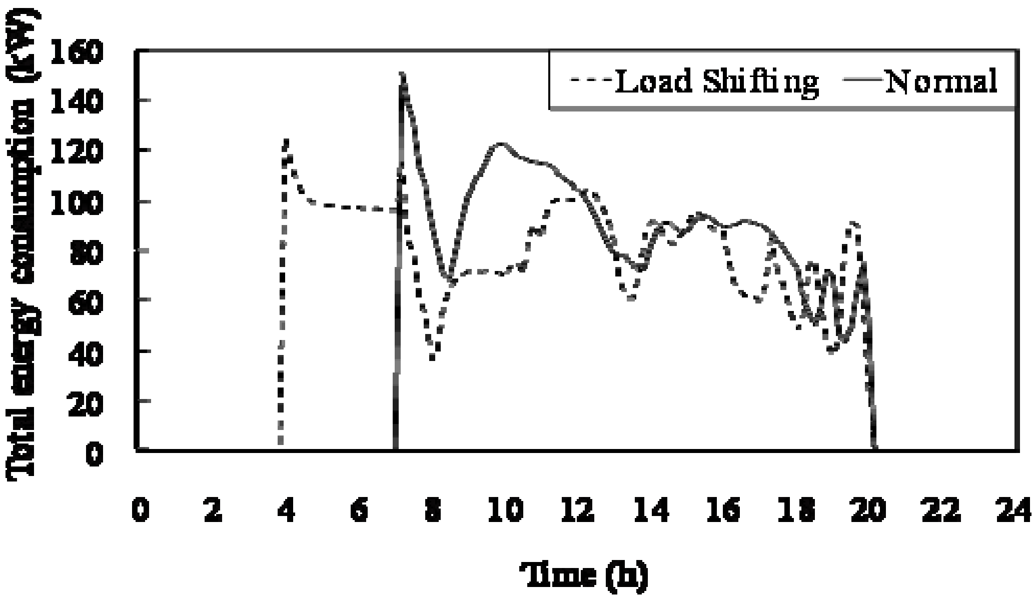

Figure 9.3 Energy consumptions of SSPCM building under load shifting control and normal control (Beijing test case)

Figure 9.3 presents a detailed comparison between the energy consumptions under load shifting control and normal control (SSPCM building) in Beijing test case. The load shifting control demonstrated significant advantage over the normal control strategy when electricity cost is of concern. The energy consumption of the SSPCM building under load shifting control was much lower between 7:00 AM and 12:00 AM. That results in reduced electricity cost during the peak period (between 8:00 AM and 11:00 AM) although the energy consumption under load shifting control was slightly higher than that under normal control between 7:00 PM and 8:00 PM. The daily electricity cost of SSPCM building under load shifting control strategy was 8.87% lower than that under the normal control strategy, while the overall electricity consumption of the building under load shifting control was even 122 kWh (10.31%) higher than that under the normal control strategy as shown in Table 9.3.

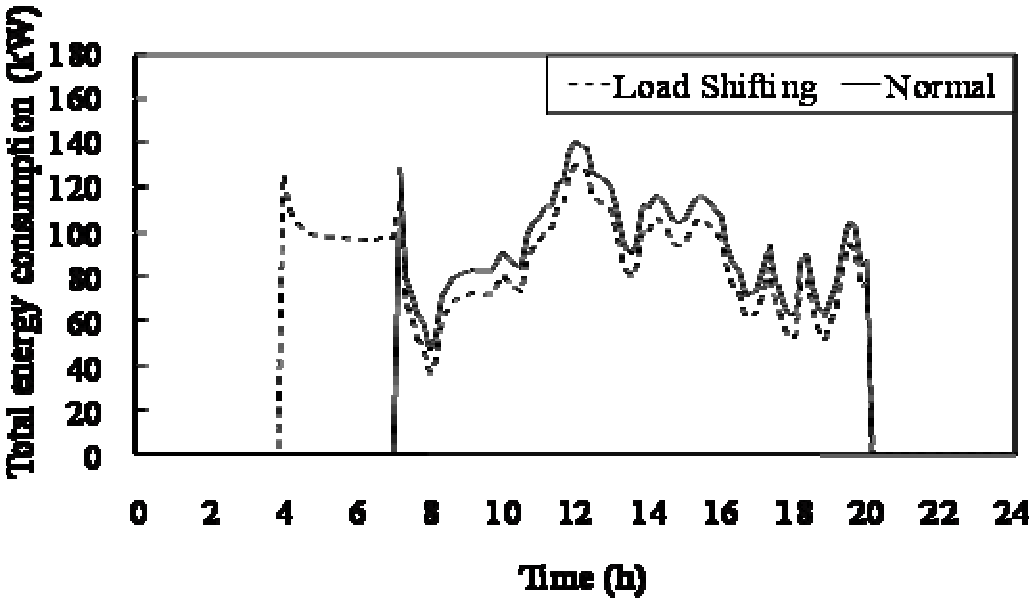

Figure 9.4 Energy consumptions of reference building under load shifting control and normal control (Beijing test case)

Figure 9.4 presents a detailed comparison between the energy consumptions under load shifting control and normal control (reference building) in Beijing test case. The daily electricity cost of SSPCM building under load shifting control strategy was 2.80% lower than that under the normal control strategy, while the overall electricity consumption of the building under load shifting control was even 183 kWh (14.91%) higher than that under the normal control strategy.

Figure 9.5 presents a detailed comparison between the energy consumptions of the reference and SSPCM buildings under the load shifting control in Hong Kong test case. Figure 9.6 presents a detailed comparison between the energy consumptions under load shifting control and normal control (SSPCM building) in Hong Kong test case.

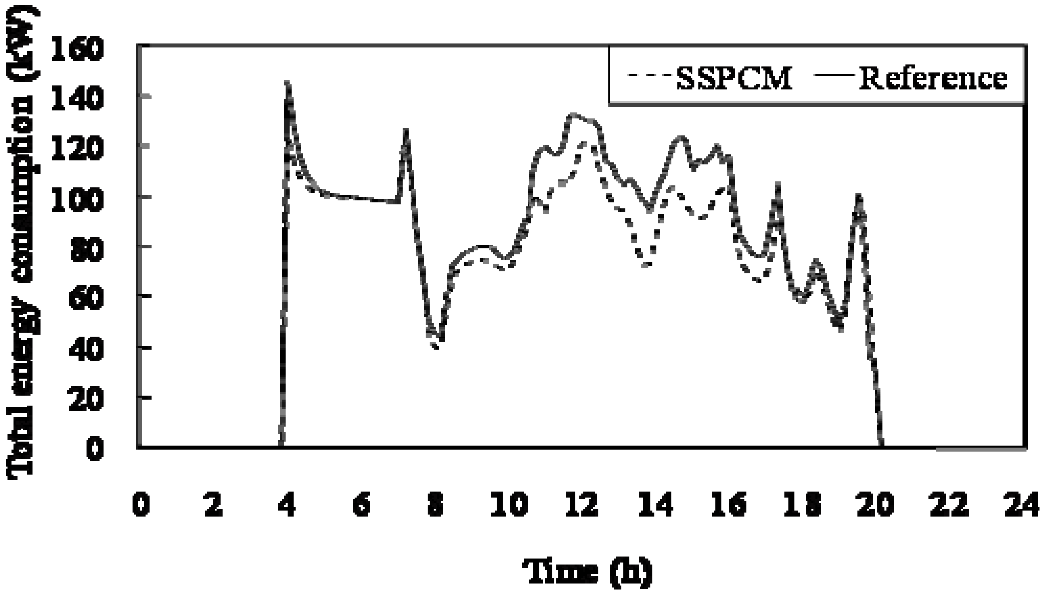

Figure 9.5 Energy consumptions of SSPCM and reference buildings under load shifting control (Hong Kong test case)

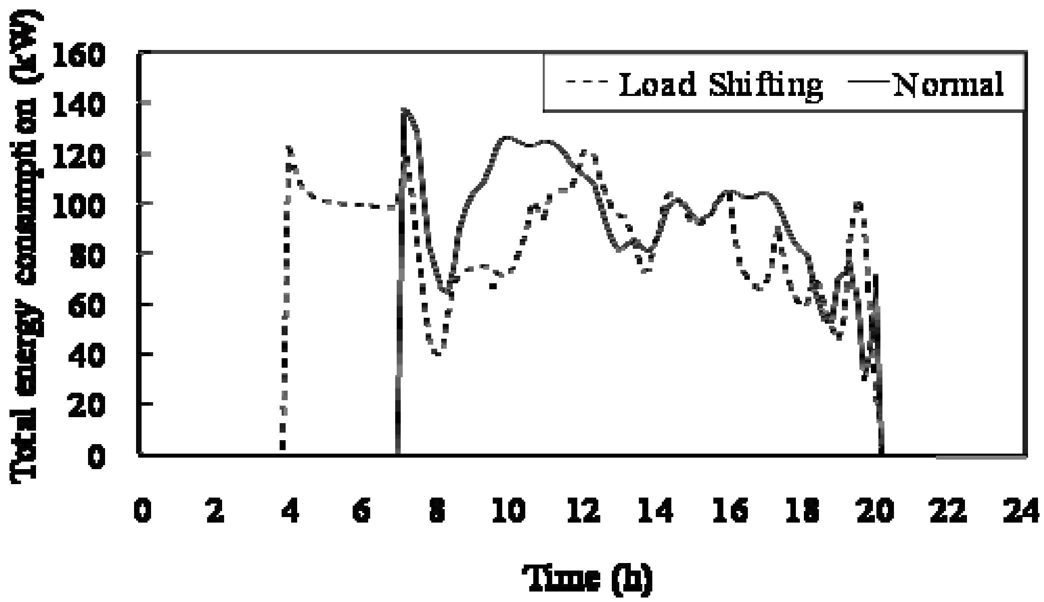

Figure 9.6 Energy consumption of SSPCM building under load shifting control and normal control (Hong Kong case)

The overall daily electricity cost in Hong Kong test case can be found in Table 9.1, and the details are listed in Table 9.2 and Table 9.3 as well. The daily electricity cost of the SSPCM building was 4.95% lower than that of the reference building under normal control. The daily electricity cost of the reference building under the load shifting control was 2.47% lower than that of the same building under the normal control. The daily electricity cost of the SSPCM building under the load shifting control was 11.44% lower than that of the reference building under the normal control in Hong Kong test case. Similarly, very significant cost saving can be achieved only when SSPCM and load shifting control are used at the same time.

Table 9.2 presents the detailed comparison between energy/electricity consumptions and indoor thermal environment of SSPCM and reference buildings when using load shifting control under two climate cases (the daily average in four test day). Table 9.3 presents a detailed comparison between energy/electricity consumptions and indoor thermal environment of SSPCM building when using load shifting and normal control respectively under two climate cases (the daily average in four test day). The results in other test days in both climate cases are slightly different but well support the same conclusions.

9.4 Dynamic characteristics of SSPCM building

Figure 9.7 presents the comparison between the indoor air (Zone 2) temperatures of SSPCM and reference buildings under load shifting control in Beijing test case. Under the load shifting control, the SSPCM building demonstrated some advantages on reducing the zone temperature swings and maintained it around the comfortable range. During the occupied period (8:00 AM to 8:00 PM), the indoor air temperatures of the

SSPCM building and reference building maintained at 22.5-25.1°C and 21.7-25.2°C respectively. The indoor air temperature was slightly low in the morning because of the pre-cooling. The indoor temperature was lower in the morning and higher in the afternoon, but still within the normal comfortable range.

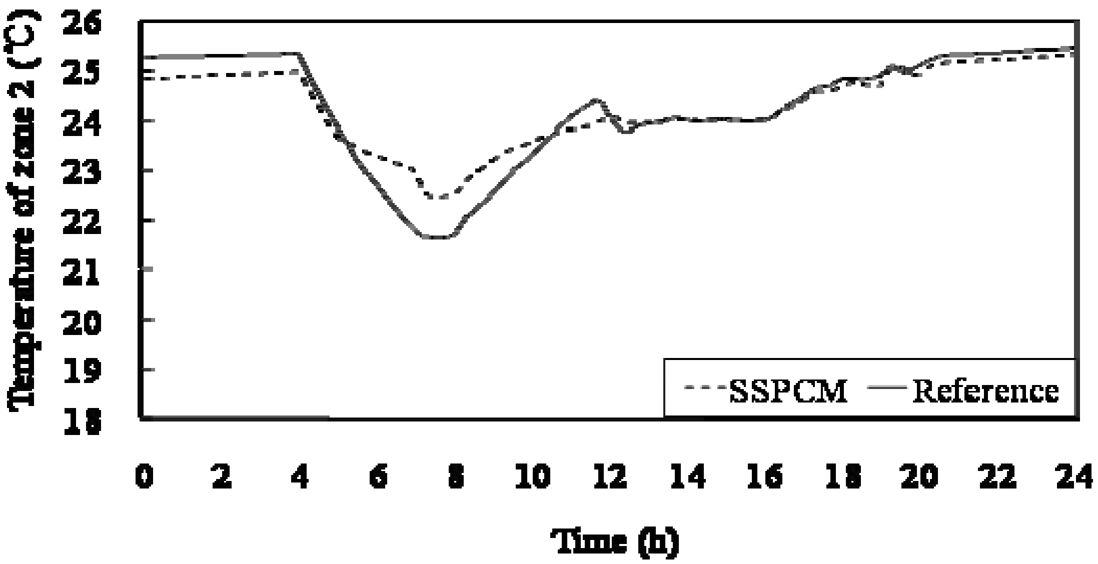

Figure 9.7 Indoor air temperatures of SSPCM and reference buildings under load shifting control (Beijing test case)

Figure 9.8 presents the comparison between the indoor air (Zone 2) temperatures of SSPCM under demand limiting and normal control in Beijing test case. The indoor temperature of SSPCM building under the demand limiting control swings more than that under the normal control. The indoor temperature of the SSPCM building under the two control strategies were all in the comfortable range during the occupied period in Beijing test case. The indoor air temperatures of SSPCM were also in the comfortable range during the occupied period under normal control and demand limiting control in Beijing test case. More details can be found in Table 9.2 and 9.3.

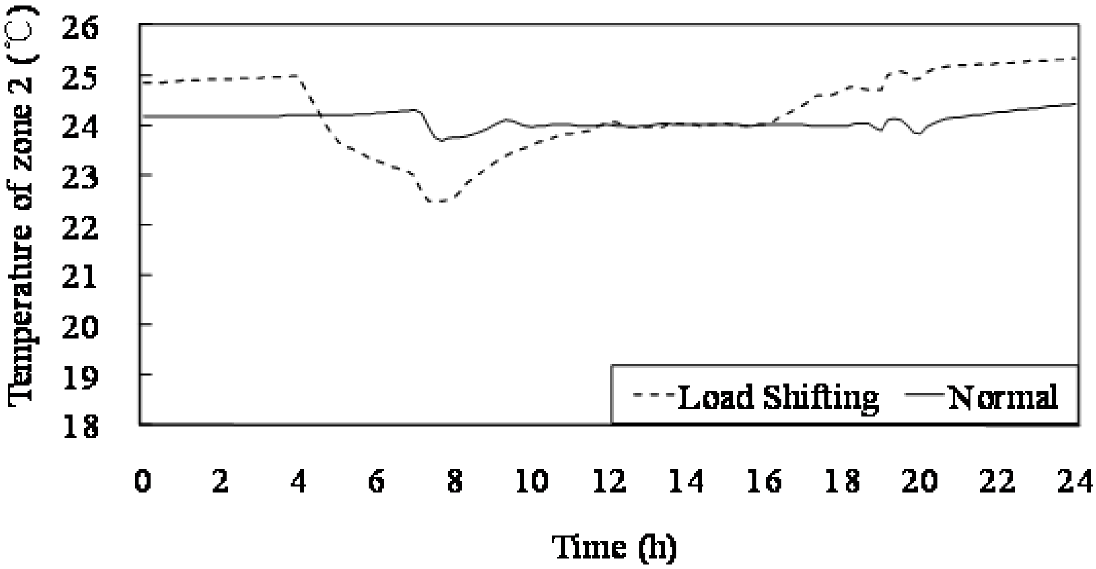

Figure 9.8 Indoor air temperatures of SSPCM building under load shifting and normal control (Beijing test case)

Figure 9.9 presents the comparison between the indoor air (Zone 2) temperatures of SSPCM and reference buildings under load shifting control in Hong Kong test case. Under the load shifting control, the SSPCM building demonstrated some advantages on reducing the zone temperature swings and maintained it around the comfortable range. During the occupied period (8:00 AM to 8:00 PM), the indoor air temperatures of the SSPCM building and reference building maintained at 22.8-25.1°C and 21.9-25.1°C respectively. The indoor air temperature was slightly low in the morning because of the pre-cooling. The indoor temperature was lower in the morning and higher in the afternoon, but still within the normal comfortable range.

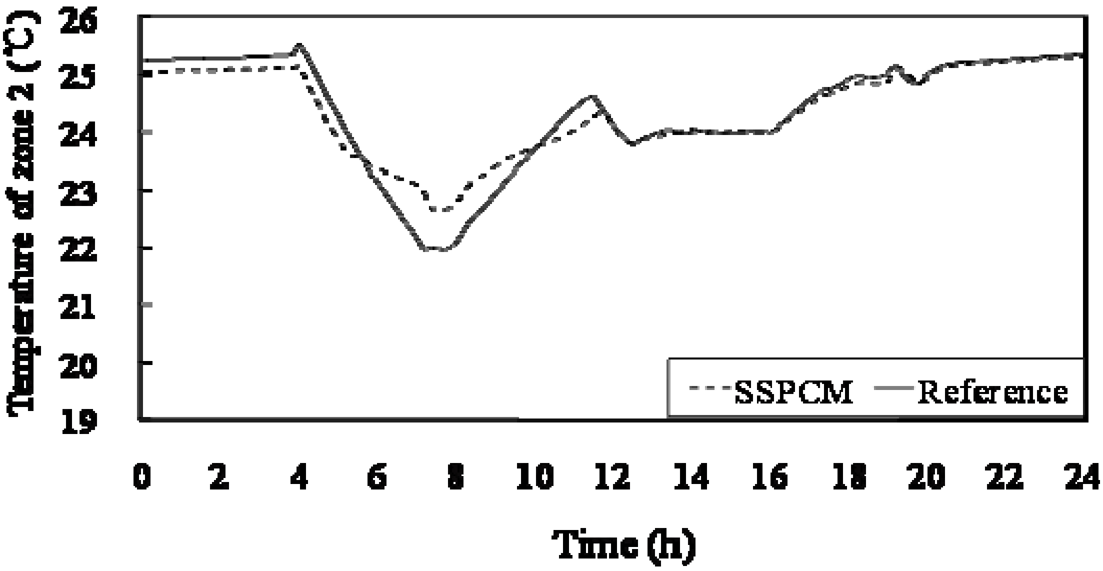

Figure 9.9 Indoor air temperatures of SSPCM and reference buildings under load shifting control (Hong Kong test case)

Table 9.2 Daily electricity consumptions/costs and indoor thermal environment of SSPCM and reference buildings - load shifting control

		Hong Kong			Beijing		
		Reference Building	SSPCM Building	Difference	Reference Building	SSPCM Building	Difference
Fan electricity consumption (kWh)		495	438	-57	458	409	-49
Coil cooling load (kJ)		11,145,600	10,319,496	-826,104	10,292,400	9,679,764	-612,636
Breakdown of electricity consumption (kWh)	8AM-11AM,6PM-11PM	376	354	-22	368	336	-32
	7AM-8AM, 11AM-6PM	818	716	-102	725	651	-74
	11PM-7AM	333	324	-9	318	318	0
Overall electricity consumption (kWh)		1527	1394	-133 (-8.71%)	1,411	1,305	-106 (-7.51%)
Daily electricity cost (Hong Kong Case: HKD, Beijing Case: CNY)		1,204.9	1,094.1	-110.8 (-9.20%)	1,117	1,019.4	-97.6 (-8.74%)
Indoor air Temp. (°C)	Average	24.2	24.1	-0.1	24.2	24.0	-0.2
	Minimum	21.9	22.8	0.9	21.7	22.5	0.8
	Maximum	25.1	25.1	0	25.2	25.1	-0.1

Table 9.3 Daily energy/electricity consumptions and indoor thermal environment under load shifting and normal control - SSPCM building

		Hong Kong			Beijing		
		Normal Control	Load Shifting Control	Difference	Normal Control	Load Shifting Control	Difference
Fan electricity consumption (kWh)		420	438	18	398	409	11
Coil cooling load (kJ)		8,908,458	10,319,496	1,411,038	8,474,928	9,679,764	1,204,836
Breakdown of electricity consumption (kWh)	8AM-11AM, 6PM-11PM	446	354	-92	431	336	-95
	7AM-8AM, 11AM-6PM	799	716	-83	752	651	-101
	11PM-7AM	0	323	323	0	318	318
Overall electricity consumption (kWh)		1,245	1,394	149 (11.97%)	1,183	1,305	122 (10.31%)
Daily electricity cost (Hong Kong Case: HKD, Beijing Case: CNY)		1,174.2	1,094.1	-80.1(-6.82%)	1,118.6	1,019.4	-99.2(-8.87%)
Indoor air Temp. (°C)	Average	24.0	24.1	0.1	24.0	24.0	0
	Minimum	23.8	22.8	-1.0	23.7	22.5	-0.8
	Maximum	24.1	25.1	1.0	24.1	25.1	1.0

9.5 Summary

Test results show that, under time-based pricing policy and load shifting control, the use of SSPCM in the building could reduce the overall building electricity cost significantly compared with the reference building without SSPCM. The daily electricity cost of the SSPCM building under the load shifting control was also reduced significantly compared with that of the SSPCM building under the normal control. The daily electricity cost of the building was reduced even more when it was enhanced by SSPCM and controlled by load shifting strategy simultaneously (11.44% and 11.29% in Hong Kong and Beijing climate cases respectively).

CHAPTER 10 CONCLUSIONS AND FUTURE WORK

In this thesis, a simplified physical model for building structure integrated with SSPCM and particularly a method to identify the parameters of the model, including the wall model and the SSPCM model were developed. Two genetic algorithm-based preprocessors were developed to identify and optimize the parameters on resistances and capacitances of the 3R2C wall model and 4R2C SSPCM model.

The indoor thermal environment and energy performance were investigated in the air-conditioned SSPCM building, and they were also studied with night ventilation in the same condition test cases.

The energy performance and indoor thermal environment were also studied in the air-conditioned SSPCM building under optimal control strategies, including normal control, demand limiting control and load shifting control.

10.1 Conclusions

Simplified building model

Test results show that the simplified 3R2C+4R2C model can provide accurate and reliable prediction of the thermodynamic performance of the building structures integrated with SSPCM layer. It was also found that the 2R1C SSPCM model cannot provide the prediction with sufficient accuracy and the deviations of temperature and heat transfer rate predictions were larger than that of the 4R2C SSPCM model in the scale of at least one order of magnitude. The nodal placement (distribution of the resistances and capacitances among the nodes) affects the outputs of the simplified model significantly and the proper nodal placement is essential to ensure that the simplified model can provide accurate and reliable outputs. At the same time, the experiences show that GA is an effective tool for optimize the nodal placement of the two models in frequency domain and time domain respectively.

The prediction errors of the model using parameters identified by minimizing both the indoor heat exchange between the internal surface of the structure and indoor air (ΔQ_{in}) and indoor temperature (ΔT_{in}) and by minimizing ΔQ_{in} only had not obvious difference. Therefore, it is suggested that parameter identification of 4R2C model to be performed by minimizing ΔQ_{in} only as it is simpler and gives similar fitness.

The simplified building model can well represent thermodynamic performance (heat transfer to indoor space) of the building envelopes integrated with SSPCM for walls of normal thickness (not more than 300mm approximately) including light wall and median wall. The Bi number (<0.1) can be also used to check if the simplified model is valid to the strictures, which matches the observation in this study. Test results also show that model is suitable the SSPCM layer of normal thickness in practical applications (not significantly more than 20mm). The simplified model is very simple in programming and has very high speed in computation. It is therefore very suitable to the applications of system performance evaluation, optimal control, diagnosis, etc.

Performance of SSPCM building and impacts of control strategies

Under demand limiting control (energy-plus-demand-based pricing policy), the use of SSPCM in the building could reduce the overall building electricity cost significantly compared with that of the reference building. The daily electricity cost of the SSPCM building under demand limiting control was reduced also significantly compared with that under normal control. More significant saving on the daily electricity cost of the building could be achieved when it was enhanced by SSPCM and controlled by demand limiting strategy (10.61% and 12.76% in Hong Kong and Beijing climate cases respectively). The use of demand limiting control can contribute significant reduction on the peak electricity demand of the SSPCM building (17.36% and 20.28% in Hong Kong and Beijing test cases respectively compared with normal control).

Under load shifting control (time-based pricing policy), the use of SSPCM in the building could reduce the overall building electricity cost significantly compared with the reference building without SSPCM. The daily electricity cost of the SSPCM building under the load shifting control was also reduced significantly compared with that of the SSPCM building under the normal control. The daily electricity cost of the building was reduced even more when it was enhanced by SSPCM and controlled by load shifting strategy simultaneously (11.44% and 11.29% in Hong Kong and Beijing climate cases respectively).

It can be concluded that the advantages of using SSPCM in buildings can be effectively or fully utilized only with the support of proper control strategies, and the load shifting control (for time-based pricing) and demand limiting control (for energy-plus-demand-based pricing) can achieve more significant electricity cost (and consumption) saving when the building envelopes are enhanced with SSPCM. The indoor air temperature under load shifting control has obvious variation during occupied period and it has less variation under demand limiting control but it can still be maintained within the comfortable range. The use of SSPCM in buildings can reduce the indoor temperature swing noticeably under load shifting control.

It is worth of noticing that the actual saving can be achieved depends on the use and the integration of the PCM materials on the building envelops. The extensive evaluation on the annual saving potentials needs more tests over much longer period, such as an entire year. For maximizing the saving, the control strategies (i.e. the pre-cooling period and the set-point of both load shifting control and demand limiting control) and the melting temperature of PCM should be optimized according to the actual characteristics of the buildings and the weather conditions. The actual effect of the SSPCM also depends on the heat transfer coefficient between indoor air and SSPCM (wall).

10.2 Further work

Simplified building model

The simplified SSPCM building model is good only for light and medium walls but not good for heavy walls. There is a need to analyze if the simplified SSPCM building can be improved to be suitable for heavy walls. The thickness of SSPCM layer is no more than 20mm in light and median walls in the test cases. The cases when the thickness of SSPCM layer is over 20mm for heavy walls need to be studied if it can be modeled using simplified building model.

Performance of SSPCM building and impacts of control strategies

As the development of the simplified SSPCM building model, the indoor thermal environment and energy performance are analyzed under normal control, demand limiting control and load shifting control. The indoor temperature of zones in the SSPCM building are lower most of the time during occupied hours and swing less than that of the reference building in the same test condition under the three control strategies. The indoor temperature of zones in these two types of buildings are in the comfortable range during the occupied hours, but the indoor temperature of zones under demand limiting and load shifting control are too cool due to the pre-cooling before 8:00 AM. Therefore, there is still an opportunity to raise the temperature to improve the comfort conditions in that period but still without sacrificing the cold storage during the pre-cooling period.

The shape stabilized phase change materials have some effects under the demand limiting control and load shifting control in the case studies of this project, the energy/cost is reduced when compared with the normal control. The indoor temperature set-point trajectory is preset as a fixed profile but not updated and optimized on-line in the case studies in this project. It is interesting and needed to study the effects of online optimization of the set-point trajectory and how on-line control can be achieved to optimize the indoor temperature set-point and maximize the energy/cost saving.

REFERENCES

Ahmad M, Bontemps A, Sallée H and Quenard D. Experimental investigation and computer simulation of thermal behaviour of wallboards containing a phase change material. Energy and Buildings 2006; 38(4):357-366.

Ahmad M, Bontemps A, Sallée H and Quenard D. Thermal testing and numerical simulation of a prototype cell using light wallboards coupling vacuum isolation panels and phase change material. Energy and Buildings 2006; 38(6):673-681.

Alawadhi EM. Thermal analysis of a building brick containing phase change material. Energy and Buildings 2008; 40(3):351-357.

Andresen I, Brandemuehl MJ. Heat storage in building thermal mass: a parametric Study. ASHRAE Transactions 1992; 98(1):910-918.

Antonopoulos KA, Koronaki EP. On the dynamic thermal behaviour of indoor spaces. Applied Thermal Engineering 2001; 21(9):924-940.

Athienities A, Chen Y. The effect of solar radiation on dynamic thermal performance of floor heating systems. Solar Energy 2000; 69(3):229–237.

Athienitis AK. Numerical model of floor heating system. ASHRAE Transactions 1994; 100(1):1024–1030

Athienitis AK, Liu C, Hawes D, Banu D and Feldman D. Investigation of the thermal performance of a passive solar test-room with wall latent heat storage. Build and Environment 1997; 32(5):405–410.

Arkar C, Vidrih B and Medved S. Efficiency of free cooling using latent heat storage integrated into the ventilation system of a low energy building. International Journal of Refrigeration 2007; 30(1):134-143.

Arkar C, Medved S. Free cooling of a building using PCM heat storage integrated into the ventilation system. Solar Energy 2007; 81(9):1078-1087.

Banu D, Feldman D, Haghighat F, Paris J and Hawes D. Energy-storing wallboard: flammability tests. Journal of Materials in Civil Engineering 1998; 10(2):98-105.

Benmansour A, Hamdan MA and Bengeuddach A. Experimental and numerical investigation of solid particles thermal energy storage unit. Applied Thermal Engineering 2006; 26(5-6):513-518.

Benard C, Gobin D and Gutierrez M. Experimental results of a latent heat solar roof used for breeding chickens. Solar Energy 1981; 26(4):347–354.

Braun JE. Reducing energy cost and peak electrical demand through optimal control of building thermal storage. ASHARE Transactions 1990; 96(2):839-848.

Braun JE. Load control using building thermal mass. Journal of Solar Energy Engineering, Transactions of the ASME 2003; 125(3):292-301

Braun JE, Montgomery KW and Chaturvedi N. Evaluating the performance of building thermal mass control strategies, HVAC&R Research 2001; 7(4): 403–428.

Braun JE, Chaturvedi N, An inverse gray-box model for transient building load prediction, HVAC&R Research 2002; 8 (1):73–99.

Butala V, Stritih U. Cold storage with phase change material for building ventilation. International Journal of Ventilation 2006; 5(2):189-198.

Butala V, Stritih U. Experimental investigation of PCM cold storage. Energy and Buildings 2008;doi:10.1016/j.enbuild.2008.10.008

Cabeza LF, Castellón C, Nogues M, Medrano M, Leppers R and Zubillaga O. Use of microencapsulated PCM in concrete walls for energy savings. Energy and Buildings 2007; 39(2):113-119.

Carbonari A, De Grassi M, Di Perna C and Principi P. Numerical and experimental analyses of PCM containing sandwich panels for prefabricated walls. Energy and Buildings 2006; 38(5):472-483.

Carroll DL. FORTRAN Genetic algorithm (GA) driver, Version 1.7a, http://cuaerospace.com/carroll/ga.html,http://cuaerospace.com/carroll/gatips.html, (2001).

Chen C, Guo HF, Liu YN, Yue HL and Wang CD. A new kind of phase change material (PCM) for energy-storing wallboard. Energy and Buildings 2008; 40(5): 882-890.

Darkwa K, Kim JS. Dynamics of energy storage in phase change drywall systems. International Journal of Energy Research 2005; 29(4):335-343.

Darkwa K, Kim JS. Heat transfer in neuron composite laminated phase-change drywall. Proceedings of the Institution of Mechanical Engineers, Part A: Journal of Power and Energy 2004; 218(2): 83–88.

Darkwa K, O'Callaghan PW and Tetlow D. Phase-change drywalls in a passive-solar building. Applied Energy 2006; 83(5):425-435.

De Grassi M, Carbonari A and Palomba G. A statistical approach for the evaluation of the thermal behavior of dry assembled PCM containing walls. Building and Environment 2006; 41(4):448-485.

De Saulles T. Free cooling systems: design and application guidance. Bracknell, England: Building Services Research and Information Association, 1996.

Dinçer I, Rosen MA. Thermal energy storage: systems and applications. England: John Wiley & Sons, LTD., 2002.

DOE. Buildings Energy Data Book. Office of Energy Efficiency and Renewable Energy, U.S. Department of Energy, 2007.

Dwarka K, Kim JS. Thermal analysis of composite phase change drywall systems. Journal of Solar Energy Engineering, Transactions of the ASME 2005; 127(3):352-356.

Emmerich SJ. Mitchell JW and Beckman WA. Demand-controlled ventilation in a multi-zone office building. Indoor environment 1994; 3:331-340.

Esen M. Thermal performance of a solar-aided latent heat store used for space heating by heat pump. Solar Energy 2000; 69(1):15-25.

Etheridge D, Murphy K and Reay D. A PCM/heat pipe cooling system for reducing air conditioning in buildings: Review of options and report on field tests. Building Services Engineering Research and Technology 2006; 27(1):27-39.

Faggembauu D, Costa M, Soria M and Oliva A. Numerical analysis of the thermal behaviour of ventilated glazed facades in Mediterranean climates, Part I: Development and validation of a numerical model. Solar Energy 2003; 75(3): 217-228.

Faggembauu D, Costa M, Soria M and Oliva A. Numerical analysis of the thermal behaviour of glazed ventilated facades in Mediterranean climates, Part II: Applications and analysis of results. Solar Energy 2003; 75(3):229-239.

Farid MM, Chen XD. Domestic electrical space heating with heat storage. Proceedings of the Institution of Mechanical Engineers, Part A: Journal of Power and Energy 1999; 213(2):83-92.

Farid MM, Khudhair AM, Siddiquei AK and Said A. A review on phase change energy storage: materials and applications. Energy Conversion and Management 2004; 45(9):1597-1615.

Farid MM, Kong WJ. Underfloor heating with latent heat storage. Proceedings of the Institution of Mechanical Engineers, Part A: Journal of Power and Energy 2001; 215(5):601-609.

Feldman D, Banu D, Hawes D and Ghanbari E. Obtaining an energy storing building material by direct incorporation of an organic phase change material in gypsum wallboard. Solar Energy Materials 1991; 22(2-3):231–242.

Ferrano F and Wong K. Prediction of thermal storage loads using a neural network. ASHRAE transactions 1990; 96(2):723-726.

Feustel HE, Stetiu C. Thermal performance of phase change wallboard for residential cooling application. Report LBL-38320, UC-1600. Lawrence Berkeley National Laboratory, University of California, USA, 1997.

Ghoneim AA, Klein SA and Duffie JA. Analysis of collector-storage building walls using phase-change materials. Solar Energy 1991; 47(3):237–242.

Gong ZX, Mujumdar AS. Finite-element analysis of cyclic heat transfer in a shell-and-tube latent heat energy storage exchanger. Applied Thermal Engineering 1997; 17(6):583–591.

Gu ZL, Liu HJ and Li Y. Thernal energy recovery of air conditioning system - Heat recovery system calculation and phase change materials development. Applied Thermal Engineering 2004; 24(17-18):2511-2526.

Hadjieva M, Kanev S and Argirov J. Thermophysical properties of some paraffins applicable to thermal energy storage. Solar Energy Materials and Solar Cells1992; 27(2):181-187.

Halawa E, Bruno F and Saman W. Numerical analysis of a PCM thermal storage system with varying wall temperature. Energy Conversion and Management 2005; 46(15-16):2592–2604.

Halford CK, Boehm RF. Modeling of phase change material peak load shifting. Energy and Buildings 2007; 39(3):298-305.

Hammou ZA, Lacroix M. A hybrid thermal energy storage system for managing simultaneously solar and electric energy. Energy Conversion and Management 2006; 47(3):273-288.

Hammou ZA, Lacroix M. A new PCM storage system for managing simultaneously solar and electric energy. Energy and Buildings 2006; 38(3):258-265.

Hasnain SM. Review on sustainable thermal energy storage technologies, Part I: Heat storage materials and techniques. Energy Conversion and Management 1998; 39(11):1127-1138.

Hassan MM, Beliveau Y. Modeling of an integrated solar system. Building and Environment 2008; 43(5): 804-810.

Hauer A, Mehling H, Schossig P, Yamaha M, Cabeza L, Martin V and Setterwall F. Annex 17: Advanced thermal energy storage through phase change materials and chemical reactions-feasibility studies and demonstration projects. International

Energy Agency Implementing Agreement on Energy Conservation through Energy Storage, 2005.

Hawlader MNA, Uddin MS and Khin MM. Microencapsulated PCM thermal-energy storage system. Applied Energy 2003; 74(1–2):195–202.

Heim D, Clarke JA. Numerical modelling and thermal simulation of PCM-gypsum composites with ESP-r. Energy and Buildings 2004; 36(8):795-805.

Heim D. Phase-change material modeling within whole building dynamic simulation. ASHRAE Transactions 2006; 112(1):518-525.

Heim D. Whole year analysis of TIM-PCM solar thermal storage wall. Proceedings of SimBuild, First National Conference of IBPSA-USA, University of Colorado, Boulder, CO, August 4-6, 2004.

Henze GP, Felsmann C and Knabe G. Evaluation of optimal control for active and passive building thermal storage, Int. J. Thermal Sciences 2004; 43(2):173–183.

Henze GP, Le TH, Florita AR and Felsmann C. Sensitivity analysis of optimal building thermal mass control. Journal of Solar Energy Engineering, Transactions of the ASME 2007; 129(4):473-485.

Henze GP, Pfafferott J, Herkel S and Felsmann C. Impact of adaptive comfort criteria and heat waves on optimal building thermal mass control. Energy and Buildings 2007; 39(2):221-235.

HKES (Hong Kong energy statistics). Census and Statistics department, Hong Kong Government, Hong Kong, 2008. Available at http://www.censtatd.gov.hk/.

Huang MJ, Eames PC and Hewitt NJ. The application of a validated numerical model to predict the energy conservation potential of using phase change materials in the fabric of a building. Solar Energy Materials and Solar Cells 2006; 90(13): 1951-1960.

Ibáñez M, Lázaro A, Zalba B and Cabeza LF. An approach to the simulation of PCMs in building applications using TRNSYS. Applied Thermal Engineering 2005; 25(11-12):1796-1807.

Inaba H, Tu P. Evaluation of thermophysical characteristics on shape-stabilized paraffin as a solid–liquid phase change material. Heat Mass Transfer 1997; 32(4): 307-312.

Incropera FP, DeWitt DP. Introduction to Heat Transfer, 3rd edition, New York, John Wiley & Sons, 1996

Ismail KAR, Castro JNC. PCM thermal insulation in buildings. International Journal of Energy Research 1997; 21(14):1281-1296.

Ismail KAR, Henrquez JR. Thermally effective windows with moving phase change material curtains. Applied Thermal Engineering 2001; 21(18):1909-1923.

Jokisalo J, Lamberg P and Sirén K. Thermal simulation of PCM structures with TRNSYS. 8th International Conference on Thermal Energy Storage, Stuttgart, Germany. 2000.

Kang YB, Jiang Y, Zhang YP. Modeling and experimental study on an innovative passive cooling system-NVP system. Energy and Buildings 2003; 35(4): 417-425.

Kang YB, Zhang YP, Jiang Y and Zhu YX. General model for analyzing the thermal characteristics of a class of latent heat thermal energy storage systems. Journal of Solar Energy Engineering, Transactions of the ASME 1999; 121(4):185-193.

Kawashima M, Dorgan C and Michell J. Hourly thermal load prediction for the next 24 hours by ARIMA, EWMA, LR and an artificial neural network. ASHRAE transactions 1995; 101(1):186-200.

Kaygusuz K. Performance of solar-assisted heat-pump systems. Applied Energy 1995; 51(2):93-109.

Kaygusuz K. Investigation of a combined solar-heat pump system for residential heating, Part 1: Experimental results. International Journal of Energy Research 1999; 23(14):1213-1223.

Kaygusuz K. Phase change energy storage for solar heating systems. Energy Sources 2003; 25(8):791-807.

Kaygusuz K, Ayhan T. Experimental and theoretical investigation of combined solar heat pump system for residential heating. Energy Conversion and Management 1999; 40(13):1377-1396.

Kelin SA. et al. TRNSYS–A Transient Simulation Program, User Manual Version 13.1. Madison: Engineering Experimentation Station, University of Wisconsin. 1990.

Khalifa AJN, Abbas EF. A comparative performance study of some thermal storage materials used for solar space heating. Energy and Buildings 2008; 41(4): 407-415.

Khudhair AM, Farid MM. A review on energy conservation in building applications with thermal storage by latent heat using phase change materials. Energy Conversion and Management 2004; 45(2):263-275.

Kim JS, Darkwa K. Simulation of an integrated PCM-wallboard system. International Journal of Energy Research 2003; 27(3):215-523.

Kintner-Meyer M, Emery AF. Optimal control of an HVAC system using cold storage and building thermal capacitance. Energy and Buildings 1995; 23(1):19-31.

Kissock JK, Hannig JM, Whitney TI and Drake ML. Testing and simulation of phase change wallboard for thermal storage in buildings. International Solar Energy Conference, Solar Engineering, 1998, 45-52.

Kissock JK, Limas S. Diurnal load reduction through phase-change building components. ASHRAE Transactions 2006; 112(1):509-517.

Kondo T, Ibamoto T. Research on thermal storage using rock wool phase-change material ceiling board. ASHRAE Transactions 2006; 112(1):526-531.

Koschenz M, Lehmann B. Development of a thermally activated ceiling panel with PCM for application in lightweight and retrofitted buildings. Energy and Buildings 2004; 36(6):567-578.

Khudhair AM, Farid MM. A review on energy conservation in building applications with thermal storage by latent heat using phase change materials. Energy Conversion and Management 2004; 45(2):263-275.

Kurklu A. Energy storage applications in greenhouses by means of phase change materials (PCMs): A review. Renewable Energy 1998; 13(1):89-103.

Kurkulu A, Wheldon A and Hadley P. Mathematical modelling of the thermal performance of a phase-change material (PCM) store: cooling cycle. Applied Thermal Engineering 1996; 16(7):615–623.

Kuznik F, Virgone J and Noel J. Optimization of a phase change material wallboard for building use. Applied Thermal Engineering 2008; 28(11-12):1291-1298.

Kuznik F, Virgone J and Roux JJ. Energetic efficiency of room wall containing PCM wallboard: a full-scale experimental investigation. Energy and Buildings 2008; 40(2):148-156.

Lai CM, Chiang CM. How phase change materials affect thermal performance: Hollow bricks. Building Research and Information 2006; 34(2):118-30.

Lamberg P. TRNSYS16: TYPE204, http://sel.me.wisc.edu/trnsys/trnlib/ library16. htm# thermalstorage, Nov. 2005.

Lawrence Berkeley Laboratory. DOE-2 Engineering Manual Version 2.1C. Berkeley, CA, Lawrence Berkeley Laboratory. 1982.

Laret L, Liebecq G and Ngendakumana P. Building. IEA Annex 10 Report, University of Liege, Belgium, 1987.

Lebrun J, Wang SW. Evaluation and Emulation of Building Energy Management Systems-Synthesis Report. IEA (BCS) Annex 17 Final Report, University of Liege, Belgium, 1993.

Lee K, Braun JE. An experimental evaluation of demand limiting using building thermal mass in a small commercial building. ASHRAE Transactions 2006; 112(1):559-571.

Lee KH, Braun JE. Model-based demand-limiting control of building thermal mass. Building and Environment 2008; 43 (10):1633-1646.

Lee KH, Braun JE. Development of methods for determining demand-limiting set-point trajectories in building using short-term measurement. Building and Environment 2008; 43(10):1769-1783.

Lee T, Hawes DW, Banu D and Feldman D. Control aspects of latent heat storage and recovery in concrete. Solar Energy Materials and Solar Cells 2000; 62(2): 217-237.

Liao Z, Dexter AL. A simplified physical model for estimating the average air temperature in multi-zone heating systems. Building and Environment 2004; 39(9):1013-1022.

Lin KP, Zhang YP, Xu X, Di HF, Yang R and Qin PH. Experimental study of under-floor electric heating system with shape-stabilized PCM plates. Energy and Buildings 2005; 37(3):215-220.

Lin KP, Zhang YP, Di HF and Yang R. Study of an electrical heating system with ductless air supply and shape-stabilized PCM for thermal storage. Energy Conversion and Management 2007; 48(7):2016-2024.

Lv SL, Feng GH, Zhu N and Li DY. Experimental study and evaluation of latent heat storage in phase change materials wallboards. Energy and Buildings 2007; 39(10):1088-1091.

Lv SL, Zhu N and Feng GH. Impact of phase change wall room on indoor thermal environment in winter. Energy and Buildings 2006; 38(1):18-24.

Manz H, Egolf PW, Suter P and Goetzberger A. TIM–PCM external wall system for solar space heating and day lighting. Solar Energy 1997; 61(6):369–379.

Medina MA, King JB and Zhang M. On the heat transfer rate reduction of structural insulated panels (SIPs) outfitted with phase change materials (PCMs). Energy 2008; 33(4):667-678.

Medved S, Arkar C. Correlation between the local climate and the free cooling potential of latent heat storage. Energy and Buildings 2008; 40(4):429-437.

Mehling H, Cabeza LF. Heat and cold storage with PCM: an up to date introduction into basics and applications. Berlin: Springer, 2008.

Mitchell JM. An Introduction to Genetic Algorithm, MIT Press, Cambridge, MA, 1997.

Mozhevelov S, Ziskind G and Letan R. Temperature moderation in a real-size room by PCM-based units. Journal of Solar Energy Engineering, Transactions of the ASME 2006; 128(2):178-188.

Nagai T, Reddy A and Massie D. Optimization method for minimizing annual energy, peak energy demand, and annual energy cost through use of building thermal storage. ASHRAE Transactions 2002; 108(1):43-53.

Nagano K, Takeda S, Mochida T, Shimakura K and Nakamura T. Study of a floor supply air conditioning system using granular phase change material to augment building mass thermal storage-heat response in small scale experiments. Energy and Buildings 2006; 38(5):436-446.

Neeper DA. Thermal dynamics of wallboard with latent heat storage. Solar Energy 2000; 68(5):393–403.

Nikolć R, Marinović-Cincović M, Gadžurić S and Zsigrai IJ. New materials for solar thermal storage-Solid/liquid transitions in fatty acid esters. Solar Energy Materials and Solar Cells 2003; 79(3):285-292.

Norford LK, Xing HY. A multiple-building optimization scheme based on statistical building load models. In: SimBuild 2006 IBPSA-USA national conference, Cambridge, MA, USA, 2006.

Onishi J, Soeda H and Mizuno M. Numerical study on a low energy architecture based upon distributed heat storage system. Renewable Energy 2001;22(1): 61-66.

Paksoy HÖ. Thermal energy storage for sustainable energy consumption: fundamentals, case studies and design. The Netherlands: Springer, 2007.

Pasupathy A, Athanasius L, Velraj R and Seeniraj RV. Experimental investigation and numerical simulation analysis on the thermal performance of a building roof incorporating phase change material (PCM) for thermal management. Applied Thermal Engineering 2008; 28(5-6):556-565.

Pasupathy A, Velraj R. Effect of double layer phase change material in building roof for year round thermal management. Energy and Buildings 2008; 40(3): 193-203.

Pasupathy A, Velraj R and Seeniraj RV. Phase change material-based building architecture for thermal management in residential and commercial establishments. Renewable and Sustainable Energy Reviews 2008; 12(1):39-64.

Peippo K, Kauranen P and Lund PD. A multicomponent PCM wall optimized for passive solar heating. Energy and Buildings 1991; 17(4):259-270.

Price BA, Smith TF. Description of the Iowa Energy Center Energy Resource Station: facility update Ⅲ. Technical Report ME-TES-00-001, The University of Iowa 2000.

Rabl A, Norford LK. Peak load reduction by preconditioning buildings at night. International Journal of Energy Research 1991; 15(9):781-798.

Reddy TA, Claridge DE. Using synthetic data to evaluate multiple regression and principal component analyses for statistical modeling of daily building energy consumption. Energy and buildings 1994; 21(1):35-44.

Reddy TA, Norford LK and Kempton W. Shaving residential air-conditioner electricity peaks by intelligent use of the building thermal mass. Energy (Oxford) 1991; 16(7):1001-1010.

Regin AF, Solanki SC and Saini JS. Heat transfer characteristics of thermal energy storage system using PCM capsules: A review. Renewable and Sustainable Energy Reviews 2008; 12(9):2438-2451.

Roth K, Westphalen D and Brodrick J. PCM technology for building materials. ASHRAE Journal 2007; 49(7):129-131.

Ruud MD, Mitchell JW and Klein SA. Use of building thermal mass to offset cooling loads. ASHRAE Transactions 1990; 96(2):839-848.

Saman W, Bruno F and Halawa E. Thermal performance of PCM thermal storage unit for a roof integrated solar heating system. Solar Energy 2005; 78(2):341-349.

Scalat S, Banu D, Hawes D, Paris J, Haghighata F and Feldman D. Full scale thermal testing of latent heat storage in wallboard. Solar Energy Materials and Solar Cells 1996; 44(1):49-61.

Schossig P, Henning HM, Gschwander S and Haussmann T. Micro-encapsulated phase-change materials integrated into construction materials. Solar Energy Materials and Solar Cells 2005; 89(2-3):297-306.

Schweigler C, Hiebler S, Keil C, Köbel H, Kren C and Mehling H. Low-temperature heat storage for solar heating and cooling applications. ASHRAE Transactions 2007; 113(1):89-96.

Reddy TA, Lukes JK and Norford LK. Benefits of multiple-building electric load aggregation: actual and simulation case studies. ASHRAE Transaction 2004; 110(part 2):130-144.

Salyer IO, Sircar AK. Review of phase change materials research for thermal energy storage in heating and cooling applications at the University of Dayton from 1982 to 1996. International Journal of Global Energy Issues 1997;9(3):183-198.

Schossig P, Henning HM, Gschwander S and Haussmann T. Microencapsulated phase-change materials integrated into construction materials. Solar Energy Materials and Solar Cells 2005; 89(2-3): 297–306.

Seem JE, Klein SA, Beckman WA and Mitchell JW. Transfer functions for efficient calculation of multidimensional transient heat transfer. Journal of Heat Transfer Transactions of the Same 1989; 111 (1):5–12.

Stetiu C, Feustel HE. Phase-change wallboard and mechanical night ventilation in commercial buildings. Lawrence Berkeley National Laboratory, University of California, 1998. Available at http://epb.lbl.gov/thermal/docs/pcm2.pdf.

Stovall TK, Tomlinson JJ. What are the potential benefits of including latent storage in common wallboard? Journal of Solar Energy Engineering, Transactions of the ASME 1995; 117(4):318-325.

Stritih U. Heat transfer enhancement in latent heat thermal storage system for buildings. Energy and Buildings 2003; 35(11):1097-1104.

Stritih U, Butala V. Energy saving in building with PCM cold storage. International Journal of Energy Research 2007; 31(15):1532-1544.

Takeda S, Nagano K, Mochida T and Shimakura K. Development of a ventilation system utilizing thermal energy storage for granules containing phase change material. Solar Energy 2004; 77(3):329-338.

Telkes M. Review of solar house heating. Heating and Ventilation 1949; 46(9): 68-74.

Telkes M. Storing solar heat in Chemicals. Heating and Ventilation 1949; 46(11): 79-86.

Telkes M. Solar energy storage. ASHRAE Journal 1974; 16(9):38-44.

Thomas HR, Rees SW. The thermal performance of ground floor slab-a full scale in situ experiment. Building and Environment 1998; 34(2):139-164.

Turnpenny JR, Etheridge DW and Reay DA. Novel ventilation cooling system for reducing air conditioning in buildings. Part I: Testing and theoretical modeling. Applied Thermal Engineering 2000; 20(11):1019-1037.

Turnpenny JR, Etheridge DW and Reay DA. Novel ventilation system for reducing air conditioning in buildings. Part II: Testing of prototype. Applied Thermal Engineering 2001; 21(12):1203-1017.

Tyagi VV, Buddhi D. PCM thermal storage in buildings: A state of art. Renewable and Sustainable Energy Reviews 2007; 11(6):1146-1166.

Vakilaltojjar SM, Saman W. Analysis and modeling of a phase change storage system for air conditioning applications. Applied Thermal Engineering 2001; 21(3): 249-263.

Verma P, Varun and Singal SK. Review of mathematical modeling on latent heat thermal energy storage systems using phase-change material. Renewable and Sustainable Energy Reviews 2008; 12(4):999-1031.

Wang SW. Modelling and simulation of Building and HVAC System-Building and HVAC Component Models Used in Simulation Exercise C.3. IEA Annex 17 Report. University of Liege, Belgium. 1992.

Wang SW. Dynamic simulation of building VAV air-conditioning system and evaluation of EMCS on-line control strategies. Building and Environment 1999; 34(6):681-705.

Wang SW, Xu XH. Simplified building model for transient thermal performance estimation using GA-based parameter identification, International Journal of Thermal Sciences 2006; 45(4):419–432.

Wang SW, Chen YM. A novel and simple building load calculation model for building and system dynamic simulation. Applied Thermal Energy 2001; 21(6): 683–702.

Wang XC, Niu JL and Van Paassen AHC. Raising evaporative cooling potentials using combined cooled ceiling and MPCM slurry storage. Energy and Buildings 2008; 40(9):1691-1698.

Weinläder H, Beck A and Fricke J. PCM-facade-panel for day lighting and room heating. Solar Energy 2005; 78(2):177-186.

Xiao M, Feng B and Gong KC. Thermal performance of a high conductive shape-stabilized thermal storage material. Solar Energy Mater Solar Cells 2001; 69(3):293–296.

Xiao M., Feng B and Gong KC. Preparation and performance of shape stabilized phase change thermal storage materials with high thermal conductivity. Energy Conversion and Management2002; 43(1):103–108.

Xu P, Haves P, Zagreus L and Piette M. Demand shifting with thermal mass in large commercial buildings (field test, simulation and results). Lawrence Berkeley National Laboratory, CEC-50020006-009, January 2006.

Xu X, Zhang YP, Lin KP, Di HF and Yang R. Modeling and simulation on the thermal performance of shape-stabilized phase change material floor used in passive solar buildings. Energy and Buildings 2005; 37(10):1084-1091.

Yamaha M, Misaki S. The evaluation of peak shaving by a thermal storage system using phase-change materials in air distribution systems. HVAC & R Research 2006; 12(3c):861-869.

Yao Y, Lian ZW, Liu S and Hou ZJ. Hourly cooling load prediction by a combined forecasting model based on Analytic Hierarchy Process, Int. J. Thermal Sciences 2004; 43(11):1107–1118.

Ye H, Ge XS. Preparation of polyethylene-paraffin compound as a form-stable solid–liquid phase change material. Solar Energy Mater Solar Cells 2000; 64(1): 37–44.

Zalba B, Marin JM, Cabeza LF and Mehling H. Review on thermal energy storage with phase change: Materials, heat transfer analysis and applications. Applied Thermal Engineering 2003; 23(3):251-283.

Zalba B, Marin JM, Cabeza LF and Mehling H. Free cooling of buildings with phase change materials. International Journal of Refrigeration 2004; 27(8):839-849.

Zhang M, Medina MA and King JB. Development of a thermally enhanced frame wall with phase-change materials for on-peak air conditioning demand reduction and energy savings in residential buildings. International Journal of Energy Research 2005; 29(9):795-809.

Zhang YP, Lin KP, Zhang QL and Di HF. Ideal thermophysical properties for free cooling (or heating) buildings with constant thermal physical property material. Energy and Buildings 2006; 38(10):1164-1170.

Zhang YP, Lin KP, Yang R, Di HF and Jiang Y. Preparation, thermal performance and application of shape-stabilized PCM in energy efficient buildings. Energy and Buildings 2006; 38(10):1262-1269.

Zhang YP, Lin KP, Jiang Y and Zhou GB. Thermal storage and nonlinear heat-transfer characteristics of PCM wallboard. Energy and Buildings 2008; 40(9):1771-1779.

Zhang YP, Lin KP, Yang R, Di HF and Jiang Y. Preparation, thermal performance and application of shape-stabilized PCM in energy efficient buildings. Energy and Buildings 2006; 38(10):1262–1269.

Zhang YP, Su Y, Zhu YX and Hu XX. A general model for analyzing the thermal performance of the heat charging and discharging processes of latent heat thermal energy storage systems. Transactions of the ASME 2001; 123(3): 232-236

Zhang YP, Xu X, Di HK, Lin KP and Yang R. Experimental study on the thermal performance of the shape-stabilized phase change material floor used in passive solar buildings. Journal of Solar Energy Engineering, Transactions of the ASME 2006; 128(2):255-257.

Zhang YP, Zhou GB, Lin KP, Zhang QL and Di HF. Application of latent heat thermal energy storage in buildings: State-of-the-art and outlook. Building and Environment 2007; 42(6):2197-2209.

Zhang YW, Faghri A. Heat transfer enhancement in latent heat thermal energy storage system by using the internally finned tube. International Journal of Heat and Mass Transfer 1996; 39(15):3165-3173.

Zhou GB, Zhang YP, Lin KP and Xiao W. Thermal analysis of a direct-gain room with shape-stabilized PCM plates. Renewable Energy 2008; 33(6): 1228-1236.

Zhou GB, Yang YP, Wang X and Zhou SX. Numerical analysis of effect of shape-stabilized phase change material plates in a building combined with night ventilation. Applied Energy 2009; 86(1):52-59.

Zhou GB, Zhang YP, Wang X, Lin KP and Xiao W. An assessment of mixed type PCM-gypsum and shape-stabilized PCM plates in a building for passive solar heating. Solar Energy 2007; 81(11):1351-1360.

Zhou GB, Zhang YP, Zhang QL, Lin KP and Di HF. Performance of a hybrid heating system with thermal storage using shape-stabilized phase-change material plates. Applied Energy 2007; 84(10):1068-1077.

Zhou Q, Wang SW, Xu XH and Xiao F. A grey-box model of next-day building thermal load prediction for energy-efficient control. International Journal of Energy Research 2008; 32(15):1418-1431.

Zhu N, Wang SW, Xu XH and Ma ZJ. A simplified dynamic model of building structures integrated with shaped-stabilized phase change materials, International Journal of Thermal Sciences 2010; 49(9):1722-1731.

Zhu N, Ma ZJ and Wang SW. Dynamic characteristics and energy performance of buildings using phase change materials: A review. Energy Conversion and Management 2009; 50(12):3169-3181.

Zhou Z, Rees SW and Thomas HR. A numerical and experimental investigation of ground heat transfer including edge insulation effects. Building and Environment 2002; 37(1):67-78.